ADDIS ABABA UNIVERSITY
ADDIS ABABA INSTITUTE OF TECHNOLOGY (AAiT)

EVALUATION OF THE PERFORMANCE OF HIGH-RESOLUTION SATELLITE RAINFALL PRODUCTS FOR STREAM FLOW SIMULATION
(Case Study: Genale Dawa River basin)

Thesis Submitted in Partial Fulfillment of the Requirements for the Degree of Master of Science in Hydraulic Engineering.

By: DAWIT GIRMA BURAYU

Advisors: Dr. BELETE BERHANU

Addis Ababa
Ethiopia

JULY, 2020

DECLARATION AND COPY RIGHT

I declare that research work titled "**EVALUATION OF THE PERFORMANCE OF HIGH-RESOLUTION SATELLITE BASED RAINFALL PRODUCTSFOR STREAM FLOW SIMULATION (Case Study: Genale Dawa River basin)**" is my own work. The work has not been presented elsewhere for assessment. Where material has been used from other sources it has been properly acknowledged or referenced. This thesis is a copyright material protected under the Berne convention, the copy right Act 1999 and other international and national enactments, in that behalf, on intellectual property. It may not be reproduced by any means, in full or in part, except short extracts in fair dealing, for research or private study, critical scholarly review or discourse with an acknowledgement, without written permission of the directorate of postgraduate studies, on behalf of both the author and Addis Ababa University.

DAWIT GIRMA
Signature----------

Addis Ababa Institute of technology (AAiT)
Addis Ababa University (AAU)

CERTIFICATION

I, the undersigned, certify that I read and hereby recommend for the acceptance by the Addis Ababa University a Thesis entitled: **EVALUATION OF THE PERFORMANCE OF HIGH-RESOLUTION SATELLITE BASED RAINFALL PRODUCTSFOR STREAM FLOW SIMULATION (Case Study: Genale Dawa River basin)** in partial fulfillment of a degree of Masters of Science in Hydraulic Engineering.

_____

Belete Berhanu (PhD)
(Advisor)

_____

Date

ACKNOWLEDGEMENT

Foremost, I owe my genuine gratitude to my advisor Belete Berhanu (PhD), for his generous advice, inspiring guidance and encouragement throughout my research work. His expert advice from title selection up to final writes up of this thesis and especially for his patience and guidance during the writing process, the insightful discussion, for his support during the whole period of the study. His technical and editorial advice was essential to the completion of this Thesis and has taught me innumerable lessons and insights on the workings of academic research in general. This thesis could not have been completed without his generous and professional assistance. What I learn from him is not just how to write a thesis to graduation requirement but how to view this from world prospective. I have been extremely lucky to have a such advisor who cared so much about my work, and who responded to my questions and queries so promptly.

I would like to extend my sincere gratitude to Ethiopian Ministry of Water and Energy; and Ethiopian National Metrology Agency for their assistance in providing me the necessary data for the study.

I would like to express my sincere gratitude to my employer Wolkite University for providing me to learn my MSc. Program. I would like to gratefully acknowledge Addis Ababa University for the financial support made through the postgraduate program of the University, which available to me during my research time.

My Last but not list, gratitude and appreciation goes to my wife Burtukan Getachew. Without her encouragement and continuous support, this Thesis cannot be completed.

ABSTRACT

Precipitation data is the most important input parameter to simulate rainfall-runoff processes, since it's strongly hooked into the accuracy of the spatial and temporal representation of the precipitation. In regions where rainfall stations are scarce, additional data sources could also be needed. Satellite platforms has provided a satisfactory alternative because of its global coverage. Although a good range of satellite-based estimations of precipitation is out there, not all the satellite products are suitable for all regions. Moreover, in data-scarce regions in which interpolation schemes are applied, it becomes difficult to have an accurate performance assessment; another comparison tool is required as rainfall-runoff models. Remotely-sensed estimates need to generate realistic and reliable data to be used in water resource assessments. Therefore there is a need to evaluate the accuracy of remote sensing techniques. This study investigated the reliability of the following satellite-derived rainfall estimates; Tropical Applications of Meteorology using SATellite (TAMSAT) and Climate Hazards Group InfraRed Precipitation with Stations (CHIRPS) in Genale Dawa river basin, Ethiopia where climate data scarcity problem extremely high. Besides, the study evaluated the performance of satellite precipitation estimates with ground observations from the most representative rain gauge for nine stations at daily, monthly and yearly timescale. Intercomparison between Satellite rainfall product and observed data were done using point to grid method selecting nine representative metrological stations namely, Bore, Robe, Delomena, Ginir, Moyale, Finchawa, KibreMengist, Negele, and Filtu. TAMSAT shows unacceptable linear correlation coefficient with rain gauges while CHRIPS shows a good linear correlation coefficient with rain gauges. Therefore bias correction was done for TAMSAT. The average correlation R is 0.45 and the average NS is 0.028 for Raw TAMSAT. After bias correction, this value was improved to the average value of R=0.87 and NS =0.764. Considering four Categorical index POD, FAR, FB and HSS, the average value were (0.49, 0.4, 0.84 and 0.41) respectively before Bias correction and improved to (0.71, 0.22, 0.92 and 0.66) respectively after bias correction. For CHRIPS average R and NS are 0.88 and 0.755 respectively and categorical index POD, FAR, FB and HSS were (0.8, 0.05, 0.85 and 0.81) respectively The study model streamflow using both CHRIPS and TAMSAT rainfall products by using the SWAT model from 1983-2017). The model is calibrated from 1998 to 2003 and validated from 2004 to 2007 using SUFI-2 algorithm embodied in the SWAT-CUP. Comparisons of the simulations to the observed streamflow for the four discharge gauging stations namely Dawa at Melka Guba, Welme at Melka Amana, Dimtu Nr. Bore and Genale Nr. Halwen. The Nash-Sutcliffe Efficiency (NSE), linear correlation coefficient (R) and BIAS indices were used to benchmark the model performance and shows very good result (having R^2 and NS=0.71-0.95 during calibration and 0.72-0.97 during validation).

Key words: *CHRIPS, Model, TAMSAT, Satellite rainfall products*, SUFI-2, *SWAT, SWAT-CUP*

ACRONYMS and ABBREVIATIONS

ARC2 Africa Rainfall Estimate Climatology version 2
AGNPS Agricultural None Point Source Model
ANSWERS Areal None Point Source Watershed Environmental response simulation
CCD Cold Cloud duration
CFSR Climate Forecast System Re-analysis
CMORPH Climate Prediction Center Morphing Method
CHRIPS Climate Hazards Group Infrared Precipitation with Stations
CN2 Curve number
DEM Digital Elevation Model
EMA Ethiopian Map Agency
ECMWF ERA European Center for Medium range Weather Forecast European Re-Analysis
EPIC Erosion productivity impact calculator
EUROSEM European soil Erosion model
FAR False alarm ratio
FBI Frequency bias index
GIS Geographic Information System
GPCP Global Precipitation Climatology Project
GSMaP MVK Global Satellite Mapping of Prediction Moving Vector with Kalman
HECHMS Hydrologic modeling system
HRU Hydrologic Response Unit
HSS Heidke skill score
HSPF Hydrologic Simulation Program-Fortran
ITCZ Inter-tropical Convergence Zone
IR Infrared
LS Linear scaling
LOCI Local intensity scaling
LULC Land use land cover
MSWEP Multi-Source Weighted-Ensemble Precipitation
MoWIE Ministry of Water, Irrigation and electricity
MW Microwave
NASA National Aeronautics and Space Administration
NOAA National Oceanic and Atmospheric Administration (USA)
NMAE National Meteorological Agency of Ethiopia
NSE Nash–Sutcliff coefficient
OWWDSE Oromia water works and design supervision enterprise
PERSIANN Precipitation Estimation from Remotely Sensed Information using Artificial Neural Networks
PBIAS percentage bias
PT Power Transiformation
QM Quantile mapping
RCMs Regional Climatic Models

RFEv2 African Rainfall Estimation
RMSE Root mean square error
SCS Soil Conservation Service
SNNP Southern Nation Nationality and peoples
SUFI-2 Sequential Uncertainty Fitting algorithm
SRE Satellite rainfall estimates
SPP Satellite precipitation product
SWAT Soil and Water Assessment Tool
SWAT-CUP SWAT Calibration and Uncertainty Procedures
TAMSAT Tropical Applications of Meteorology using SATellite data and ground-based observations
TARCAT African Rainfall Climatology and Time-series
TMPA TRMM Multi-satellite Precipitation Analysis
TIR Thermal infrared
TRMM Tropical Rainfall Measuring Mission
USDA States Department of Agriculture
USGS United States Geological Survey
WEPP Water Erosion Prediction Project
WGEN Weather Generator
WLRC Water, Land resources center

Table of Contents

LIST OF TABLES

LIST OF FIGURES

APPENDEX TABLE

1. INTRODUCTION

1.1 Background

Accurate estimations of rainfall on fine spatial and temporal resolutions are vital for several water resource-related applications. Hence, for a better understanding of the impact of rainfall on the environment, it is crucial that one uses good spatial and high temporal resolution rainfall measurements (1). Many countries are stricken by precipitation variability and semi-permanent changes in each precipitation amounts and distribution over recent decades. However, the amount of rain gauges throughout Africa is little and erratically distributed, and also the gauge network is deteriorating (2). Therefore, ground-based precipitation measurements are either few or nonexistent. This drawback is common in our country, particularly in Genale-Dawa basin. Satellite-based precipitation estimates with high spatial and temporal resolution and enormous areal coverage provide a possible alternative source of data for hydrological models in areas where conventional rain gauge precipitation measurements are not readily available or sparsely available and no radar technology for measuring representative rainfall magnitude (3) (1) (2). These applications would even have far-reaching effects for several developing countries whose ground-based rain gauges are sparse and no radar technology for measuring representative rainfall magnitude. However, there are errors associated with satellite-based rainfall estimates which prompt several questions. How accurate are satellite-based rainfall products? Can high- resolution satellite rainfall products be used for hydrological applications? Lack of knowledge on the accuracy of those satellite products is a challenge to the hydrological community especially under complex terrain. During the last twenty years, satellite-based instruments are designed to collect observations mainly at thermal infrared (IR) and microwave (MW) wavelengths which will be used to estimate rainfall rates. Observations in the IR band are available in passive modes from (near) polar-orbiting (revisit times of 1–2 days) and geostationary orbits (revisit times of 15–30 min), while observations in the passive and active MW band are only available from the (near) polar-orbiting satellites. Many algorithms are developed to estimate rainfall rates by combining information from the more accurate (but infrequent) MW with the more frequent (but less accurate) IR to require advantage of the complementary strengths (4). Satellite rainfall products are subject to the various source of errors related to temporal sampling, instrument, algorithm, gaps in revisit times, indirect relationship between remotely sensed signals and rainfall rate and also its performance varies with region, elevation, and season (4). Therefore; it's very important to assess the performance of these estimates. Several studies assessed the performance of satellite rainfall products on streamflow simulation capability using hydrological models. For instance, comparing the Climate Prediction Center morphing method (CMORPH), Precipitation Estimation from Remotely Sensed Information Using Neural Networks (PERSIANN) and the Real-time version of the Tropical Rainfall Measuring Mission (TRMM) Multi-satellite Precipitation Analysis (TMPA) 3B42RT) and TMPA 3B42 data with rain gauge data for two medium-scaled watersheds of the Ethiopian highlands as input to the hydrological model. These results revealed 3B42RT and CMORPH simulations show reliable skills in their simulations but

underestimate large flood peaks, while 3B42 and PERSIANN simulations have inconsistent performance. Also this result showed the simulation based on the satellite-only product (3B42RT) gave a better performance than the satellite-gauge product (3B42) (5).

Regarding our country Ethiopia, some studies have been conducted to evaluate performance, validation, Inter-comparison of satellite-based rainfall products especially for Blue Nile basin e.g (1) (6) (4) (7). In other parts of Ethiopia high- resolution rainfall products have been evaluated for different purposes (8) (9). This study also involves a collection of historical rainfall data from existing rain gauges and observed streamflow measurements and application of SWAT hydrological model to simulate streamflow. The rainfall data sets and the modeling activities were used to characterize and determine performance in input precipitation data; high-resolution satellite rainfall products (CHRIPS and TAMSAT) in this case.

The aim of this study is to evaluate the performance of high-resolution satellite rainfall products (CHRIPS and TAMSAT) as input for streamflow simulation in Genale-Dawa river basin, Ethiopia.

1.2 Statements of the Problem

Precipitation is one among the essential meteorological inputs of a hydrologic model and therefore the key drive for a hydrologic cycle. Errors in precipitation estimation can bring significant uncertainties in streamflow simulation and prediction (10)

To gain an exact relationship between rainfall and runoff in modeling, suitable data are required. However, scarcity of data is a common problem in most of the basins within the world especially in undeveloped and developing countries. For solving this problem, new approaches are needed to get hydrological prediction in data-sparse regions. With technological progress, getting time series data using satellite products become important and this represents a possible solution for ungauged basins.

In developing countries, the availability of ground measuring stations is extremely limited with a scarce density of the hydro-meteorological network and uneven distribution making it challenging for accurate measurement of streamflow data for water resource development.

Rainfall measurement is typically accomplished using rain gauge stations. However, there are small numbers of stations available especially in mountainous regions of Ethiopia. In mountainous regions, rainfall is extremely variable and changes in rainfall distribution can occur over short distances and within a short period of time (6). In addition to the sparse network distribution issue, gathering available information from the existent surface observation network and performing ground surveys also are common problems. Among Ethiopian river basins facing this problem, Ganale Dawa river basin encompasses series challenge. Existing basic data for the basin are very limited. This inevitably limits the waterworks to be undertaken therein & provides for hydrologic uncertainty. Remote sensing and satellite technology have provided another platform to retrieve precipitation data insufficient spatial and temporal resolution which is crucial

source, especially in data-scarce regions. By using satellite images, various efforts have been administered to estimate rainfall. These estimates, enhanced by gauge data, can improve rainfall analyses that are currently interpolated solely from sparse rain-gauge data.

A wide range of satellite-based estimations of precipitation is out there in high spatial and temporal resolution, which makes them useful for distributed hydrological models. However, not all the satellite products are suitable for all the regions (i.e. their suitability and performance varies from region to region). There is, therefore, a requirement to quantify their uncertainties before selecting the acceptable product for the region. Therefore, hydrologists are still uncertain in applying these products directly in hydrological applications knowing that many uncertainties are still involved in such techniques (7).

This study intended to evaluate the performance of two widely used, high-resolution, easily available and highly suitable for fully and semi distributed hydrologic model; satellite rainfall datasets (namely, CHRIPS and TAMSAT) for simulating streamflow modeling in Genale Dawa river basin to capture the gauged data scarcity problem.

1.3 Objectives

1.3.1 General Objective

The main objective of this study is to evaluate the performance of high-resolution satellite-based (CHRIPS and TAMSAT) rainfall estimates for streamflow simulation as the case of Genale Dawa river basin in Ethiopia.

1.3.2 Specific Objectives

1. To Validate the TAMSAT rainfall data set for Genale Dawa river basin
2. To model surface flow using satellite rainfall data (CHRIPS and TAMSAT) with the help of SWAT as a tool and evaluate the results.

1.4 Research Question

The basic questions that will be answered by this research are:-

1. Can high – resolution satellite rainfall products accurately estimate rainfall compared to ground-based rain gauge rainfall observation over Genale Dawa river basin?
2. How good are a high – resolution satellite rainfall products for prediction of streamflow in Genale Dawa River Basin?

1.5. The significance of the study

Hydrological models are mainly used for the planning and design of water resources, for flood protection measures or, for flood forecasting. These models are applied to simulate the rainfall-runoff processes and they rely on the precipitation data with a proper resolution in space and time. Decision-makers, planners and water resource managers need to know the amount of water available therefore must be able to assess the input or precipitation. Rain gauges can be used to measure precipitation; however, they are often sparse. Given the practical limitations of hydro-metrological station has brought about the utilization of satellite remote sensing as a potential methods of quantifying rainfall such as visible and infrared techniques that derive qualitative or quantitative appraise of rainfall from satellite imagery. Inadequate hydro-metrological network

coupled with inadequate maintenance of rainfall gauge measuring instruments, human error and inaccessible areas such as sloping areas has resulted in the existence of gaps in rainfall measurements as most occasions are not recorded requires a means to improve on the available data accessible from the gauge precipitation network. Satellite precipitation estimation will, therefore, be important to address issues such as precipitation occurrence, magnitude and apportionment at all-time scales for many applications in meteorology, climatology, hydrology, and environmental sciences. Beside this, it will provide many information required in the management of water resources and flood forecasting. To utilize these rainfall estimates appropriately it is essential to know of their accuracy and expected error characteristics.

As different sources of rain data are available; this study is to investigate the reliability of the TAMSAT and CHIRPS. Furthermore, to investigate the cause of the errors, this will be the important step towards closing the gap between the estimates and the actual ground measurements. The study will also contribute to the literature on the comparison of remotely sensed precipitation data and the actual ground measurements.

1.6. Organization of the Thesis

The paper is organized into five chapters: Chapter one is an introduction part where the background, statement of the problem, objectives of the study and research questions are discussed. In chapter two, review of related literatures where rainfall runoff process in a watershed, rainfall-runoff modeling, stream flow analysis, description of satellite rainfall products, application of high-resolution satellite rainfall products in hydrological modeling and application of SWAT model worldwide and in Ethiopia are reviewed.

In Materials and Methods chapter, Description of the study area, hydrological model selection criteria, model inputs data collection and analysis, model setup and model performance evaluation is elaborated. The fourth chapter describes with the result and discussion which are satellite rainfall products versus rain gauges, stream flow modeling, satellite rainfall simulation of stream flow and overall discussion are made. The stream flow modeling includes sensitivity analysis, calibration and validation of stream flow simulation, and the performance evaluation of the model. Finally, in section five, conclusion and recommendations of the study are provided.

2. LITERATURE REVIEW

2.1 Introduction

This chapter describes the literature review related to the objective of this study. First we describe rainfall measurement technique and satellite rainfall products. Then understanding spatial distribution of rainfall to compute average areal rainfall is also very important in rainfall – runoff modeling, since most of the time the output of models is subject input uncertainty. Next, a description of hydrological cycle and rainfall – runoff processes are given and an overview of rainfall – runoff models is also discussed. Moreover, application of high – resolution satellite rainfall products in hydrological modeling was presented.

2.2 Rainfall Measurement

Precipitation is one of the main components in the hydrological cycle and knowledge of rainfall and its variability is therefore crucial to understand and to predict the global climate system. Also rainfall data with very fine resolution and high quality are of primary importance for hydrological computations (8) (9). In spite of its important role in our lives and global climate, the measurement of rainfall is extremely difficult because of its high spatial and temporal variability. In practice, the density and configuration of an in-situ gauge network is decided based on the supply of funds, accessibility of site and the function of the network. As a result most of the time rain gauges in developing countries are commonly installed in towns that are located along main roads that provide accessibility. However, relatively remote and mountainous areas may remain uncovered by the rain gauge network. To come up with solution for this problem Satellite remote sensing is the good way to provide rainfall data on a global scale. The satellite rain fall estimates have different spatial and time resolutions and give a stream of invaluable data on the side of operational meteorology and numerous other disciplines. In recent years, the utilizations of these satellites have become a long ways past the dreams of the individuals who structured and worked the frameworks. A few satellite precipitation algorithms have been developed to estimate rainfall from visible, thermal infrared (TIR) and microwave radiation using satellite imagery (11). The estimation of precipitation by downpour measures is laden with certain issues, yet those moderately straightforward instruments will long keep on giving the information against which precipitation appraisals by different methods must be balanced. Satellites measure an indispensable of space at a point in time. Obvious and infrared procedures infer subjective or quantitative evaluations of precipitation from satellite symbolism through aberrant connections between vitality reflected by mists (or cloud splendor temperatures) and estimated precipitation.

2.3 Rainfall – runoff modeling

Understanding the rainfall – runoff relation has been a subject of hydrological research for a long time (11). According to study, runoff occurs due to a complex interaction between surface, unsaturated, and saturated flow. In the same time researches in the field of hydrology focused on stream flow simulation processes using hydrological model. Hydrological models are the main tool where all the hydrological processes are combined and simulations are performed to obtain a

certain output. A model is a representation of the real world into a conceptual world. Models can be predictive (to obtain a specific answer to a specific question) or investigative (to further understanding hydrological processes) (12).Depending on the aim of the investigation, models can be deterministic, which do not consider randomness (used for forecasting), or stochastic, where the model outputs are at least partially random (used for prediction). Although all the hydrological processes are random, when the variability in the output is small in comparison with the one of the known factors, deterministic models can be used (13). Within the deterministic models, three types of models are distinguished based on spatial discretization. In rainfall-runoff modeling, models are characterized as lumped, semi distributed (White box) models account for spatial variability of topography, geology, soil type and land use within a catchment. These models use grid layers with elements. Within this sub-catchment the characteristics are lumped. Also another classification is known: event models that represent a single runoff event occurring over a period of time from one hour to several days. In general event models tend to be lumped. Considering the spatial scale, these models can range from lumped to distributed models. Based on the objectives of this study Soil and Water Assessment Tool (SWAT) model was used to simulate stream flow for both in situ dataset and satellite rainfall products.

2.4. Stream flow analysis

Catchment response to the event is characterized by measuring the discharge (volume rate of flow) at the outlet. This is described by a hydrograph. It is clear that hydrograph is a spatial and temporally integrated response of catchments which is determined by spatially and temporal variation of input (rainfall), and travel time of each drop of water form where it strikes on the stream network to outlet. After begins of the rainfall event the flow rate to basin increases rapidly and at same moment it reaches the peak discharge. Each hydrograph has a different shape because it depends on the catchment input (rainfall), and the catchment characteristics. Knowledge of climatic factors (precipitation, evaporation, and transpiration), geometric factors (size, shape, elevation, and stream density), geology, soil type, and land use as well as channel factors (size, shape of the channel, cross-section, slope, length, roughness, and number of tributaries) is very important.

Catchment response to an event is characterized by the discharge (volume flow rate) at the outlet that is described by a hydrograph. Sometime after the start of the event the flow rate begins to increase till the well-defined peak discharge. At this moment the hydrograph rises, which characterized by the rising limb. After that the hydrograph declines as a result of ending of direct runoff, which is described by the recession limb. At the recession period, the discharge is related primarily to the base flow. From this description, one can identify the hydrograph.

2.5. Description of satellite rainfall products

Several remote sensing methods have been developed for estimating the precipitation. Satellite-based estimations of rainfall can provide the data for the areas where there is no rainfall

stations or can help to improve the data in those areas where there is a low density ofstations (3).The great advantage of space-based precipitation estimates is their global coverage, providing information on rainfall frequency and intensity in regions that are inaccessible to other observing systems like rain gauge and radar. The disadvantage is that they are indirect estimates of rainfall, depending on the properties of cloud top (in the case of IR algorithms) and cloud liquid and ice content (in the case of passive microwave algorithms). The two high-resolution satellite based rainfall data that are used in this study are described in this section.

2.5.1. CHRIPS

CHIRPS is developed by the US Geological Survey and the Climate Hazards Group at the University of California at Santa Barbara. The data inputs used for CHIRPS creation are as follows: (i) the Climate Hazards Precipitation Climatology; (ii) quasi-global 3-hourly geostationary TIR satellite observations from the Climate Prediction Center and the National Climatic Data Center; (iii) atmospheric model rainfall fields from the National Oceanic and Atmospheric Administration Climate Forecast System; (iv) the TRMM-3B42 product from NASA; and (v) in situ precipitation observations obtained from a variety of sources, including national and regional meteorological services (5). Unlike TAMSAT, which implements a temporally and spatially varying threshold to compute the CCD, CHIRPS uses a constant rain/no-rain temperature threshold of 235 K. Calibration regression coefficients were then derived by comparing TRMM-3B42 rainfall estimates (2000–2013) and pentadal CCDs. These calibration parameters were then applied to the complete CCD record to produce a time series of rainfall estimates. Next, these pentadal rainfall estimates were expressed as a fraction of their long-term mean (1981–2013) and then multiplied by the Climate Hazards Precipitation Climatology. Rain gauge measurements were then merged using a modified form of the inverse distance weighting algorithm to create the CHIRPS product. Finally, daily estimates of rainfall were created by disaggregating the pentadal estimates using daily CCD observations. In this study, we used the CHIRPS version 2.0 dataset, which provides quasi-global daily rainfall estimates from January 1981 onwards at 0.05° (about 5 km) spatial resolution (ftp://ftp.chg.ucsb.edu/pub/org/chg/products/CHIRPS-2.0). (5) have provided a more detailed description of the CHIRPS product

2.5.2. TAMSAT

TAMSAT is produced by the research group of the University of Reading; it provides rainfall estimates across Africa based both on TIR images obtained every 15 min (30 min prior to June 2006) and on ground-based observations. The TAMSAT algorithm is based on linear relationships between rain gauge records and the number of hours when the brightness temperatures of TIR pixels fall below a certain rain/no-rain temperature threshold called the cold cloud duration (CCD). Optimal threshold temperatures and calibration parameters were derived by comparing CCDs at various temperature thresholds to a large database of historic rain gauge measurements (Tarnavsky 2014). The calibration process was divided into two stages. In the first stage, daily CCD totals were derived at a range of thresholds between

-60 °C and -30 °C. These were then summed to a dekadal (version 2.0) or pentadal (5 days) (version 3.0) time-step, and a set of contingency tables was prepared for every threshold. The tables compared greater-than-zero CCDs at the pixel scale with rainfall occurrences from the collocated rain gauge records. In the second stage, calibration parameters were obtained by linear regressions of CCD totals for the selected temperature threshold versus historical rain gauge accumulations. In version 3.0, the calibration parameters were corrected with a bias adjustment that varied spatially and temporally. The rainfall estimates were then disaggregated to daily values in proportion to the CCD observed on each day. The TAMSAT daily rainfall estimates have been available for all of Africa since January 1983 at a spatial resolution of 0.0375° (about 4 km) http://tamsat.org.uk/view/estimates/index.cgi/rainfall/. In this study we used the newly developed TAMSAT version 3.0 daily rainfall estimates.

2.6 Application of high – resolution satellite rainfall products in hydrological modeling

A number of studies have been carried out to assess the capability of satellite rainfall products (CHRIPS and TAMSAT) through stream flow simulation using hydrological modeling. Some of the studies that evaluated the performance of satellite rainfall products for hydrological simulation are summarized as follow: These studies revealed the capability of satellite rainfall products in the application of hydrological modeling for both worldwide and in case of Ethiopia.

Table 2-1 Studies on performance of satellite rainfall products in Ethiopia

Products Evaluated	**Title and Hydrological model used**	**Study area**	**Main Result**	**Reference**
CHRIPS (V2) TAMSAT 2 TAMSAT 3 ARC2	*Comparison of new satellite Precipitation products over the Upper Blue Nile Basin, Ethiopia*	Upper Blue Nile	CHIRPS exhibited better performance, TAMSAT 3 has shown a comparable performance, ARC 2 product was found to have the weakest performance	(1)

CHRIPS TARCAT PERSIANN ARC 2 TRMM		Upper Blue Nile	CHRIPS perform best, TARCAT performs next, PERSIANN has the list performance	(18)
TRMM, CHIRPS, RFEv2, ARC2, PERSIANN, GPCP, CMAPC,MORPH	Comparison and validation of eight satellite rainfall products over the rugged topography of Tekeze-Atbara Basin	Tekeze Atbara river	CHIRPS and TRMM have a consistently good agreement with ground rainfall at different spatiotemporal scales	(19)
TRMM 3B42 GSMaP_MVK+ PERSIANN	Performance of High Resolution SatelliteRainfall Products over Data Scarce Parts of Eastern Ethiopia	WABESHEBELLE	Performance of High Resolution Satellite Rainfall Products over Data Scarce Parts of Eastern Ethiopia	(6)
TAMSAT ARCV 2 CMORPH TRMM3B42	Investigation of Errors in Satellite Precipitation Estimates over Ethiopia	Blue Nile	TAMSAT exhibits good skill in detecting rainy events but underestimates precipitation amount, while ARC underestimates both rainfall amount and rainy event frequency	(20)

SREs TAMSAT CHRIPS ARC	Investigation of satellite rainfall estimates	Blue Nile	TAMSAT and CHIRPS estimated the amount of rainfall reasonably good, ARC did not perform satisfactorily SREs perform low	(21)
ARC TAMSTA CHRIP CHRIPS	Validation of the chirps satellite rainfall estimate	Ethiopia and Tanzania	CHIRP/CHIRPS performed better than ARC and TAMSAT both over Ethiopia and Tanzania	(22)
GPCP NOAA-CPC CMAP TRMM-3B43 TAMSAT CMORPH RFE ARC TRMM-3B42 GPCP-1DD	Validation of satellite rainfall products over complex topography	East Africa	From the products compared CMORPH and TAMSAT have shown the best agreement with the reference data. CMORPH has shown superior performance over 1DD and 3B42.	(23)
TMPA, CMORPH, PERSIANN, MSWEP) and ECMWF ERA	Evaluation of High-Resolution Multisatellite and Reanalysis Rainfall Products	Upper Blue Nile	CMORPH exhibits the best accuracy of the wet season MSWEP detects higher percentiles values better than satellite estimate in the wet and poor in the secondary rainy seasons.	(24)

GPCC 7.0 CHIRPS v2.0 PERSIANN-CDR MSWEP 2.0 ARC2	Performance of satellite-based and GPCC 7.0 rainfall products in an extremely data-scarce country.	BLUE NILE	ARC2 performs the best in capturing the variability in the maximum monthly rainfall. Performance from MSWEP 2.0 on the annual scale is better. (PERSIANN-CDR) is mostly (relatively) for median maximum monthly rainfall; GPCC 7.0 (CHIRSPS v2.0) is mostly (partly) suitable as an estimator for the monthly median.	(25)
CHIRPS ARC2 CHIRP ORH RCMs	Evaluation of multiple climate data sources for managing environmental resources	East Africa	CHIRPS, followed by ARC2 and CHIRP, is the best performing rainfall product compared to ORH, individual CHIRPS captures the daily rainfall characteristics well. Compared to CHIRPS, ARC2 showed higher underestimation of the total and daily rainfall. ORH, I-RCM, and RCMs are the worst performing products.	(26)
TAMSAT PERSIAN CDR CMORPH v1.0 CHIRPS TRMM 3B42RT v7 ARC v2	Statistical Evaluation of High Resolution Satellite Precipitation Products	Eastern part of Ethiopia	Results indicated that in terms of rainfall amount estimation, TAMSAT has relatively better capability while for detecting rain event, ARC v2 was found capable in Eastern Ethiopian. All precipitation products underestimate precipitation amount with profound bias level.	(27)

2.7 Hydrological model

Hydrology is principally concerned with the study of the motion of the earth's waters through the hydrologic cycle, and the transport of constituents such as sediment and pollutants in the water as it flows (12). Hydrological modelling is very important for prediction of runoff and soil erosion, and is a major tool for research hydrologists and water resources engineers for planning and management of water resources. Hydrological models can be used to estimate river flows at ungauged sites, fill gaps in incomplete data series or predict future runoff and river flows. The need for hydrological models is increasing both in aspects of coverage and functionality. Also more and more researchers and practitioners require access to hydrological models and in particular model simulation results. Hence, hydrological models need to be more robust, transparent and defensible as they are increasingly relied on to make informed decisions on sharing and managing of limited water resources (13). Distributed hydrological models consider the spatial non-uniformity of hydrological characteristics and processes in the river basin. These models are based on our understanding of the physics of the hydrological processes which control catchment response and use physically based equations to describe these processes. These models can be applied for the study of the effects of land use changes and human intervention on the catchment behavior.

Hydrological models are tools that describe the physical processes controlling the transformation of precipitation to stream flows. There are different hydrological models designed and applied to simulate the rainfall runoff relationship under different temporal and spatial dimensions. The focus of these models is to establish a relationship between various hydrological components such as precipitation, Evapotranspiration, surface runoff, ground water flow and soil water movement (infiltration). Many of these hydrological models describe the canopy interception, evaporation, transpiration, snowmelt, interflow, overland flow, channel flow, unsaturated subsurface flow and saturated subsurface flow. These models range from simple unit hydrograph based models to more complex models that are based on the dynamic flow equations. Simulation programs implementing watershed hydrology and river water quality models are important tools for watershed management for both applied and operational research purposes. A hydrological model represents the water cycle of a drainage basin and studies the response of this basin to climatic and physical conditions. Three different categories of hydrological models can be distinguished: physically process based, empirical and statistically based. Physically process based models are described by mathematically formulated fundamental physical laws, where each basin is represented by a concept; a reservoir for instance. They are useful for inferring the distribution, magnitude, and past, present and future behavior of a process with limited observations.

These equations can relate the changes of water properties across the surface. These physical processes vary both temporally and spatially. They consider the spatial and temporal changes of different factors (14). Physically based distributed watershed models play also a major role in analyzing the impact of land management practices on water, sediment, and agricultural chemical yields in large complex watersheds.

Empirical models are a synthesis and a summary of field or experimental observations. Their fundamental parameters are not compulsory physically related. Empirical models are based on defining important factors through field observation, measurement, experiments and statistical methods**.** They are useful in predicting the hydrology or soil erosion, but are site specific and require long-term data. Empirical models are the result of several years of research data and numerically evaluate the effects of climate, soil properties, topography and crop management.

Statistically based models use many observations to estimate the behavior of watersheds and their interactions. They can be physically or empirically based. In addition to categorizing both soil erosion and hydrological models with respect to the way they are being synthesized, another distinction is the difference between distributed and global models. In global models, the watershed is one single entity and in distributed models, many units represent the variability of hydrological parameters on the surface. Spatial variability is handled by dividing a drainage basin into smaller geographical units, such as sub basins, land cover classes, elevation zones or a combination of them. The hydrological response units (HRUs) represent areas where the modeling simplified and where the hydrological response is supposed to be homogeneous.

In recent years, distributed watershed models are increasingly used to study alternative management strategies in the areas of water resources allocation, flood control, impact of land use change and climate change, and finally environmental pollution control. Many of these models share a common base in their attempt to incorporate the heterogeneity of the watershed and spatial distribution of topography, vegetation, land use, soil characteristics, rainfall and evaporation. Some of the watershed models developed in the last two decades are CREAMS (Chemicals, Runoff, and Erosion from Agricultural Management Systems) (Knisel,, EPIC - Erosion Productivity Impact Calculator (Williams, 1995), AGNPS (Agricultural None Point Source model) (Young et al.,1987), SWAT (Soil and Water Assessment Tool) (Arnold et al., 1998) and HSPF (Hydrologic Simulation Program – Fortran) (Bicknell 2001), ANSWERS (Areal Nonpoint Source Watershed Environmental Response Simulation) (Beasley and Huggins, 1982), EROSION-3D (SCHMIDT, 1995), EUROSEM (European Soil Erosion Model) (Morgan et. al., 1997), WEPP (Water Erosion Prediction Project) (Foster and Lane, 1987), HECHMS (Hydrological Modelling System)etc.

Understanding the rainfall – runoff relation has been a subject of hydrological research for a long time (15). According to study, runoff occurs due to a complex interaction between surface, unsaturated, and saturated flow. In the same time researches in the field of hydrology focused on stream flow simulation processes using hydrological model. Hydrological models are the main tool where all the hydrological processes are combined and simulations are performed to obtain a certain output. A model is a representation of the real world into a conceptual world. Models can be predictive (to obtain a specific answer to a specific question) or investigative (to further understanding hydrological processes) (16). Depending on the aim of the investigation, models can be deterministic, which do not consider randomness (used for forecasting), or stochastic, where the model outputs are at least partially random (used for prediction). Although all the hydrological processes are random, when the variability in the output is small in comparison with the one of the known factors, deterministic models can be used (17). Within the deterministic models, three types of models are distinguished based on spatial discretization. In rainfall-runoff modeling, models are characterized as lumped, semi distributed (White box) models account for spatial variability of topography, geology, soil type and land use within a catchment. These models use grid layers with elements. Within this sub-catchment the characteristics are lumped. Also another classification is known: event models that represent a single runoff event occurring over a period of time from one hour to several days. In general event models tend to be lumped. Considering the spatial scale, these models can range from lumped to distributed models. Based on the objectives of this study Soil and Water Assessment

Tool (SWAT) model was used to simulate stream flow for both in situ dataset and satellite rainfall products.

There are many reason for decision which is important for choosing the right hydrological model for a given problem. These necessity are always project dependent, since every project has its own specific requirements and needs. Besides, some necessity are also user-depended (and therefore subjective). From the various project-dependant selection necessity, there are four common, basic ones that must be always answered (28):

- Required model results important to the project and therefore to be evaluated by the model (Does the model predict the variables required by the project such as long-term sequence of flow?),
- Hydrologic processes that are required to be modeled to estimate the desired results adequately (Is the model capable of simulating single-event or continuous processes?),
- Suitability of input parameter (Can all the inputs required by the model be provided within the time and cost constraints of the project?),
- Does the investment appear to be worthwhile for the objectives of the project?

The reasons for choosing SWAT model for this study are;

- The model simulates many hydrological process in the watersheds
- It is less requirement of input data, and
- It is readily and freely exist.

A major drawback to large area hydrologic modeling of SWAT is the spatial detail required to correctly simulate environmental processes. For example, it is difficult to capture the spatial variability associated with precipitation within a watershed. Another drawback is data files can be difficult to manipulate and can contain several missing records. The model simulations can only be as accurate as the input data. The third limitation is that, the SWAT model doesn't simulate detailed event-based flood.

2.7.1 Description of SWAT model

Soil and Water Assessment tool (SWAT), developed by the United States Department of Agriculture (USDA) – Agricultural Research Service (ARS) in early 1990s (29), is a continuous, semi distributed hydrologic model that runs on a daily time step. Hydrologic response units (HRUs), defined by combinations of land cover and soil combinations, are the computational elements of SWAT. The daily water budget in each HRU is calculated using daily rainfall, runoff, evapotranspiration, percolation, and return due the subsurface and groundwater flow. Flow amount in each HRU is calculated by the SCS curve number method (SCS, 1986).The interface of SWAT model is compatible with ArcGIS that can integrate numerous available geospatial data to accurately represent the characteristics of the watershed. In SWAT model, the impacts of spatial heterogeneity in topography, land use, soil and other watershed characteristics on hydrology are described in subdivisions.

There are two scale levels of subdivisions; the first is that the watershed is divided into a number of sub watersheds based upon drainage areas of the attributes, and the other one is that each sub watershed is further divided in to a number of Hydrologic Response Units (HRUs) based on land use and land cover, soil and slope characteristics.

One of the most merits of SWAT is that it is often important to model watersheds with less monitoring data. For simulation, SWAT needs digital elevation model; land use and land cover map, soil data and climate data of the study area. These data are considered as an input for the analysis of hydrological simulation of surface runoff and groundwater recharge.

SWAT splits hydrological simulations of a watershed in to two major phases: the land phase and the routing phase. The land phase of the hydrological cycle determines the amount of water, sediment, nutrient, and pesticide loadings to the main channel in each sub watershed. While the routing phase controls the movement of water, sediment and agricultural chemicals through the channel network to the watershed outlet. The prior one is modeled in SWAT based on the water balance equation (30)

$$SWt = SWo + \sum_{i=1}^{t}(Rday - Qsurf - Ea - Wsleep - Qgw) \qquad (2.1)$$

Where, SWt is the final soil water content (mm)
SWo is the initial water content (mm)
t is the time (days)
Rday is the amount of precipitation on day i (mm)
Qsurf is the amount of surface runoff on day i (mm)
Ea is the amount of evapotranspiration on day i (mm)
Wsleep is the amount of water entering the vadose zone from the soil profile on day i (mm), and Qgw is the return flow on day i (mm)
The SWAT model simulates eight major components: hydrology, weather, sedimentation, soil temperature, crop growth, nutrients, pesticides, and agricultural management (30). Major hydrologic processes that can be simulated by this model include evapotranspiration, surface runoff, infiltration, percolation, shallow aquifer and deep aquifer flow, and channel routing (29). Stream flow is determined by its components (surface runoff and ground water flow from shallow aquifer). But the brief description of some of the SWAT computation procedures which are considered in this study are presented under the following subsections.

1. Surface runoff

Runoff refers to the part of rainfall that is not lost to interception, infiltration, and evapotranspiration (31). Surface runoff occurs whenever the rate of rainfall is greater than the rate of infiltration. SWAT proposed two methods for estimating the surface runoff: the Soil Conservation Service (SCS) curve number method and the Green and Ampt infiltration method). The Green and Ampt method needs sub-daily time step rainfall which made it difficult to be used for this study due to unavailability of sub-daily rainfall data. We selected the SCS curve number method for this study.

The general equation for the SCS curve number method is expressed by equation

$$Qsur = \frac{(Rday - Ia)^2}{(Rday - Ia + S)} \quad (2.2)$$

defining , Q_{sur} as the accumulated runoff or rainfall excess (mm),
R_{day} as the rainfall depth for the day (mm water),
I_a as initial abstraction which includes surface storage, interception and infiltration prior to runoff (mm water), and
S as retention parameter (mm water).
The retention parameter varies spatially due to changes with land surface features such as soils, land use, slope and management practices. This parameter can also be affected temporally due to changes in soil water content. It is mathematically expressed as:

$$S = 25.4 * (\frac{1000}{\text{CN}} - 10) \quad (2.3)$$

Where, CN is the curve number for the day and its value is the function of land use practice, soil permeability and soil hydrologic group.

The initial abstraction, I_a, is commonly approximated as 0.2S. Therefore

$$Qsur = \frac{(Rday - 0.2S)^2}{(Rday + 0.8S)} \quad (2.4)$$

For the definition of hydrological groups, the model uses the U.S. Natural Resource Conservation Service (NRCS) classification. The classification defines a hydrological group as a group of soils having similar runoff potential under similar storm and land cover conditions. Thus, soils are classified in to four hydrologic groups (A, B, C, and D) based on infiltration which represent high, moderate, slow, and very slow infiltration rates, respectively.

2. Potential evapotranspiration

Potential Evapotranspiration is a common term that include evaporation from the plant (transpiration) and evaporation from the water bodies and soil. Evaporation is the primary mechanism by which water is removed from a watershed. An exact estimation of evapotranspiration is critical in the assessment of water resources and the impact of land use change on these resources.

There are many methods that are adopted to estimate potential evapotranspiration (PET). SWAT offers three methods for PET calculation: Penman-Monteith, Priestley-Taylor, and Hargreaves methods. The methods have various data needs of weather variables. The Penman-Monteith rule needs solar radiation, air temperature, relative humidity and wind speed; while the Priestley-Taylor rule needs solar radiation, air temperature and relative humidity; But, the Hargreaves rule needs air temperature only and therefore, adopted for this study.

3. Ground water flow

To simulate the ground water, SWAT partitions groundwater into two aquifer systems: a shallow, unconfined aquifer which gives return flow to streams in the watershed and a deep, confined aquifer gives return flow to streams outside the watershed (32). In SWAT the water balance for a shallow aquifer is calculated as:

$$AQshi = AQshi - 1 + Wrchrg - Qgw - Wrevap - Wdeep - Wpump.sh \quad (2.5)$$

Representing, $AQ_{sh,i}$ as the amount of water stored in the shallow aquifer on day i(mm),
$AQ_{sh,\ i-1}$ as the amount of water stored in the shallow aquifer on day i-1(mm)
W_{rchrg} as the amount of recharge entering the aquifer on day i (mm)
Q_{gw} as the ground water flow, or base flow, or return flow, into the main channel on day i (mm)
W_{revap} as the amount of water moving in to the soil zone in response to water deficiencies on day i (mm)
W_{deep} as the amount of water percolating from the shallow aquifer in to the deep aquifer on day i (mm), and
$W_{pump,sh}$ as the amount of water removed from the shallow aquifer by pumping on day I (mm)

4. Flow routing phase

Another component of the simulation of the hydrology of a watershed is the routing phase of the hydrologic cycle. It consists of the movement of water, sediment and other constituents (e.g nutrients pesticides) in the stream network. The change in channel dimensions with time due to down cutting and widening is also included. Similar to the case for the overland flow, the rate and velocity of flow is calculated by using the manning‟s equation. The main channels or reaches are assumed to have a trapezoidal shape by the model.
Two methods are available to route the flow in the channel network: the variable storage and Muskingum methods. The variable storage method uses a simple continuity equation in routing the storage volume, whereas the Muskingum routing method models the storage volume in a channel length as a combination of wedge and prism storages. In the latter method, when a flood wave advances into a reach segment, inflow exceeds outflow and a wedge of storage is produced. As the flood wave recedes or retreat, outflow exceeds inflow in the reach segment and a negative wedge is produced. In addition to the wedge storage, the reach segment contains a prism of storage formed by a volume of constant cross-section along the reach length. While calculating the water balance in the channel flow, the transmission and evaporation are also well considered by the model.

The equation of the variable storage routing is given by:

$$\Delta Vstored = Vin - Vout \quad (2.6)$$

2.7.2. SWAT model application worldwide

The SWAT model has good reputation for best use in agricultural watersheds and its uses have been successfully calibrated and validated in many areas of the USA and other

continents (33). The studies indicated that the SWAT model is capable in simulating hydrological process and erosion/sediment yield from complex and data poor watersheds with reasonable model performance statistical values. (29) Modeled the hydrology of the 3050 km^2 Sondu River basin in Kenya using land use, soil and elevation data with limited spatial resolution (1 - 10 km^2). The objective was to assess impacts of land use changes as a result of changes to intensive dairy farming. The simulation Nash-Sutcliffe efficiency (NSE) coefficient of < 0.1 was attributed to inadequate rainfall and other model input data. The use of one rain gauge station situated at the upper end of the catchment was not representative of the basin.

In modeling the hydrology of the Mitano River basin in Uganda, Kingston and Taylor (2010) used the gridded 0.5^o CRUTS3.0 database as the climatic input. Although there was a good agreement between observed and simulated monthly means and flow duration curves, the model performance after calibration was poor, resulting in an NSE of -0.09. According to the author, the poor performance in the hydrological modeling was attributed to "model observation divergences with the calibration period that are simply too large to be resolved by an auto-calibration routine".

SWAT has gained worldwide recognition as a hearty interdisciplinary watershed modeling tool as proved by universal SWAT conferences, hundreds of SWAT- related papers presented at numerous other scientific meetings, and numerous articles published in peer-reviewed journals (34).

To design and construct structures, like, dams, there is a need to determine the amount of steamflow. For un-gauged watersheds, in Iran it is necessary to calculate their inflows through hydrological simulation. SWAT is one of the models that is widely used for such purposes. For computing the stream flow, the model requires weather data, as well as physiographic data related to the basin surface, such as curve number and roughness coefficient. Besides, the strike of each input data on the computation of water flow has also been evaluated. Specifically, with an advance of 13.43 percent in the curve number and 0.15 in the over land roughness coefficient of the basin the simulated value of the average monthly discharge 2.52 and 0.01% closer to the observed average flow value. Using all the climatic parameters, the average mean flow of the period increased with an error of 14.32 percent (35)

The Study by (36) entitled as Runoff simulation by SWAT model using high-resolution gridded precipitation in the upper Heihe River Basin, Northeastern Tibetan Plateau, and come up with valid result. The SWAT model comprehend at monthly streamflow simulation compared with gauged runoff from 2000 to 2014; the coefficients of determination are higher than 0.71, the Nash–Sutcliffe efficiencies are above 0.76 and the t bias are controlled within ±15%. The meadow and limited vegetation are the major water yield landscapes, and the elevation band at 3,500 m to 4,500 m is the major water yield area in this basin. Rainfall and evapotranspiration shows a slightly increasing trend, whereas water yield and soil water content presented a slightly decreasing trend. This result indicates that the high-resolution precipitation data well depicts its spatial heterogeneity, and scale transformation significantly promotes the application of the

distributed hydrological model in inland river basins. The variation of water balance components can be quantified to give references for the integrated assessment and management of basin water resources in data scarce areas.

2.7.3. SWAT model application in Ethiopia

The SWAT model application was calibrated and validated in some parts of Ethiopia, frequently in Blue Nile basin (37).used SWAT to model the hydrological water balance of the Lake Tana basin in Ethiopia with the target of testing the suitability of the SWAT model for streamflow simulation. These authors calibrated and validated on four tributaries of Lake Tana using SUFI-2, GLUE and ParaSol algorithms. This study shows that the SWAT model was more sensitive to HRU definition thresholds than to sub-basin discretization. Besides, the study shows that more than 60% of the observed river discharge falls within the 95% confidence bounds.

As (38) used the SWAT model performed to predict the Legedadi reservoir sedimentation. According to this study, the SWAT model performed very well in computing sediment yield to the Legedadi reservoir. The study further put that the model proved to be worthwhile in capturing the process of stream flow and sediment transport of the watershed of the Legedadi reservoir.

In addition to the above, (39) assessed surface runoff generation and soil erosion rates for a small watershed in the Awash River basin of Ethiopia using the SWAT model. Comparing monthly predicted runoff against the measured values, the study demonstrates that distribution of observed and simulated runoff was quite uniform throughout the simulation period. The study presents a high correlation value of 0.831. It further reports a NSE of 0.789 to demonstrate that the model was able to generate monthly runoff close to the observed. The literature reviewed and presented above showed that SWAT is capable of simulating hydrological and soil erosion process with reasonable accuracy and can be applied to large and complex watersheds.

The study Conducted by (40) targets to evaluate the performance of the ArcSWAT model in simulating stream flow for the Weyib river catchment in Ethiopia. Two techniques that are widely used in models evaluating, namely quantitative statistics (four very common statistical indices) and graphical method (hydrograph analysis technique), were applied to estimate the performance of the ArcSWAT model in this study. the results of calibration and validation of the model was R2 of 0.95, NSE of 0.92, RSR of 0.26 and Pbias of 1.31 for model calibration while R2 of 0.97, NSE of 0.95, RSR of 0.20 and Pbias of 2.48 for the validation stage. As of the monthly model demonstration ratings, for all the four evaluation criteria (R2, NSE, RSR and Pbias), the model performed very well during both calibration and validation periods.

Study on SWAT-Modeling of the Impact of future Climate Change on the Hydrology and the Water Resources in the Upper Blue Nile River Basin, Ethiopia (41). The SWAT-model was calibrated and validated on flow observed at the Eldiem gauging station) at the baseline period. Model performance is evaluated using standard performance parameters, i.e. PBIAS, NS and R2.

All these statistical indexes shows a good adjustment of the modeled to the observed streamflow for both the calibration and validation period.

The study conducted by (4) on the Assessment of High-Resolution Satellite precipitation Products through Stream flow Simulation in a Modeling of a Small Mountainous Watershed in Ethiopia, using SWAT model selecting CMORPH, TRMM, TMPA, PERSIANN Correlation was high between CMORPH and 3B42RTmonthly estimates (R=0.97) and lower between the other satellite products. At the monthly time scale, rain gauge had the highest correlation with CMORPH and 3B42RT (R = 0.83), modest correlation with PERSIANN (R = 0.72), and poor relation with 3B42 (R = 0.54). Compared with rain gauge values, all satellite rainfall products underestimated total precipitation: CMORPH and 3B42RT by 23%–25%, PERSIANN by 51%, and 3B42 by 61%. The region exhibits a well-defined rainy season, from March to October, with peaks in June and July. The seasonal variability of precipitation observed by the metrological station was better captured by CMORPH and 3B42RT as compared to PERSIANN and 3B42.

As (42), Model to overcome this challenge, the Climate Forecast System Reanalysis (CFSR) global weather data was evaluated and compared with the limited conventional weather data available in the Upper Awash Basin. The Soil and Water Assessment Tool model was utilized to compare the performance of the two weather datasets at simulating monthly stream flow. Calibration, validation, and uncertainty analysis, was done by the sequential uncertainty fitting algorithm. The model performance statistics indicate that the CFSR global weather data performed well to the in situ weather data for simulating the observed stream flow at Melka Kunture. At Keleta, where the rain gauge data is scarce, the CFSR performed better.

The performance and applicability of the Soil and Water Assessment Tool (SWAT) model in analyzing the character of hydrologic parameters on the stream flow variability and computation of monthly and seasonal water yield at the outlet of Shaya mountainous watershed (43), specify that the calibrated SWAT model fulfill better for simulation of monthly stream flow.

2.8 Bias correction Methods

Significant advance has been realize in recent years in the elaboration and accessibility of real-time satellite precipitation products (SPPs). However, SPPs still show important biases that need to be corrected before the rainfall calculate can be necessity for any hydrologic relevancy such as real-time or seasonal prediction. These biases are due to the incorrect estimation of climate variables and their temporal variations, or the incorrect detection of rainfall events. One indicator of the latter is the simulation of too many days of low rainfall intensity (< 1 mm), an appearance assumed as the drizzle effect or drizzling. Biases can rely highly on elevation, aspect, latitude, climate, and rain-showing mechanisms thus it is important to perform location-specific and in some cases season-specific bias corrections. Numerous bias correction methods, starting from simple scaling techniques to the more sophisticated distribution mapping techniques, are developed to correct biased satellite rainfall outputs (44). Linear scaling, local intensity scaling, power transformation, distribution mapping and quantile mapping are among the bias correction methods applied for many studies yet. For temperature correction methods including linear scaling, variance scaling and distribution mapping are used for many studies. Among different types bias correction methods five of them are described below.

2.8.1 Linear scaling (LS) of precipitation and temperature

The LS method endeavor to completely agree the monthly mean of corrected values with that of observed ones (45). It operates with monthly correctaion values based on the differences between observed and raw data (raw RCM simulated data in this case). Precipitation is typically corrected with a multiplier and temperature with an additive term on a monthly basis.

$$Pd,cor = Pd,raw * (\frac{\mu(Pm,obs)}{\mu(Pm\ raw)}) \quad (2.7)$$

$$Tcor,m\ d = T\text{raw m d} + \mu(\text{Tobs m}) - \mu(\text{Traw m}) \quad (2.8)$$

Where Pcor;m;d and Tcor;m;d are corrected precipitation and temperature on the dth day of mth month, and Praw;m;d and Traw;m;d are the raw precipitation and temperature on the dth day of mth month. μ represents the expectation operator.

2.8.2 Local intensity scaling of precipitation

The Local intensity scaling method (46) improves the wet-day frequencies and intensities and can completely correct the raw data which have too many drizzle days (days with short precipitation). It normally involves two steps: firstly, a wet threshold for the mth month Pthres;m is determined from the raw precipitation series to ensure that the threshold exceedance matches the wet-day prevalence of the observation; next, a scaling factor

$$Sm = \frac{\mu(\text{Pobs;m;d/Pobs;m;d>0})}{\mu(_{\text{Praw}}\text{;m;d/Praw;m;d>}P\text{thres;m})} \quad (2.9)$$

Is computed and applied to ensure that the mean of the impoved precipitation is equal to that of the observed precipitation:

$$\text{Pcor; m; d} = \begin{cases} 0 \\ \text{Praw; m; d } *_{\text{Sm}} \end{cases} \text{ if Praw; m; d } < P\text{thres; m} \quad (2.10)$$

2.8.3 Power transformation (PT) of precipitation

The LS and LOCI account for the bias in the mean precipitation, it does not correct biases in the variance. The Power transformation method uses an exponential form to further improve the standard deviation of precipitation series. Since Power transformation has the limitation in adjusting the wet-day probability (45), the Local intensity scaling method is applied to adjust precipitation prior to the improvement by Power transformation method. Therefore, to implement this Power transiformation method, firstly, we estimate bm, which minimizes

$$\text{f (bm)} = \frac{\sigma(\text{Pobs;m})}{\mu(\text{Pobs;m})} - \frac{\sigma(P^{bm}LOCI;m)}{\mu(P^{bm}LOCI;m)} \quad (2.11)$$

Where bm is the exponent for the mth month, σ represents the standard deviation operator, and P Local intensity scaling;m is the Local intensity scaling corrected precipitation in the mth month. If bm is larger than 1, it indicates that the Local intensity scaling -corrected precipitation underestimates its coefficient of variance in month m.

The corrected precipitation series are obtained based on the Local intensity scaling corrected precipitation Pcor;m;d

$$Sm = \frac{\mu(\text{Pobs;m})}{\mu(P^{bm}LOCI;m)} \quad (2.12)$$

$$Pcor; m; d = Sm * P^{bm} LOCI; m; d \quad (2.13)$$

2.8.4 Variance scaling of temperature

The Power Transformation is an effective method to correct both the mean and variance of precipitation, but it cannot be used to correct temperature time series, as temperature is known to be approximately normally distributed. The Variance scaling method was developed to correct both the mean and variance of normally distributed variables such as temperature (46). Temperature is normally corrected using the Variance scaling method.

$$T_{cor;\, m;\, d} = \left[\left[T_{raw;\, m;\, d} - \mu(T_{raw;\, m})\right] * \frac{\sigma(T_{obs;m})}{\sigma(T_{raw;m})} + \mu(T_{obs;\, m}) \quad (2.14)$$

2.8.5 Quantile mapping (QM) of precipitation

The Quantile Mapping is a non-parametric bias correction mechanism and is generally applied for all options distributions of precipitation without any assumption on precipitation distribution. This approach originates from the empirical transformation and was correctly implemented in the bias correction of simulated rainfall. It can effectively correct bias in the mean, standard deviation and wet-day frequency as well as quantiles (45).

For rainfall, the bias correction of precipitation using Quantile Mapping can be expressed in terms of the empirical CDF (ecdf) and its inverse ($ecdf^{-1}$)

$$P_{cor;\, m;\, d} = ecdf^{-1} obs; m(ecdfraw(Praw; m; d)) \quad (2.15)$$

3.0 MATERIALS and METHODS

3.1 Description of the Study Area

3.1.1 Location

Genale Dawa river basin lies in the southern part of Ethiopia, covering parts of Oromia, SNNP, and Somali regions. Geographically located between 3^0 30' and 7^0 20' North latitude and $37^0$05' and 43^0 20' East longitude. The basin covers an area of 172889 km^2. It is the third-largest river basin, after Wabi Shebelle and Abbay river basins. Neighboring river basins are the Wabi Shebelle to the north and east, Rift Valley basin to the west. Genale Dawa river basin have very scarce metrological station and Mountainous topography and provided as area where satellite rainfall products are beneficiary

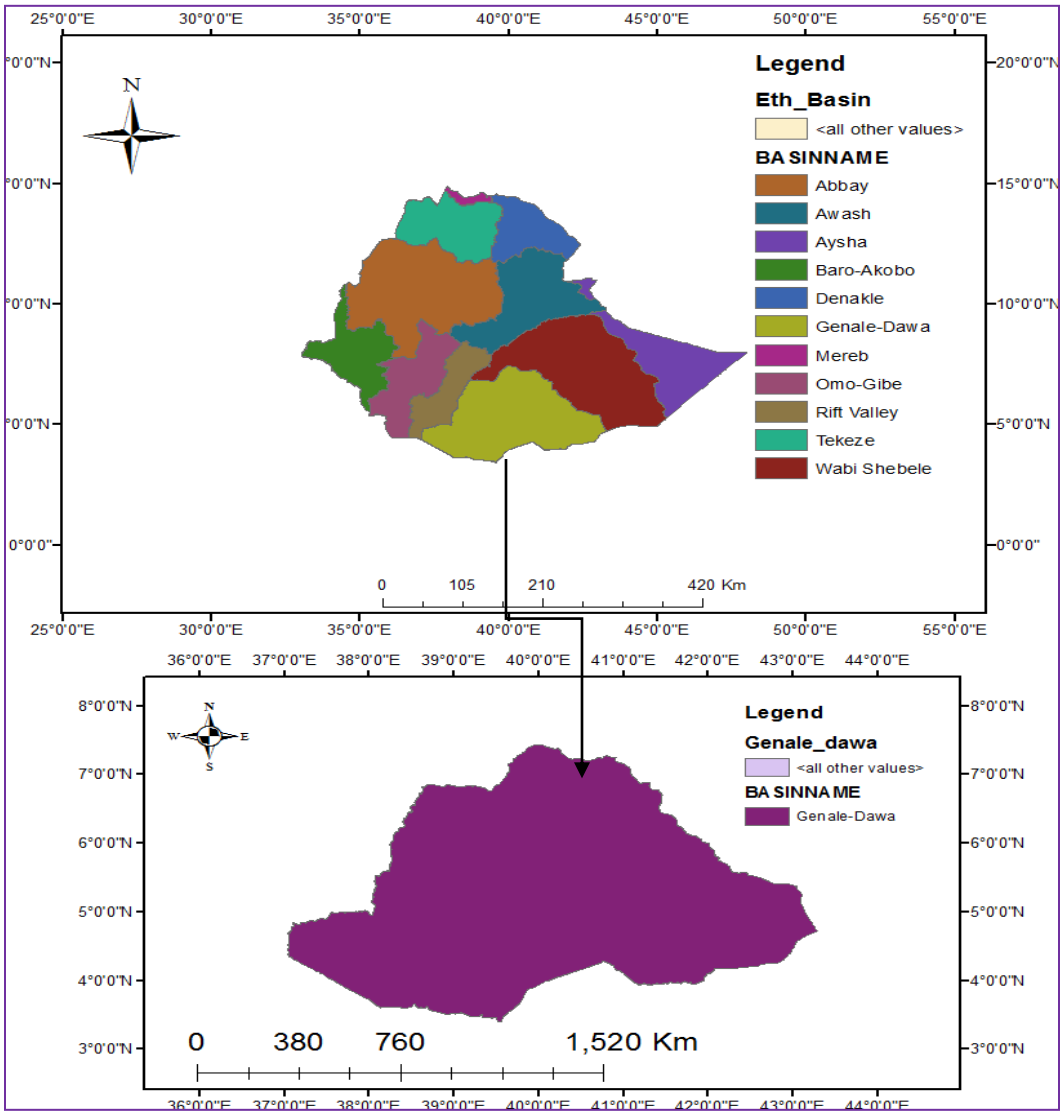

Figure 3-1 Study area map

3.1.2 Climate and Hydrology

The climate of the country is mainly controlled by the seasonal migration of the Inter-tropical Convergence Zone (ITCZ), which is conditioned by the convergence of trade winds of the northern and southern hemisphere and the associated atmospheric circulation. It is also highly influenced, regionally and locally, by complex topography of the country. The easterly and southeasterly moist air currents ascend over the highlands in spring, produce the main rainy season in southeastern Ethiopia in general, and in Genale Dawa basin in particular and bring "small rains" of spring (March to May) to most parts of the country. Southeast (Genale Dawa river basin), therefore, gets its first maxima rainfall during spring and receives the year's secondary maxima rainfall during autumn from the Indian Ocean easterlies. While the basin receives little rainfall in summer compared to spring (March to May) and autumn (September to November) due to the case that the Southerly Indian Ocean air currents lie in the lee side of the highlands in summer and Atlantic westerly's reach the southeastern lowlands (Genale Dawa) after losing their moisture on the highlands to the west.

In general, the Genale Dawa river basin climatic zone comprises (Lemma, 1996):

- Hot arid climate to the south-eastern region along the Somalia border and border to the Wabi-Shebelle basin.
- Hot Semi-arid in the lower central zone of the basin and south-west region.
- The tropical rainy climate in the extreme south and high central basin areas.
- The warm temperate climate in the mid-western area and boundary divide.
- The warm temperate rainy climate in the Sidamo Mountains and intermediate zone south of the Bale Mountains.
- The cool highland climate at the highest elevations in the Bale Mountains.

3.2 Methodology

The general methodology for the study can be described by the following flow chart;

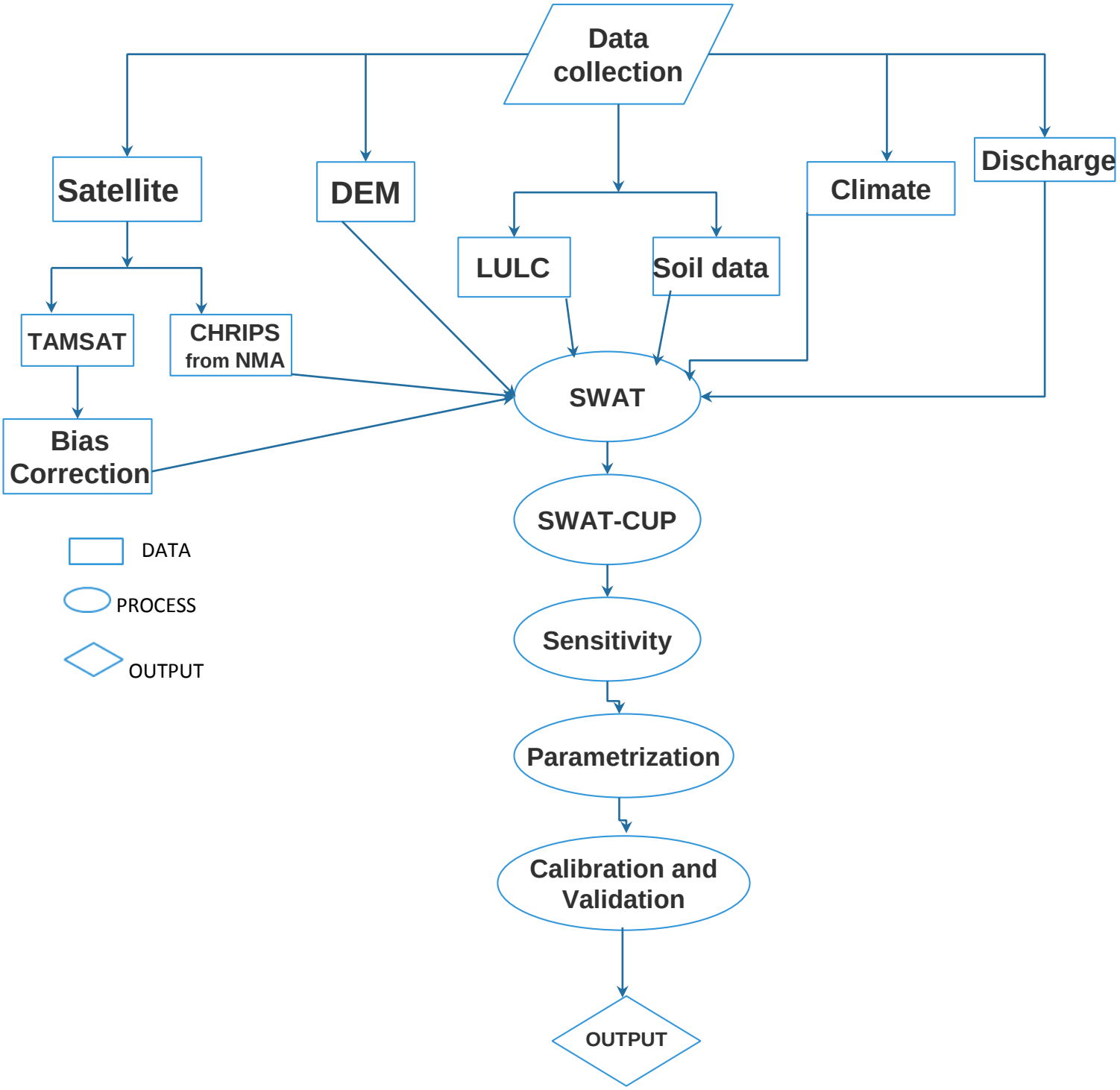

Figure 3-2 Methodology

3.3 Dataset and Data Sources for SWAT Model

3.3.1 Digital Elevation Model

The digital elevation model ASTER DEM was obtained from NASA (National Aeronautics and Space Administration) (2015). It is a product of the Ministry of Economy, Trade, and Industry of Japan and NASA. The DEM (see Fig. 3-3) was used to delineate the watershed and the drainage patterns of the surface area analysis. Sub-basin parameters such as slope gradient, slope length of the terrain, and the stream network characteristics such as channel slope, length, and width were derived from DEM. The resolution of DEM used is 30 m. It is necessary for the stream network processing in SWAT. The calculations establishing the river system are included in the Arc SWAT procedure facilitating the application. They are based on the functions Fill, Flow Direction and Flow Accumulation included in Arc Map Hydrology toolbox from the Arc GIS program. Further, the sub-basins are generated. In total there were 18 sub-basins established for Genale Dawa River basin based on their homogeneity property. The basin has Minimum Elevation and a maximum elevation of 88m and 4389m respectively.

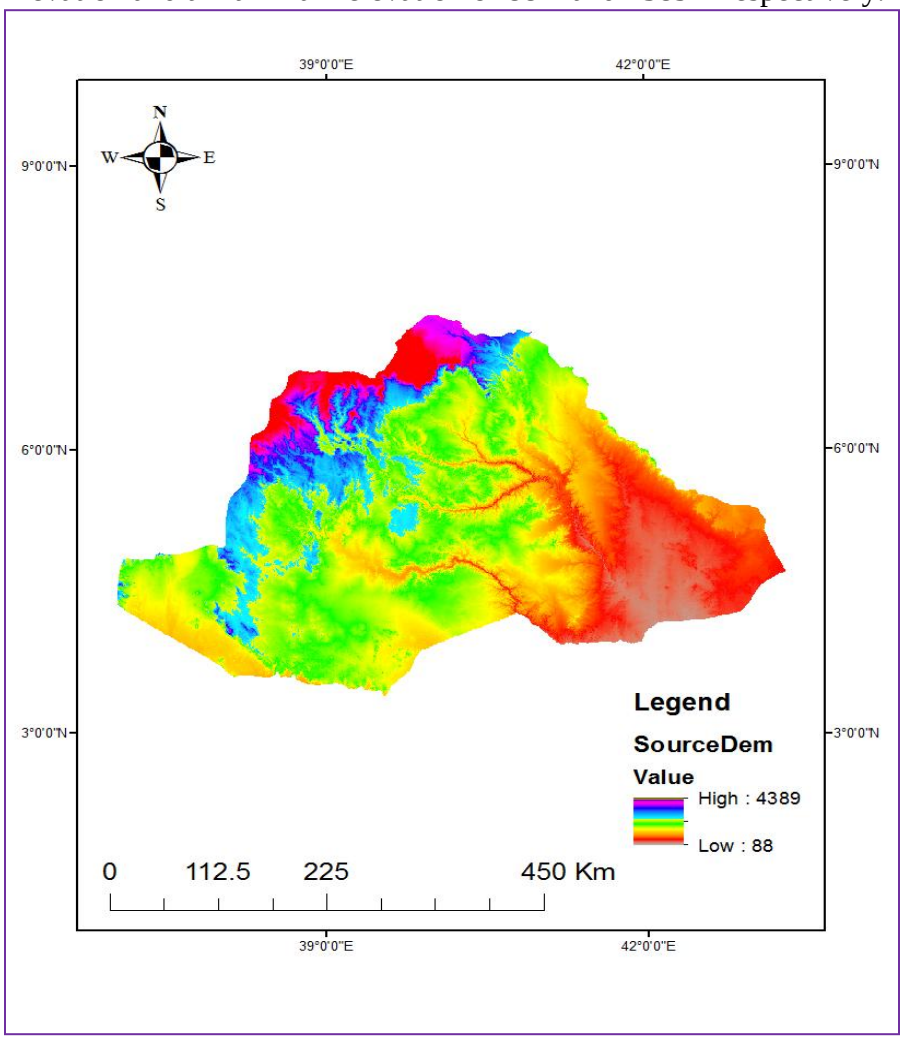

Figure 3-3 Digital Elevation Model (Source: ASTER DEM)

3.3.2. Soil map and soil properties

Different types of soil texture and physical-chemical properties are required for SWAT simulations. These data were obtained from various sources. Soil map and major soil Physio-chemical properties for the Genale Dawa river basin was obtained from Water Land Resource Center, Addis Ababa University (WLRC). However, several properties like moisture bulk density, saturated hydraulic conductivity, percent clay content, percent silt content and percentage sand content of the soil which are required by SWAT model were not incorporated. Due to this deficient information, additional data were substantiated from another source like 'soil geo-database of Ethiopia' prepared by (Belete B, 2013).

Table 3-1 Major soil distribution within Genale Dawa river basin

S no	SNAM	SOIL TYPE	HYDGRP	AREA(KM^2)	Percentage of the area Covered
1	ACha	HaplicAcrisols	A	281.43	0.16
2	AR	ARENOSOLS	A	9824.35	5.68
3	CLha	HaplicCalcisols	D	17497.51	10.12
4	Cmca	CalcaricCambisols	D	16400.88	9.50
5	Cmdy	DystricCambisols	C	5693.40	3.30
6	Cmeu	EutricCambisols	D	9588.21	5.54
7	CM	CAMBISOLS	C	1109.56	0.64
8	CMcr	Chromic Cambisols	C	27800.63	16.1
9	FLca	CalcaricFluvisols	D	6178.63	3.57
10	FLeu	EutricFluvisols	A	1488.05	0.86
11	GL	GLEYSOLS	B	84.10	0.05
12	LP	LIPTOSOLS	A	22553.64	13.04
13	LVha	HaplicLuvisols	B	1591.56	0.92
14	LVvr	VerticLuvisols	D	1497.75	0.86
15	LVcr	Chromic Luvisols	A	17643.10	10.20
16	NT	NITISOLS	C	3603.66	2.10

17	NTro	RhodicNitisols	D	8938	5.17
18	RG	REGOSOLS	D	3581	2.1
19	SCha	HaplicSolonchaks	D	504.64	0.3
20	SCcc	Chromic Solonchaks	C	1902.11	1.1
21	SNcc	SOLONETZ	D	2833.76	1.64
22	VR	VERTISOLS	A	4933.2	2.85
23	VRcc	CalcaricVertisols	A	4380	2.53
24	LavaFlow	LavaFlow	B	207	0.12
25	ANvi	VerticAndosols	B	71.16	0.04
26	VRpe	PetrivVertisols	D	928.4	0.54
27	LPli	Lithic Liptosols	D	1772.72	1.03
Total				172888.6	100

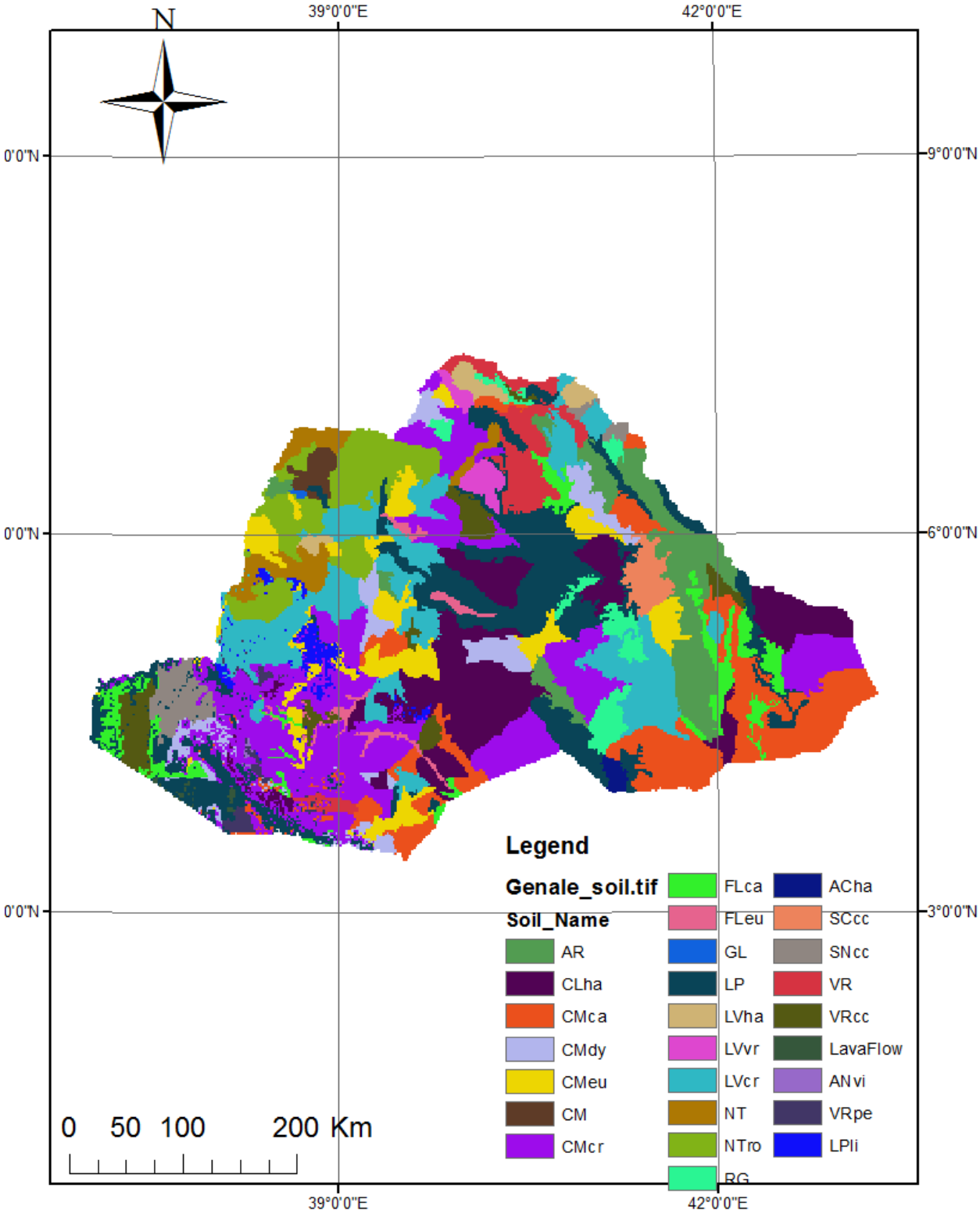

Figure 3-4 Soil distribution map of Genale Dawa River basin (*Soil geo-database of Ethiopia prepared by (Belete B. 2013)*

3.3.3 Land- use land covers maps

Land use land cover (LULC) is one of the furthermost significant spatial input data by SWAT model that disturb water runoff, evapotranspiration, surface erosion and other hydrological execution in a given basin. Spatial distribution and specific land use parameters were required for modeling. SWAT has predefined land uses identified by four-letter codes and it uses these codes to link land use maps to SWAT land-use databases in the GIS interface. Hence, while preparing the lookup table, the land use types were made compatible with the input needs of the model. The classified land use map and its attribute were adjusted to the SWAT model requirement format and database. The LULC map and datasets were acquired from Water Land Resource Center, Addis Ababa University (WLRC). It was developed during 2016 having 30mx30m resolution

Table 3-2 Land use/cover classification within Genale Dawa river basin

S No	LAND USE CODE	LANDUSE TYPE	AREA (Km^2)	Percentage of the area Covered
1	FRSE	Forest	11609.68	6.7
2	FRSD	Woodland	70653.57	40.87
3	RNGB	Shrub/Bush	55004.67	31.81
4	AGRR	Cropland	14229.64	8.23
5	RNGE	Grassland	17738.3	10.26
6	BARR	Barrenland	2584.80	1.5
7	WETL	Wetland	44.7	0.026
8	WATR	Water body	7	0.004
9	FRST	Afroalpine	814.67	0.47
10	URMD	Settlements	201.58	0.12
TOTAL			172888.6	100

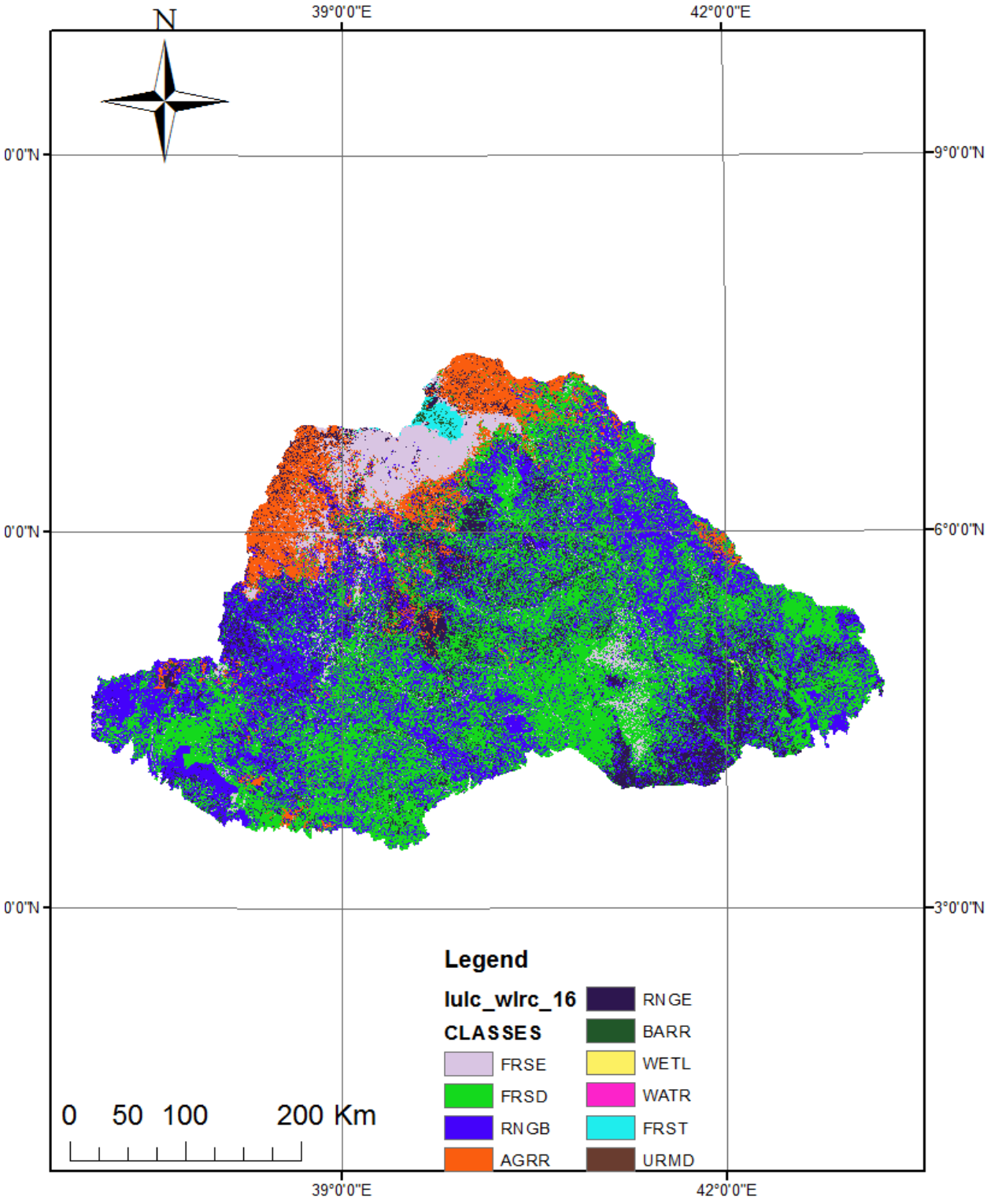

Figure 3-5 Land use land cover map of Genale Dawa river basin (Source: Water Land Resource Center, Addis Ababa University (WLRC), 2016)

3.3.4 Weather data

Weather data are among the main demanding input data for the SWAT simulation. The weather input data required for SWAT simulation includes daily data of Precipitation, maximum and minimum temperature, relative humidity, wind speed, and solar radiation. These were obtained from the Ethiopian National Meteorological Agency. The weather data used were represented from six stations inside Genale Dawa River basin. The climatic data used for this study covers 22 years from January 1996 to December 2017. However, missing values were identified in some of the climatic variables. These values were assigned with no data code (-99) which then filled by the weather generator embodied in the SWAT model. Finally, the weather data were prepared in Text format with lookup tables as required by the model.

Table 3-3 ***List of Selected weather monitoring Stations and Available data sets for rainfall and climatic variables***

No	Station	Latitude	Longitude	Elevation	Data coverage
1	Robe	7.13	40.05	2480	1996-2017
2	Delomena	6.41	39.83	1313	1997-2017
3	Ginir	7.13	40.7	1750	1996-2017
4	KibreMengist	5.87	38.97	1680	1996-2017
5	Moyale	3.55	39.03	1166	1996-2017
6	Filtu	5.11	40.64	1225	1987-1999
7	Bore	6.35	38.61	2712	2000-2017
8	Negele	5.41	39.56	1544	1996-2003
9	Finchuwa	5.4	38.27	1634	1996-2017

Station	Types of data collected	Time step
Robe	Precipitation, temperature, humidity, sunshine hours and wind speed	Daily
Delomena	Precipitation, temperature, humidity, sunshine hours and wind speed	Daily
Ginir	Precipitation, temperature, humidity, sunshine hours and wind speed	Daily
KibreMengist	Precipitation, temperature, humidity, and wind speed	Daily
Moyale	Precipitation, temperature, humidity, sunshine hours and wind speed	Daily
Filtu	Precipitation, temperature, humidity, sunshine hours and wind speed	Daily
Bore	Precipitation	Daily
Negele	Precipitation, temperature, humidity, sunshine hours and wind speed	Daily
Finchuwa	Precipitation	Daily

3.3.5 Satellite rainfall products

In this study two high-resolution, satellite-based rainfall estimations (SREs) were evaluated, which estimates precipitation at the same spatial and temporal resolution. The SREs considered are (i) Climate Hazards Group Infrared Precipitation with Stations (CHIRPS) with a relatively high spatial and temporal resolution (i.e., 5 km resolution at daily temporal scale) and quasi-global coverage. This data was resampled to 4Km and bias-corrected by Ethiopian National Metrological Agency. (ii) Tropical Applications of Meteorology using SATellite data and ground-based observations (TAMSAT) which was established by the University of Reading in 1977. TAMSAT produces daily rainfall estimates for all of Africa at 4km resolution. The satellite data used for this study covers 35 years from January 1983 to December 2017.

Table 3-4 Description of satellite rainfall products

Product	**Main principles data**	**Spatial Resolution**	**Spatial coverage**	**Rainfall Gauge**	**Minimum Time steps interval (temporal resolution)**	**Producer**	**Period of availability**
TAMSAT	Meteosat TIR	0.0375^{o}(4km)	Africa	Yes	Daily	University of Reading	1983-Present
CHIRPS	IR and Gauge	0.05^{o} (5km)	Global	Yes	Daily	USGS	1983-Present

3.3.6 Hydrological data

In rainfall-runoff modeling, the streamflow data (available throughout the entire year) was used for calibration and validation of the results obtained from model simulation. The daily stream flow data (1998 - 2007) is a relatively long period and were collected from the Ministry of Water, Irrigation, and Energy of Ethiopia for the Genale Dawa river basin.

Table 3-5 ***Basic Hydrometric monitoring description for Genale Dawa River Basin***

		CALIBRATION	VALIDATIPON
No	Station Name	Years	Years
1	Dawa at Melka Guba	1998-2003	2004-2007
2	Welmel at Melka Amana	1998-2003	2004-2007
3	Dimtu Nr Bore	1998-2003	2004-2007
4	Genale at Halwen	1998-2003	2004-2007

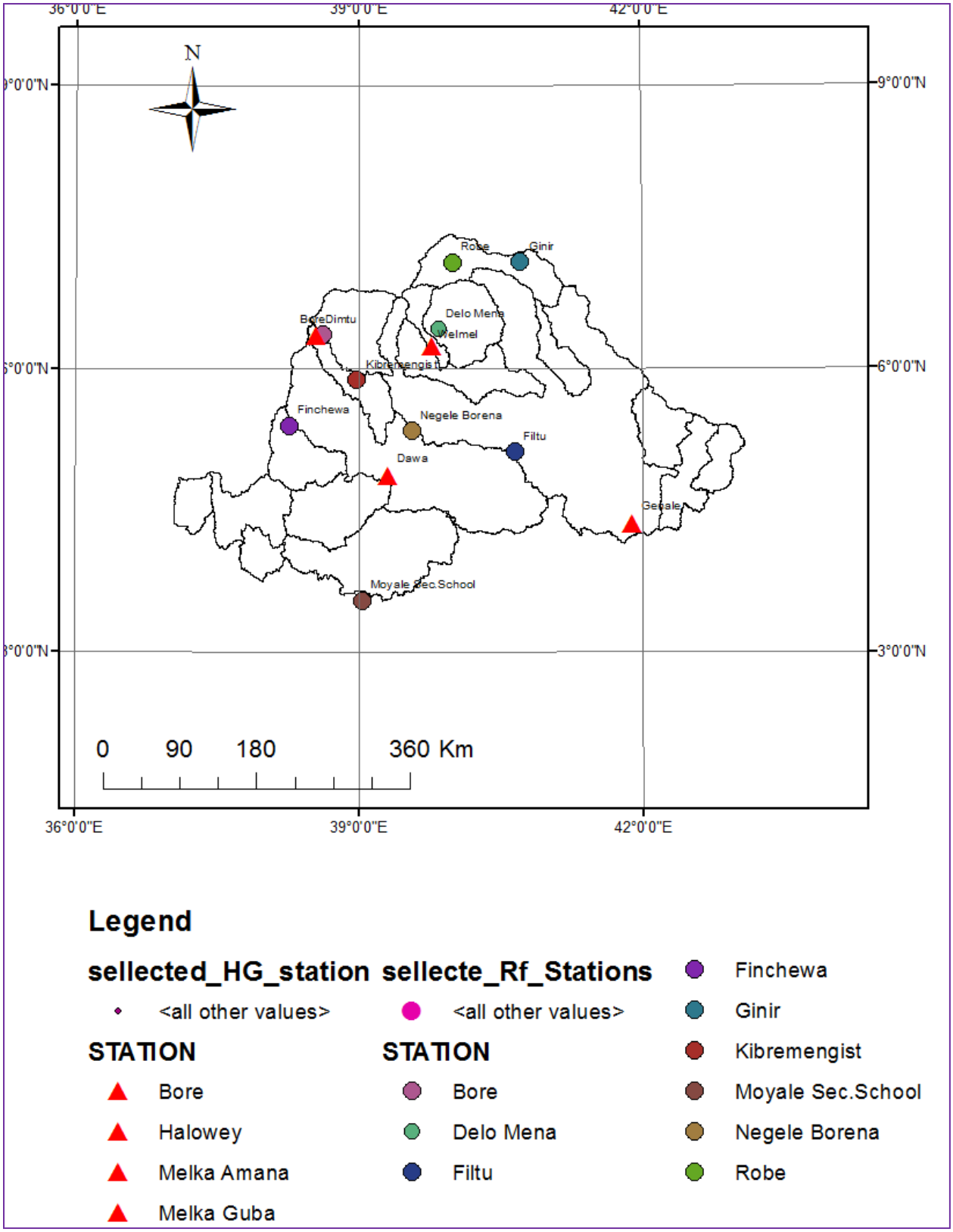

Figure 3-6 Selected metrological and hydrologic gauging stations

3.3.7 Weather generator

In developing countries, there is a lack of a full and realistic long period of climatic data. Therefore, the weather generator solves this problem by generating data from the observed one (47). The weather generator model integrated with SWAT used to fill missing values in measured records and also to simulate the data if the simulation option is selected. The Model requires the daily values of all climatic variables from measured data or generated from values using monthly average data over a number of years. The WGEN was provided with all the necessary statistical information from the meteorological records of the watershed to fill the missing portion properly. After loading this WGEN parameter and location table, the daily meteorological data (daily precipitation, daily minimum, and maximum air temperature, relative humidity, sunshine hour and wind speed) with the missing data filled with a missing data identifier of -99 and including the corresponding location table prepared according to the SWAT format were loaded to the model. The Metrologic stations which were selected in the study are Robe, Delomena, Ginir, Moyale, KibreMengist and Bore station selected to be the principal station for the weather generator. The SWAT Model contains a weather generator model called WGEN (48). It is used in SWAT model to generate climatic data or to fill missing data using monthly statistics which is calculated from existing daily data. From the values of weather generator parameters, the weather generator first separately generates precipitation for the day. The maximum temperature, minimum temperature, solar radiation, and relative humidity are then generated. Lastly, wind speed is generated independently.

To generate the data, weather parameters were developed by using the weather parameter calculator pcpSTAT and dew point temperature calculator dew02. The pcpSTAT program calculates the monthly daily average and standard deviation as well as the probability of wet and dry days, skew coefficient, and the average number of precipitation days in the month by reading of the daily values of the variables. Average daily dew point temperature was calculated using the dew point calculator (dew02) from daily maximum temperature, daily minimum temperature, and average relative humidity

3.4 Software used in the study

In this study different software have been used for different purposes as described below in the

Table 3-6 Details of all software used in the study works

No	Software	Purposes	Website
1	ArcGIS 10.7	To prepare study the area map To prepare Slope, LULC, soil map	Student trial licenses, sources from AAU FTP portal
2	ArcSWAT2012	To delineate watershed To simulate stream flow	https://swat.tamu.edu/software/SWAT/
3	SWAT -CUP2019	For sensitivity analysis To calibrate Stream flow To validate stream flow	https://swat.tamu.edu/software/SWAT-CUP/
4	XLSTAT	To test homogeneity of data To test Trend of data	www.xlstat.com
5	CMhyd	For bias correction of TAMSAT rainfall product with ground data	https://swat.tamu.edu/software/cmhyd/
6	PcpSTAT	Calculates the daily average and standard deviation as well as probability of wet and dry days, skew coefficient, and average number of precipitation days in the month by reading of the daily values of the variables during preparation of WGEN.	https://swat.tamu.edu/software/PcpSTAT/
7	dew02	To calculate Average daily dew point temperature from daily maximum temperature, daily minimum temperature and average relative humidity during preparation of WGEN.	https://swat.tamu.edu/software/dew02/
8	Data tool	To calculate statistical indexes during bias correction and comparison of satellite rainfall product with ground rainfall.	https://agrimetsoft/software/DT/
9	Netcdf- Extractor	To extract Netcdf satellite data to point data	https://agrimetsoft/software/Netcdf-extract/

3.5 Checking consistency, homogeneity and trend of selected rainfall station

3.5.1 Checking the Consistency of data at rain gauge stations

Even though, it is difficult to carry out direct analysis to detect possible errors of climatic data; it is possible to check the data consistency of individual stations with some reference stations. The data qualities of stations with regard to possible temporal variations have been checked by the double mass curve. As a result, the stations are found to be consistent. Robe (a synoptic station with best data record) was taken as a reference station to check the data consistency of other neighboring stations. Robe station was selected as the reference station because this station was

found with the best data consistency using a double mass curve considering the annual cumulative precipitation of all stations.

The cumulative precipitation values of doubtful station, X say ΣPx, and cumulative values of group average say ΣPav are then plotted on a graph paper. Px' (corrected precipitation) and given by the following formula.

$$Px' = Px\frac{M'}{M} \qquad (3\text{-}1)$$

Where, Px'= corrected precipitation at station x

Px= original recorded precipitation at station x

M'= corrected slope of double mass curve

M= original slope of double mass curve

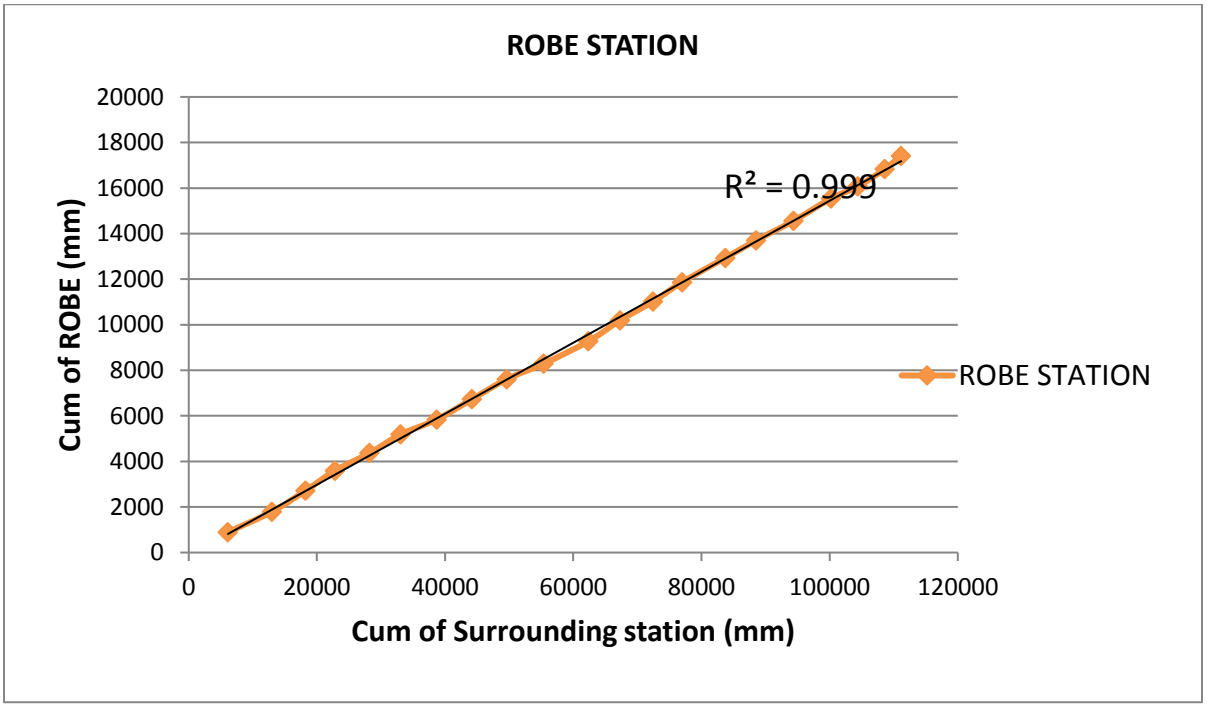

Figure 3-7 *Double mass curve for consistency check*

3.5.2 Homogeneity Tests for rainfall Time series

Reliable data which are free from artificial trends or changes are important in any research. Data reliability was checked by applying the homogeneity test. In this case, XLSTAT is used for the homogeneity test. Use this tool to determine using one of four selected tests (Pettitt, Buishand,

SNHT, or von Neumann), if we may understand a series is homogeneous over time, or if there is a time at which a change occurs.

Homogeneity tests imply an abundant number of tests for which the zero hypothesis is that a time series is homogenous between two given periods. The differences of the tests comes from the reality that there are many possible choices of hypotheses: change in distribution, changes in average (one or more times) or presence of a trend. Among the proposed tests, SNHT test is chosen.

The Standard Normal Homogeneity Test was developed by Alexanderson (1986) to determine a change in a series of climate data. The test is applicable to a series of ratios that compare the observations of a measuring station with the typical of several stations. The ratios are then standardized. The series of Yi corresponds here to the standardized ratios. The zero and alternative hypotheses are determined whether they follow the distribution.

H0: The T variables Xi follow an N (0, 1) distribution. Ha: Between times 1 and ν the variables follow an N ($\mu 1$, 1) distribution, and between ν+1 and T they follow an N ($\mu 2$, 1) distribution. The Petitt statistic is defined by:

$$To = Max\ 1 \leq t < T[v\overline{z1}^2 + (n-v)v\overline{z2}^2] \quad \text{3.2a}$$

$$z1 = \frac{1}{v}\sum_{t=1}^{v} Xt \quad \text{3.2b}$$

$$Z2 = \frac{1}{n-v}\sum_{t=v+1}^{T} Xi \quad \text{3.2c}$$

The T_o statistic derives from a calculation comparing the likelihood of the two alternative models. The model corresponding to Ha implies that $\mu 1$ and $\mu 2$ are estimated while determining the v parameter maximizing the likelihood. XLSTAT evaluates the p-value and an interval around the p-value by using a Monte Carlo method. If v is known, it is enough to run a z test on the two series of ratios. The SNHT test allows identifying the most likely v.

3.5.3 Test for Absence of Trend

Mann-Kendall Trend Tests: Use this tool to determine with a nonparametric test if a trend can be determined in a series, even if there is a seasonal component in the series. This test has first been applied by Mann (1945) then more studied by Kendall (1975) and improved by Hirsch et al (1982, 1984) who allowed taking under consideration seasonality. The null hypothesis H0 for these tests is that there's no trend within the series. The three alternative hypotheses that there's a negative, non-null, or positive trend are often chosen. The Mann-Kendall tests are supported the calculation of tau coefficient of correlation measure of association between two samples, which is itself supported the ranks with the samples. To compute the p-value of this test, XLSTAT can calculate, as within the case of the Kendall tau test, a particular p-value if there are not any ties within the series and if the sample size is less than 50. If an accurate calculation is not possible, a normal approximation is used, for which correction for continuity is optional but recommended. If the time series does have a trend, the data cannot be used for frequency analyses or modeling.

In the particular case of the trend test, the first series is an increasing time indicator generated automatically for which ranks are obvious, which simplifies the calculations. The S statistic used for the test and its variance are given by:

$$S = \sum_{x=1}^{x-1} \sum_{j=i+1}^{x} \operatorname{sgn}(xj - xi) \quad \text{.....3.3a}$$

$$Var(S) = \frac{n(n-1)(2n+5)}{18} \quad \text{.....3.3b}$$

Where n is the number of observations and x_i (i = 1...n) are the independent observations. To calculate the p-value of this test, XLSTAT can calculate, as in the case of the Kendall tau test, an exact p- value if there are no ties in the series and if the sample size is less than 50. If an exact calculation is not possible, a normal approximation is used, for which a correction for continuity is optional but recommended.

3.6 Comparison of Satellite rainfall products versus rain gauges

To better understand the impacts of rainfall inputs on the output of the model, we begin by comparing rainfall magnitudes derived from satellite rainfall products (i.e. TAMSAT and CHRIPS) and rain gauge that have been used in Arc SWAT modeling for Genale Dawa River Basin. The comparison performed for the study period of 1996- 2017 in which all the data products are available ignoring missing gauged data.

There are two commonly used methods for evaluating the satellite rainfall products, namely, point to grid (point-based) and grid to grid (interpolated grid to satellite grid) methods. In point-based comparison methods, individual gauge stations based rainfall are compared with the grid-based satellite and reanalysis rainfall products, whereas, in the grid to grid comparison, the gauge based observed rainfall are interpolated to the same resolutions of the selected grid-based satellite and reanalysis rainfall products and then evaluated. Grid to grid method of evaluation is appropriate where the area is covered with a high number and uniformly networked gauge stations. In areas with sparsely distributed and limited number of rain gauge stations and complex terrain as in the case of the present study, point to grid method is the best way to evaluate each satellite and reanalysis rainfall product independently using their native resolution (49). Hence, point to grid method is adopted for this study.

In the present study, both statistical indices and categorical statistical indices were adopted to evaluate the precision of the satellite rainfall products. Statistical indices evaluate the performance of the Satellite rainfall product in estimating the cumulative rainfall over a timeframe. Evaluation of cumulative rainfall was based on the calculation of mean error (ME), mean absolute error (MAE), the Pearson correlation (R) the Nash-Sutcliffe efficiency coefficient (NSE), the root mean square error (RMSE) and bias as follows:

$$R = \frac{\sum(O-\overline{O})(S-\overline{S})}{\sqrt{\sum(O-\overline{O})^2}\sqrt{\sum(S-\overline{S})^2}} \quad (3\text{-}4)$$

$$RSME = \sqrt{\frac{1}{N}\sum(S-O)^2} \quad (3\text{-}5)$$

$$ME = \frac{1}{N}\sum(S - O) \quad (3\text{-}6)$$

$$MAE = \frac{1}{N}\sum(|S - O|) \quad (3\text{-}7)$$

$$NSE = 1 - \frac{\sum(O-S)^2}{\sum(O-\overline{O})^2} \quad (3\text{-}8)$$

$$Bias = \frac{\sum S}{\sum O} \quad (3.9)$$

Where O is the rainfall total at a reference gauging station, $\bar{O}$ is the mean observed rainfall total at a reference gauging station, S is a rainfall total for a satellite product, and N is the number of data pairs compared. The dimensions of ME and MAE are mm, whereas NSE and Bias are dimensionless. ME and MAE both provides information on the average estimation error. ME ranges from –∞ to ∞, whereas MAE ranges from 0 to ∞, and a perfect score for both is 0. MAE was used here instead of the root mean square error to avoid the effect of extremely high rainfall values or outliers ((50).The Bias statistic indicates how well the mean estimate and gauge mean correspond; its value ranges from 0 to ∞, with 1 being a perfect score. Values of Bias >1 and positive ME values indicate an overestimation, whereas values of Bias <1 and negative ME indicate an underestimation. NSE shows the skill of the estimates relative to a reference (in this case, the mean of the gauge observations); it ranges from –∞ to 1, with higher values indicating better agreement between the Satellite rainfall and gauge measurements. Negative NSE values indicate that the reference mean is a better estimate than the SREs; 0 indicates that the reference mean is as good as the Satellite rainfall. (50) Have noted that correlation coefficients are insensitive to additive and proportional differences between satellite products and gauge measurements; hence, they were not used in the assessment of cumulative rainfall, because correlation coefficients can be large even when the magnitudes of the Satellite rainfall and gauge measurements differ considerably.

A categorical statistical index evaluates the rainfall detection capabilities of satellite rainfall product. To evaluate the rainfall detection capabilities of the Satellite rainfall product (rainfall threshold ≥1 mm), we used a suite of binary skill scores that encapsulated information on rain/no-rain days in a contingency table (Table 3-7). The contingency table was constructed to compute categorical statistics that included the probability of detection (POD), false alarm ratio (FAR), frequency bias index (FBI), and Heidke skill score (HSS) as follows:

Table 3-7 Contingency table for comparing rain gauge measurements and satellite-based rainfall estimates.

	Gauge >=1 mm	Gauge <1 mm
Satellite >=1 mm	A (Hit)	B (false detection)
Satellite <1 mm	C (Miss)	D (Correct No rain)

$$POD = \frac{A}{A+C} \quad (3\text{-}10)$$

$$FAR = \frac{B}{A+B} \quad (3\text{-}11)$$

$$FBI = \frac{A+B}{A+C} \quad (3\text{-}12)$$

$$HSS = \frac{2(AD-BC)}{(A+C)(C+D)+(A+B)(B+D)} \quad (3\text{-}13)$$

Where A, B, C, and D represent hits (the satellite successfully detected rain), false alarms (the satellite failed to detect the no-rain case), misses (the satellite failed to detect rain), and correct negatives (the satellite successfully detected the no-rain case), respectively (Table 3-7). POD quantifies the proportion of observed rainfall days that were correctly estimated by the satellite product. FAR is the proportion of satellite-estimated rainfall days when there was in fact no rain. Both POD and FAR range from 0 to 1, with 1 being a perfect POD and 0 being a perfect FAR. FBI, which ranges from 0 to ∞, compares the rainfall-day detection frequency of the Satellite rainfall product with that of the rain gauge measurements: an FBI of less than (greater than) 1 indicates an underestimation (overestimation) of rainfall days. HSS, which ranges from –∞ to 1, is a measure of the overall skill of the rainfall-day estimates after rain events detected by random chance have been removed: an HSS less than 0 indicates that random chance is better than the Satellite rainfall product; an HSS of 0 means the Satellite rainfall product has no skill; and an HSS of 1 indicates a perfect estimation of rainfall days by the Satellite rainfall product. Compared with the other metrics, HSS is advantageous because it measures the ability of the satellite to observe rain events relative to events that occur at random.

In this study the rainfall data from TAMSAT show significant variation when compared with observed rainfall data, while CHRIPS which is re sampled by Ethiopian Metrological Agency and shows good result in comparison. Therefore TAMSAT rainfall product need bias correction before using for simulation.

3.7 Bias correction

Using accurate satellite-based precipitation estimates has the potential to reduce the uncertainty in streamflow simulation. Thus, we investigated whether an improvement in the streamflow simulation performance of the hydrological model is possible through bias correction of the TAMSAT rainfall product with the local rain gauge network. Due to the availability of a relatively scarce rain gauge network within the study area, we employed a simple multiplicative bias correction procedure. Multiplicative bias correction schemes and suggested the use of a multiplicative error model for bias removal of daily satellite-based precipitation products. In the procedure, monthly bias factors were used to correct the daily TAMSAT data product. Bias correction methods are often applied to correct the climate input data provided by satellite rainfall products or remote sensed climate data for systematic statistical deviations from observational data. They generally adjust the long-term mean by adding the typical difference between the simulated and observed data over the period to the simulated data, or by applying an

associated multiplicative correction factor. In addition, differences between the variance of the simulated and observed data are often corrected. In this study, Climate Model data for hydrologic modeling (CMhyd) was used as a bias correction tool. CMhyd is powerful software that has different inbuilt algorithms and methods.

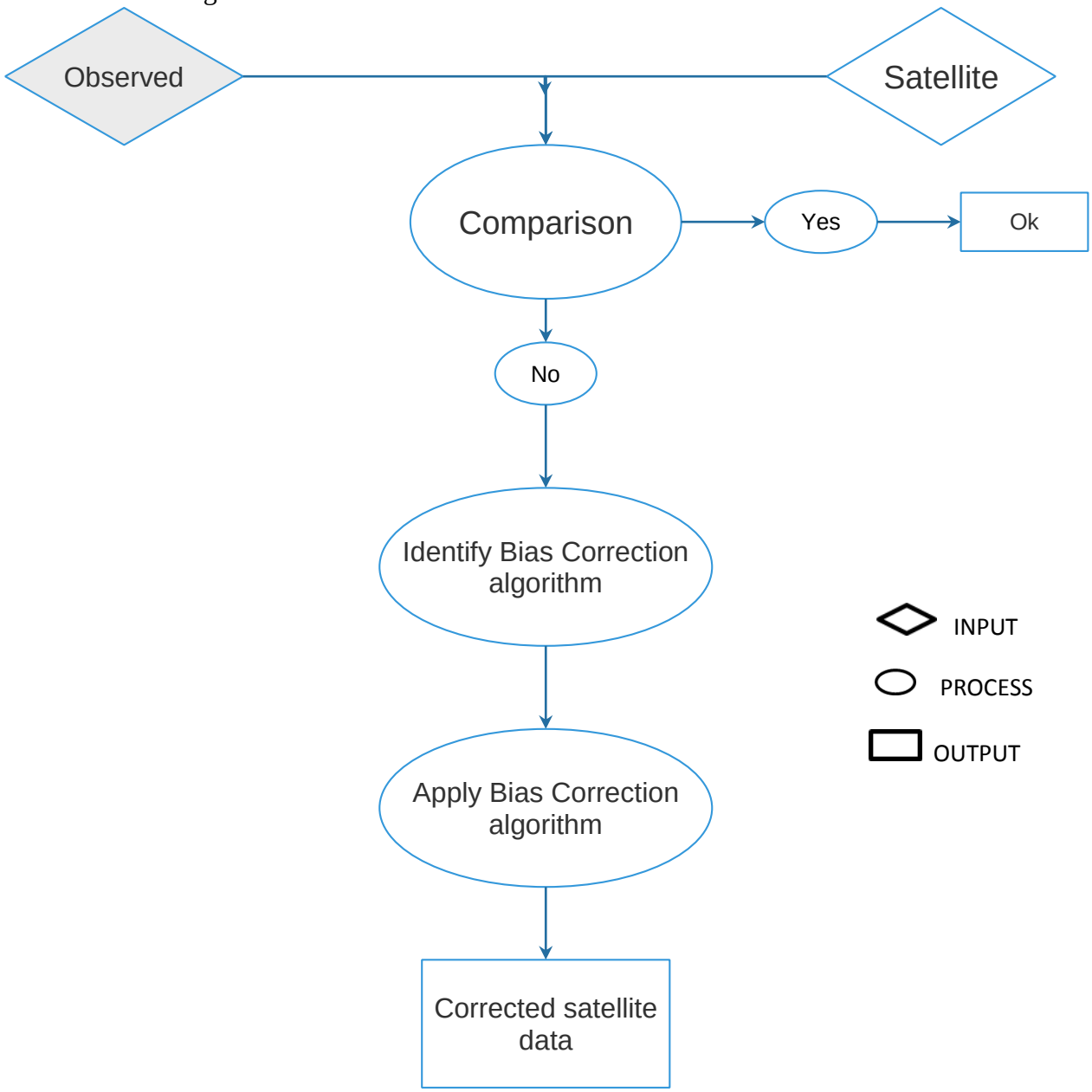

Figure 3-8 Bias correction work flow

Studies on the comparison of TAMSAT with ground-observed rainfall data showed that TAMSAT is a good alternative data set for hydrological modeling on a large scale confirmed that TAMSAT precipitation can reproduce the observed rainfall pattern in Ethiopia, but it overestimated or underestimated the observed values. Therefore, a bias correction method that focuses mainly on the magnitude rather than the pattern or trend of the datasets is needed. From among the various arrays of rainfall data adjusting techniques, most of which are statistical, the

linear scaling (LS) bias correction method was selected for this study as it aims to match the monthly mean of corrected values perfectly with that of the observed ones. It operates with monthly correction values based on the difference between observed and raw data. The change factor for precipitation is a multiplier that is computed from the ratio of the monthly mean of the observed to the raw dataset:

$$Pd,cor = Pd,raw * (\frac{\mu(Pm,obs)}{\mu(Pm\ raw)} \qquad (3.14)$$

Where P d,cor is the corrected daily precipitation and Pd,raw is the daily raw precipitation data from TAMSAT, μ(Pm,obs)is the long-term mean value of monthly rainfall of observed data and μ(Pm raw)is the long-term mean value of the monthly raw rainfall data.

3. 8 SWAT Model Setup

3.8.1 Watershed delineation

The first step in creating SWAT model input was delineation of the watershed from a DEM. Inputs entered into the SWAT model were organized to have spatial characteristics. The SWAT model provides three spatial levels: the watershed, the sub basins, and the hydrologic response units (HRUs). Each level was characterized by a parameter set and input data. The largest spatial level, the watershed, refers to the entire area being represented by the model.

For modeling purposes, a watershed was partitioned into 18 sub watersheds or sub basins. The use of sub basins in a simulation was particularly beneficial when different areas of the watershed were dominated by land uses or soils dissimilar enough in properties to impact hydrology. By partitioning the watershed into sub basins, the user was able to reference different areas of the watershed to one another spatially. Moreover, the selection and implementation of appropriate conservation measure can be aided by reliable predictions of watershed response under different land use scenarios.

The watershed and subwatershed delineation was performed using 30 m resolution DEM data using the Arc SWAT model watershed delineation function. The watershed delineation process includes five major steps, DEM setup, stream definition, outlet and inlet definition, watershed outlets selection and definition and calculation of sub-basin parameters. Automated watershed delineation embedded in Arc SWAT interface was used to delineate the watershed. Delineation of the watershed and sub-watershed was done by means of DEM data. DEM was imported into the SWAT model and projected to UTM zone 37, the projection area of Ethiopia. A mask was manually delineated over the DEM to remove the specific part, to delineate the border of the watershed and digitize the stream networks Genale -Dawa River basin, which reduces the time of processing and burn-in a polyline stream dataset that in turn helps the sub-basin reach to follow the known stream reach. For this study suggested the size of the sub-basin area (2,258 ha) to define the smallest drainage area essential to custom the origin of a stream was used. Based on the area of the basin, only one outlet is defined, which is later taken as a point of testing and verification of the simulated flows. As a result, actual Genale-Dawa river basin outlet is delineated. Lastly, calculations of sub-basin parameters were made.

3.8.2 Determination of hydrological response units

After watershed delineation, sub-basins were subdivided into small hydrologic response units (HRUs) that have unique land use, soil, and slope. The land use, soil, and slope datasets were projected into the same projections as DEM. After projection of the land use, soil, and slope datasets were reclassified, overlapped and connected with the SWAT catalogs and ready for HRU definition. To define the distribution of HRUs, multiple HRU description choices were made as it better refer to the heterogeneity inside the basin and as it precisely replicate the hydrologic executions. The threshold level set for land use, soil and slope were used to define the number of HRUs within the sub-basin as well as the watershed. Besides the land use and soil, HRUs were also classified based on slope classes. For these specific areas, multiple slope classification was used and the classifications were made based on the suggested minimum, maximum, mean and median slope statistics of the basin. The minimum threshold area of 10% for land use, 10% for soil class and 10% for slope were used. The land use, soil and slopes percentage areas covering less than the threshold area level were eliminated, and then the remaining areas were reclassified so that a hundred percent of the land area in the sub-basin could be used in the simulation execution. The third step in HRU definition is the selection of slope classification options (single or multiple). For this study, multiple slope option (an option for considering different slope classes for HRU definition) was selected and the slope class was classified to five and the range was 0-5%, 5-10%, 10-15%, 15-20% and above 20%.

3.8.3 Sensitivity analysis

The sensitivity analysis was made using a built-in SWAT sensitivity analysis tool that uses the Latin Hypercube One-factor-At-a-Time (LH-OAT) (Van Griensven, 2005). The inputs were the observed daily flow data, the simulated annual flow data and the sensitive parameter in relation to flow with the absolute lower and upper bound and default type of change to be applied (method application) were used.

LH-OAT combines the OAT design and LH sampling by taking the Latin Hypercube samples as initial points for OAT design. The LH-OAT sensitivity analysis method combines thus the robustness of the Latin Hypercube sampling that ensures that the full range of all parameters has been sampled with the precision of an OAT designs assuring that the changes in the output in each model run can be unambiguously attributed to the input changed in such a simulation leading to a robust and efficient sensitivity analysis method (Van Griensven, 2005).

3.8.4 Model calibration

Calibration describes the effort to support the model with fitted parameters for a given set of local conditions to reduce the prediction uncertainty (51). Calibration was carried out with the SWAT Calibration and Uncertainty Program (SWAT-CUP) 2019, Version 5.2.1.1, which facilitates the calibration process (52).

All rainfall- runoff hydrological models (lumped or distributed) are a simple representation of the real world processes. Besides this, the lumped model parameter represents an average value over the entire watershed. Model inputs and values of parameters are associated with several uncertainties. Therefore model calibration is an important task to improve the result of model

simulation. Proper model calibration is necessary to consider a good fit between simulated and observed watershed runoff volume (water balance), the shape of the hydrograph, the peak flow, and the base flow. Generally, model calibration involves the determination of model parameters that gives the best possible correspondence between observed and simulated runoff from a catchment. Calibration can be performed in two ways: either manually or automated. In ArcSWAT2012 Manual Calibration Helper used for adjusting to parameters across a user-defined group of HRUs or sub-basins. Auto calibration and Uncertainty of ArcSWAT2012 is used for automated calibration. Many of auto-calibration and uncertainty analysis tools for SWAT were developed and are currently available to assist in the optimization process (53).This study is based on SWAT-CUP and its Sequential Uncertainty Fitting algorithm (SUFI-2) to achieve a proper calibration. In SUFI-2, parameter uncertainty accounts for all sources of uncertainties such as uncertainty in driving variables (e.g., rainfall), conceptual model, parameters, and measured data (52). The intelligence of SWAT-CUP allows model parameters to be predefined and optimized throughout the auto-calibration process or manually adjusted iteratively between calibration batches (53).The SUFI-2 algorithm in the SWAT-CUP software package was used for model calibration, validation, sensitivity, and uncertainty analysis of the Genale Dawa River Basin. Among various evaluation coefficients allowed in SUFI-2, Nash-Sutcliff (NSE) was chosen for model optimization in SWAT-CUP.

3.8.5 Model validation

Validation was also done to compare the model outputs with an independent data set without making further adjustments to the parameter values. Model validation is a comparison of the model outputs with an independent data set without making further adjustments which may be adjusted during the calibration process. Model performance in calibration and validation periods may not be similar. Recent studies revealed that there are some difficulties in climate model validation. That is because of the complexity of the nature of climate and time-dependent uncertainties of modeling dataset. Another reason is the hydrologic condition in the calibration period may not be the same as the hydrologic condition during the validation period. The streamflow observed data of ten years, from 01 January 1998 to 31 December 2007, derived from four gauging stations that were used for auto-calibration. Before performing the Auto-calibration process the data was divided into two parts: 01 January 1998 to 31 December 2003 for calibration and 01 January 2004 to 31 December 2007 for validation.

3.8.6 Selection of parameters for Sensitivity Analysis

Before calibration to start parameters those were sensitive for Genale Dawa River basin was arranged from articles published. Parameters required for calibration are described in (table 3.8) below.CN2,ESCO,SOL_AWC,CANMX,REVAPMN,GWGMN, SLOPE, SOL_K,GW_REVAP, CH_K2, ALPHA_BF,GW_DELAY, CH-K2, RCHRG-DP, SURLAG, HRU-SLP, SLSUBBSN, ALPHA-BNK

Table 3-8 ***Parameter definitions and initial ranges used in SUFI-2.***

NO	Stream flow parameters selected for calibration	Description of parameters	Ranges
1	CN2	SCS runoff curve number	25 - 98
2	ESCO	Soil evaporation compensation factor	0 - 1
3	SOL_AWC	Available water capacity of the soil layer.	(-0.25) - 0.25
4	CANMX	Maximum canopy storage	0-10
5	REVAPMN	Threshold depth of water in the shallow aquifer for "revap" to occur (mm).	0-500
6	GWQMN	Threshold depth of water in the shallow aquifer required for return flow to occur	0-5000
7	SLOPE	Average slope steepness	(-0.25) - 0.25
8	SOL_K	Saturated hydraulic conductivity.	(-0.25) - 0.25
9	GW_REVAP	Groundwater "revap" coefficient.	0-0.2
10	CH_K2	Effective hydraulic conductivity in main channel alluvium.	0-500
11	ALPHA_BF	Base flow alpha factor (days).	0-1
12	CH_N2	Manning's n value for the main canal	0-0.3
13	GW_DELAY	Groundwater delay (days).	0-500
14	RCHRG_DP	Deep aquifer percolation fraction.	0-1
15	SURLAG	Surface runoff lag time [days]	0-24
16	HRU_SLP	Average slope steepness	0-1
17	SLSUBBSN	Average slope length	10-150
18	ALPHA_BNK	Baseflow alpha factor for bank storage	0-1

The work flow concerning SWAT model, calibration and validation using SWAT-CUP is summarized in the following flowchart

3.9 Model performance evaluation

To evaluate the model simulation outputs relative to the observed data, model performance evaluation is necessary. There are various methods to evaluate the model performance during the calibration and validation periods. For this study, the objective functions to measure the model's goodness of fit for discharge was Nash-Sutcliffe Efficiency (NSE), Determination coefficient (R^2), The Root Mean Square Error (RMSE), and PBIAS.

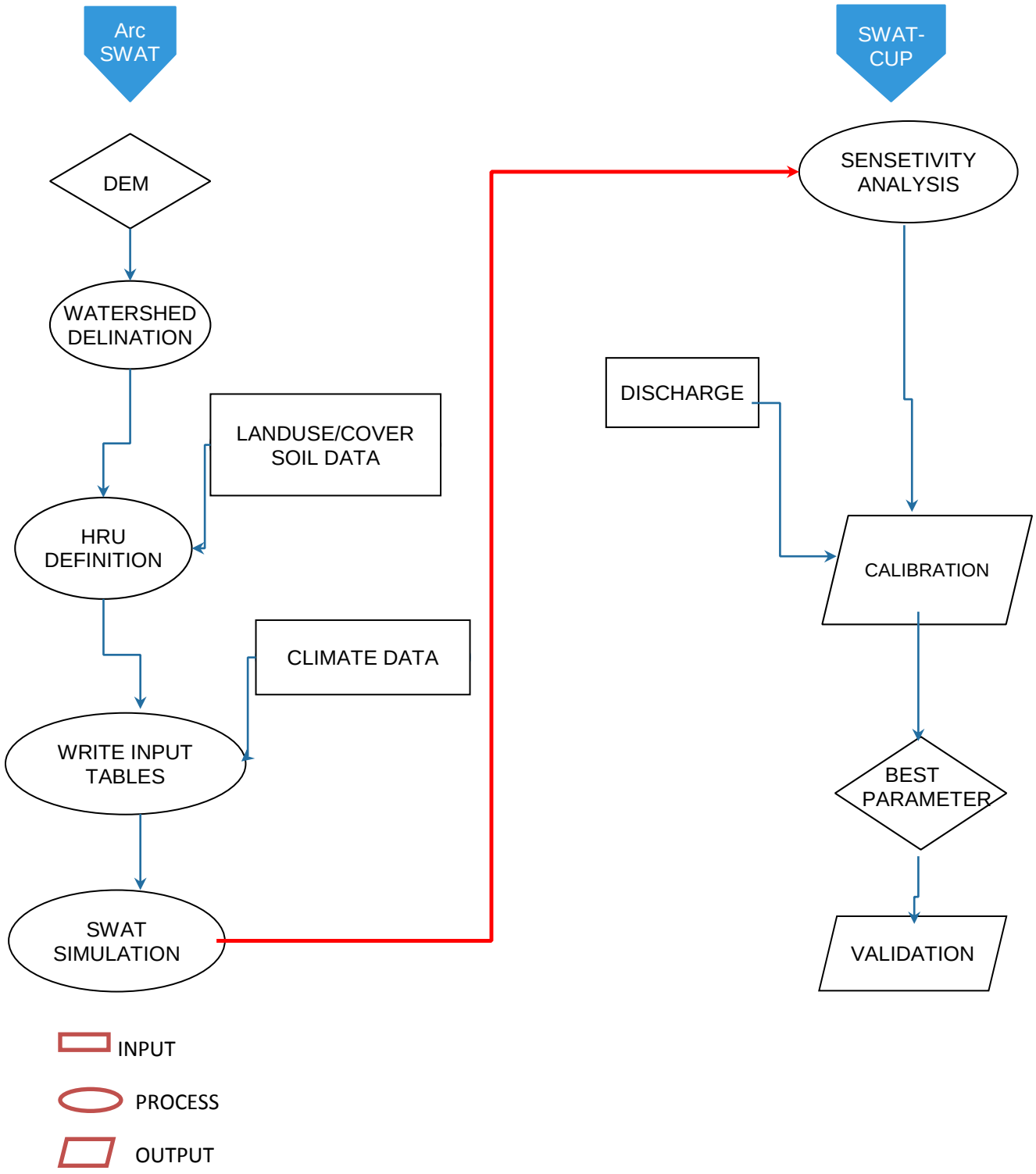

Figure 3-9 Arc SWAT and SWAT-CUP work flow

4. RESULTS AND DISCUSSIONS

4.1 Data Processing and Model Set Up

Data processing, in this case, includes trend tests and homogeneity tests for monthly precipitation data of nine stations in Genale Dawa River basin. Moreover, monthly flow data of four stations in the basin is also tested depending on the availability of flow data. A comparison of satellite rainfall product versus rain gauge is done for both TAMSAT and CHRIPS rainfall products. After comparison, it was seen that there is a magnitudinal variation between TAMSAT product and rain gauge. Therefore, Bias correction was done for TAMSAT.

4.2. Trend and Homogeneity Test

4.2.1. Trend test for observed Rainfall

Monthly rainfall data from 1996 to 2017 is employed for trend analysis. In this test, seasonal Mann Kendall test is applied, and we take into account the seasonality of the series. This means that for monthly data with seasonality of 12 months, one will not try to find out if there is a trend in the overall series, but if from one month of January to another, and from one month February and another, and so on, there is a trend. Based on alpha value of 0.05 (95% significance level), if p value is greater than alpha value, therefore the series is homogeneous. Table 4.1a, Table 4.1b and Table 4.1c shows the summary result of the test. According to the Wijngaard et al. (2003) classification, The Nine selected rainfall stations were found homogeneous having the Null Hypothesis greater than significance level alpha (p- value = (0.28 - 0.98)) considering Mann-kendall test.

As the computed p-value is greater than the significance level alpha=0.05, one cannot reject the null hypothesis H0.

Table 4-1a ***seasonal trend test for monthly rainfall of Weather gauging stations***

NO	Station	Observations	Obs. with missing data	Obs. without missing data	Minimum	Maximum	Mean	Std. Deviation
1	Bore	192	0	192	0	467.6	137.31	98.55
2	DeloMena	226	0	226	0	507.8	88.68	100.61
3	Filtu	116	0	116	0	249.4	36.1	57.38
4	Finchawa	230	0	230	0	402	66.85	80.64
5	Ginir	237	0	237	0	497.8	86.05	92.86
6	Kibremengist	219	0	219	0	358.3	83.6	86.13
7	Moyale	252	0	252	0	504.7	46.79	68.54
8	Negele	95	0	95	0	274.5	48.98	64.33
9	Robe	237	0	237	0	249.3	70.93	53.79

Table 4-1b Kendall's tau value and p-value (Two-tailed) of stations

NO	Station	Kendall's tau	p-value (Two-tailed)	Alpha
1	Bore	0.015	0.757	0.05
2	DeloMena	-0.007	0.877	0.05
3	Filtu	-0.060	0.362	0.05
4	Finchawa	0.048	0.284	0.05
5	Ginir	0.054	0.221	0.05
6	Kibremengist	-0.003	0.949	0.05
7	Moyale	-0.031	0.466	0.05
8	Negele	0.001	0.987	0.05
9	Robe	-0.025	0.576	0.05

Note: p-values are greater than alpha (0.05), hence data of all stations are consistent

4.2.2. Homogeneity test of observed Rainfall

Considering alpha value of 0.05 (95% significance level), if p value is greater than alpha value, therefore the series is homogeneous. Table 4.2 shows the summary result of the test. According to the Wijngaard et al. (2003) classification, The Nine selected rainfall stations were found homogeneous having the Null Hypothesis greater than significance level alpha (p- value = (0.06-0.97) for SNTH test. We followed the same procedure as trend test and found that data are homogeneous (see table below).

Table4-2 *Alexanderson's SNHT test for Homogeneity of monthly rainfall data*

No	Station	Kendall's tau(τo)	p-value (Two-tailed)	Alpha
1	Bore	3.528	0.680	0.05
2	DeloMena	1.685	0.978	0.05
3	Filtu	12.426	0.064	0.05
4	Finchawa	2.228	0.913	0.05
5	Ginir	5.274	0.395	0.05
6	Kibremengist	7.973	0.133	0.05
7	Moyale	3.752	0.604	0.05
8	Negele	6.296	0.234	0.05
9	Robe	1.812	0.970	0.05

As shown in table all p-values are greater than alpha (0.05), hence data are homogenous.

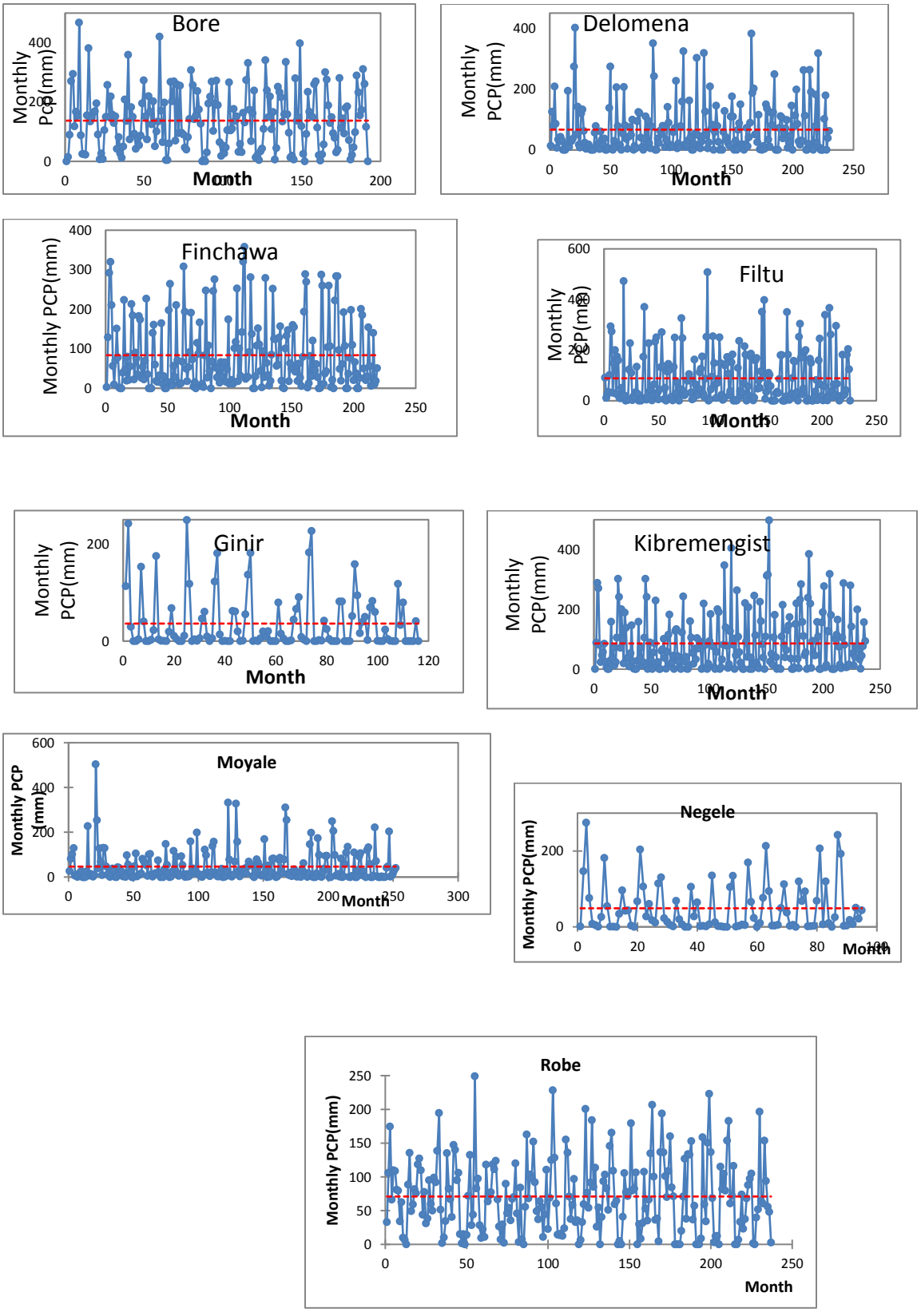

Figure 4-1*Graphical representation of homogeneity test of monthly flow data*

The section below emphasizes on the overall trend of the data series on each station. Time series plot, MannKendall Trend Test and descriptive statistical analysis were used in determining the trend associate stream flow and water level for each station. Results obtained show a significant trend at 95% confidence level for certain stations. Trend line also drawn to show the trend clearly. The *p*-values smaller than 0.05 must be fulfilled before the trend test was concluded to be significant.

4.2.3. Trend test and homogeneity test for monthly flow data

Similarly, discharge homogeneity and trend test were done at discharge gauging stations. Based on alpha value of 0.05 (95% significance level), if p value is greater than alpha value, therefore the series is homogeneous. Table 4.3a, Table 4.3b and Table 4.4 shows the summary result of the test. According to the Wijngaard et al. (2003) classification, The four selected rainfall stations were found homogeneous having the Null Hypothesis greater than significance level alpha (p-value = (0.06 - 0.92)) considering Mann-kendall test and (0.06 - 0.65) for SNTH test.

Table 4-3a ***seasonal trend test for monthly Discharge***

NO	Station	Observations	Obs. with missing data	Obs. without missing data	Minimum	Maximum	Mean	Std. deviation
1	Dawa@MelkaGuba	120	0	120	7.64	877.4	128.96	137.24
	Welmel@MelkaAmana	119	0	119	11.65	2224.51	470.92	432.83
3	Dimtu Nr Bore	120	0	120	1.7	724.73	160.36	147.17
4	Genale@Halwen	120	0	120	5.03	11023.36	2860.4	2313.07

Table 4-3b Kendall's tau and p-value (Two-tailed) values of HG stations

Station	Kendall's tau	p-value (Two-tailed)	Alpha
Dawa @Melka Guba	0.041	0.508	0.05
Welmel@Melka Amana	0.092	0.140	0.05
Dimtu Nr Bore	0.033	0.601	0.05
Genale@Halwen	0.114	0.065	0.05

Note: p-values are greater than alpha (0.05), hence data of all stations are consistent

Table 4-4 *Alexanderson's SNHT test for Homogeneity of monthly Discharge*

Station	Kendall's tau(τo)	p-value (Two-tailed)	Alpha
Dawa @Melka Guba	5.896	0.263	0.05
Welmel@Melka Amana	5.726	0.304	0.05
Dimtu Nr Bore	2.064	0.917	0.05
Genale@Halwen	9.962	0.058	0.05

As shown in table all p-values are greater than alpha (0.05), hence data are homogenous.

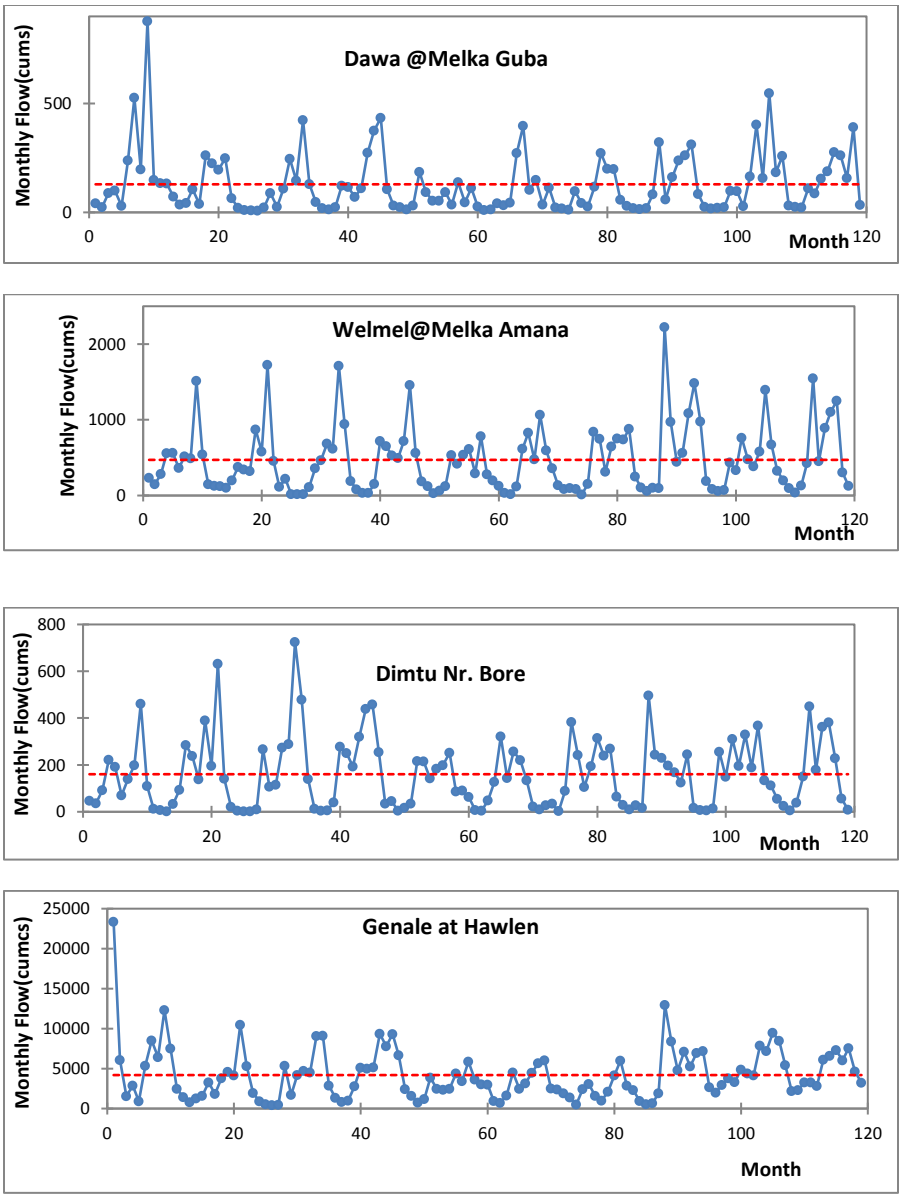

Figure 4-2 *Graphical representation of homogeneity test of monthly observed flow data*

4.3 Bias correction of TAMSAT rain fall product

Satellite-based precipitation estimates exhibit large systematic and random biases. The systematic errors (*i.e.*, bias) persist when the estimates are aggregated over time and, hence, may cause large uncertainties in hydrologic modeling. Besides, models could augment or suppress rainfall biases to larger or smaller streamflow based on the response mode of the model. Therefore, the bias in rainfall products should be assessed and corrected before satellite rainfall products can be used in hydrologic applications. When comparing TAMSAT rainfall product with the in-situ rainfall of selected stations, it shows a large discrepancy.

The raw gridded TAMSAT rainfall dataset for the Genale Dawa river basin wasaccessed from http://www.met.reading.ac.uk/~tamsat. The basin is covered with 9998 grid points with a spatial resolution of ~3.75 km and a 35 year temporal resolution (1983–2017). In order to use the

corrected dataset for hydrological modelling and other purposes, the raw TAMSAT rainfall dataset was adjusted with LS bias correcting techniques. Both statistical and categorical tests clearly describe that the raw TAMSAT rainfall dataset has biased in both directions (underestimation and overestimation) of the daily rainfall. However, the overall magnitude of the raw TAMSAT rainfall dataset overestimates or underestimates the daily rainfall of the basin, indicated with a values of R, NSE and RSME (0.26 - 0.58), (-0.41 - 0.26) and (5.21 - 10.3) respectively for all representative station. Categorically the values of POD, FAR, FBI and HSS (0.38 - 0.6), (0.26 - 0.65), (0.75 - 1.22), (0.25 - 0.47) respectively. The adjusted TAMSAT rainfall dataset was the best fit with the observed dataset, with a small range of RMSE (1.77–5.6) and strong range of NSE co-efficients (0.74 – 0.91) and a strong R (0.84 - 0.95). The bias correction gave a better result and lower values of PBIAS, ranging from 0.98 to 1.25. The categorical improvement is indicate by a strong value of POD, FAR, FBI and HSS (0.75 - 0.85), (0.17 - 0.3), (0.75 - 1.1) and (0.58 - 0.89) respectively. The detail of Continuous evaluation statistics, Categorical evaluation indices and the magnitude of maximum and minimum rainfall for the corrected TAMSAT is discussed in three tables below

Table 4-5 Continuous Evaluation Statistics for raw and bias corrected TAMSAT

	CONTINUOUS EVALUATION STATISTICS									
	TAMSAT raw					TAMSAT corrected				
STATION	R	ME	BIAS	RSME	NSE	R	ME	BIAS	RSME	NSE
ROBE	0.37	0.05	1.02	6.43	0.03	0.89	-0.004	1	2.6	0.8
DELOMENA	0.26	0.04	1.02	9.55	-0.4	0.87	0.1	1.05	4.04	0.75
GINIR	0.38	0.08	1.03	10.3	0.26	0.92	0.23	1.1	3.4	0.85
KIBRMENGIST	0.47	0.08	1.03	7.45	0.02	0.84	0.30	1.11	4.26	0.67
MOYALE	0.44	0.14	1.1	6.67	0.06	0.91	0.11	1.1	2.6	0.81
BORE	0.53	0.08	0.98	9.08	0.06	0.82	-0.67	1.1	5.46	0.61
FILTU	0.55	0.22	1.18	5.88	0.07	0.86	0.3	1.2	5.62	0.70
NEGELE	0.58	0.06	1.04	5.21	0.15	0.95	-0.024	0.98	1.77	0.90
FINCHAWA	0.43	0.3	1.13	7.74	0.07	0.88	0.14	1.06	3.55	0.77

Table 4-6 Categorical Evaluation Statistics for raw and bias corrected TAMSAT

	CATAGORICAL STATISTICS							
	TAMSAT raw				TAMSAT corr			
STATION	POD	FAR	FB	HSS	POD	FAR	FB	HSS
ROBE	0.55	0.32	0.81	0.45	0.77	0.17	0.94	0.687
DELOMENA	0.53	0.382	0.86	0.44	0.67	0.23	0.88	0.62
GINIR	0.47	0.37	0.75	0.43	0.75	0.20	0.94	0.71
KIBREMENGIST	0.55	0.33	0.83	0.47	0.64	0.26	0.86	0.58
MOYALE	0.39	0.41	0.67	0.4	0.57	0.22	0.75	0.621
BORE	0.60	0.26	0.81	0.44	0.72	0.2	0.90	0.58
FILTU	0.38	0.52	0.79	0.36	0.73	0.3	1.05	0.68
NEGELE	0.50	0.38	0.82	0.47	0.73	0.15	0.86	0.74
FINCHAWA	0.42	0.65	1.22	0.25	0.83	0.23	1.09	0.76

Table 4-7 Maximum and Minimum precipitation for raw and bias corrected TAMSAT

	TAMSAT raw		TAMSAT corrected		Observed	
STATION	Min	Max	Min	Max	Min	MAX
ROBE	0.0	55.6	0.0	109.30	0.0	112.3
DELOMENA	0.0	82.0	0.0	108.0	0.0	109.3
GINIR	0.0	90.0	0.0	159.0	0.0	162.0
KIBREMENGIST	0.0	85.0	0.0	90.95	0.0	94.0
MOYALE	0.0	100.0	0.0	124.0	0.0	126.2
BORE	0.0	92.0	0.0	94.0	0.0	96.3
FILTU	0.0	70.0	0.0	89.0	0.0	90.3
NEGELE	0.0	50.0	0.0	102.55	0.0	103.0
FINCHAWA	0.0	96	0.0	99.0	0.0	100.7

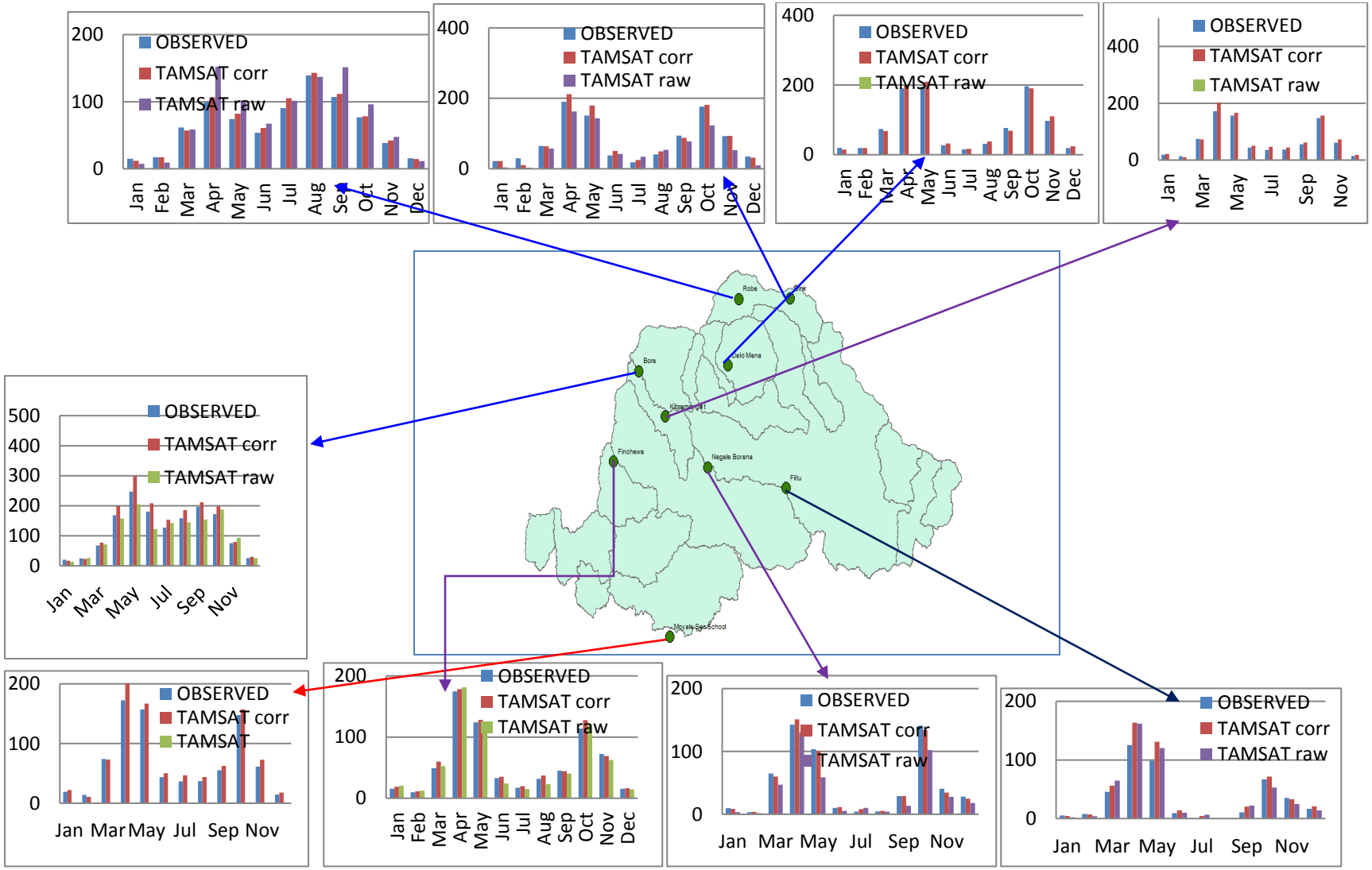

Figure 4-3 Stations and grid-based comparison of mean monthly rainfall datasets.

4.4. Comparison of Satellite rainfall products versus rain gauges

4.4.1. Comparison of Daily Rainfall

Good performance of a product for rainfall detection would be characterized by a combination of high POD, high FBI, low FAR, and high HSS. For all the nine selected stations, TAMSAT had the lower rainfall detection skill: compared to CHRIPS. It correctly identified more than 71.62% of the observed rainy days (POD). While, CHIRPS had the highest rainfall detection skill: it correctly dictate more than 81% of the rainfall events for all the nine selected stations. The POD values reveal that both the SREs missed moderate rainfall events in all the nine selected stations. FAR values indicated that around 22% and 5% of the estimated rainy days were falsely estimated by the TAMSAT and CHRIPS respectively. In general, FAR was relatively low for all the nine selected stations. FBI values were 86% and 92.1% for CHIRPS and TAMSAT respectively, an indication that these two SREs underestimated the frequency of rainfall. The main problem with the SREs over the study region therefore seems to be the moderate overestimation (TAMSAT) and underestimation (CHIRPS) of rainfall occurrence. The HSS values were high, the implication being that the skill of the SREs in detecting rainfall occurrences was much better than random chance. Generally, CHRIPS demonstrates better rainfall detection capability on most of the evaluation metrics compared to TAMSAT over all the nine selected stations (Table 4.8).

At a daily time scale (Table 4.8), the ME was small relative to the average daily rainfall ($\bar{O}$) for both the SREs. There were small random errors in the TAMSAT estimates for all the nine selected stations, as indicated by the lower ME values 0.05 and -0.44 for TAMSAT and CHRIPS respectively (Table 4.8). TAMSAT and CHIRPS estimated the amount of rainfall reasonably well (high efficiency, low random errors, and bias <10%) at daily time scales. The better accuracy of the TAMSAT estimates may have resulted from the use of thresholds that varied spatially and temporally and from the high temporal resolution. The fact that TAMSAT is bias-adjusted, and CHIRPS is bias-adjusted and includes contemporaneous station data could also result in better rainfall estimation. CHIRPS had the NSE and R (> 0.75, >0.88) respectively and TAMSAT had the NSE and R (> 0.76, >0.88) respectively. All the evaluation statistics confirm that TAMSAT and CHIRPS performed better and the differences in the evaluation statistics between TAMSAT and CHIRPS were very small for all selected nine stations.

In all stations, the CHRIPS has scored higher POD, FB and HSS, with an average values of 0.8097,0.8575 and 0.8118, respectively, while raw TAMSAT have scored lower POD,FB and HSS values, 0.49 ,0.84 and 0.42 and bias-corrected TAMSAT scored 0.716225488, 0.220670874, 0.920867473, 0.663972613 respectively. The POD result showed that more than 80% of the observed rainfall events from the rain gauge measurements were correctly detected by the CHRIPS, while raw TAMSAT correctly detected less than 49%, and the corrected TAMSAT detect more 71% of the rainfall from the rain gauge over data Genale Dawa. Considering continuous evaluation statistics all evaluation statistics (correlation(R), bias, RMSE NSE, and ME) are very good for CHRIPS and very poor for raw TAMSAT for all selected Stations. In general, the result shows a good agreement between the weather stations and satellite estimates. The overall performance of the CHRIPS and TAMSAT (before and after Bias Correction) at daily time scales is summarized in Table 4-8.

Table 4-8 Comparison of categorical Evaluation Statistics for raw, bias corrected TAMSAT and CHRIPS

	Product			
Evaluation Statistics		TAMSAT raw	TAMSAT Corr	CHRIPS
	POD	0.49	0.71	0.81
	FAR	0.40	0.22	0.05
	FB	0.84	0.92	0.86
	HSS	0.41	0.66	0.81
	R	0.45	0.88	0.88
	ME	0.11	0.05	-0.44
	BIAS	1.06	1.08	0.8
	RSME	7.6	3.70	3.5
	NSE	0.028	0.76	0.75

Figure 4.4 clearly shows that the inter-annual variation of rain observed by rain gauges was generally captured by both of satellite rainfall products for all selected stations. The CHRIPS product shows a small underestimation of annual maximum rainfall for the whole study period and all selected station from 39.9 to 6938.8 mm/yr, but shows better performance in capturing inter-annual variation of rainfall. TAMSAT product shows overestimation of annual maximum rainfall from 84.4 to 2054.81mm/yr for the whole study period when compared with Observed data. In capturing both magnitude and trend of annual rainfall bias corrected TAMSAT shows better performance. The detail was expressed in the annex table.

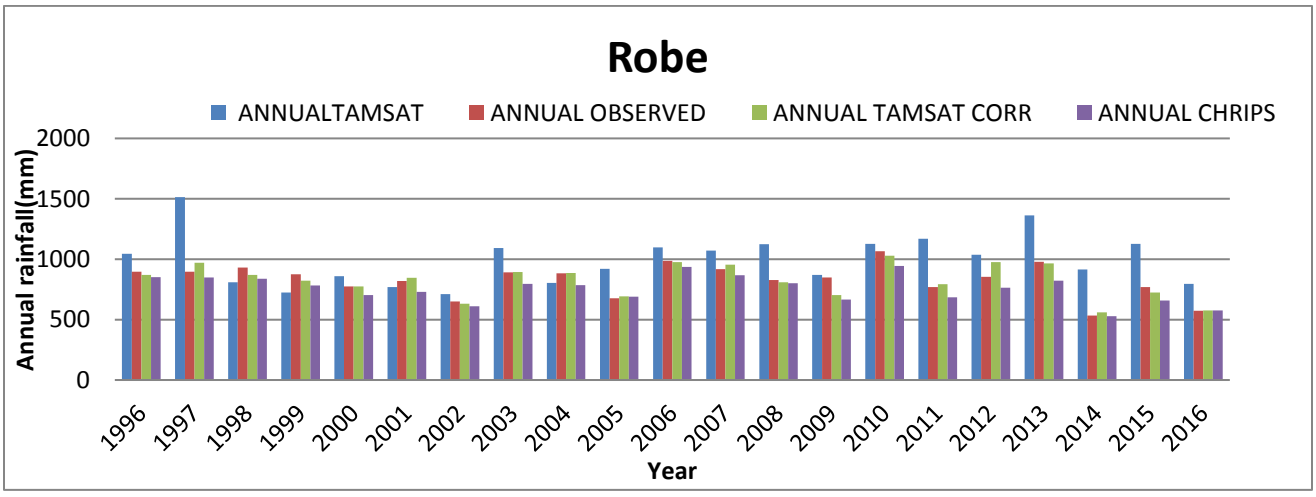

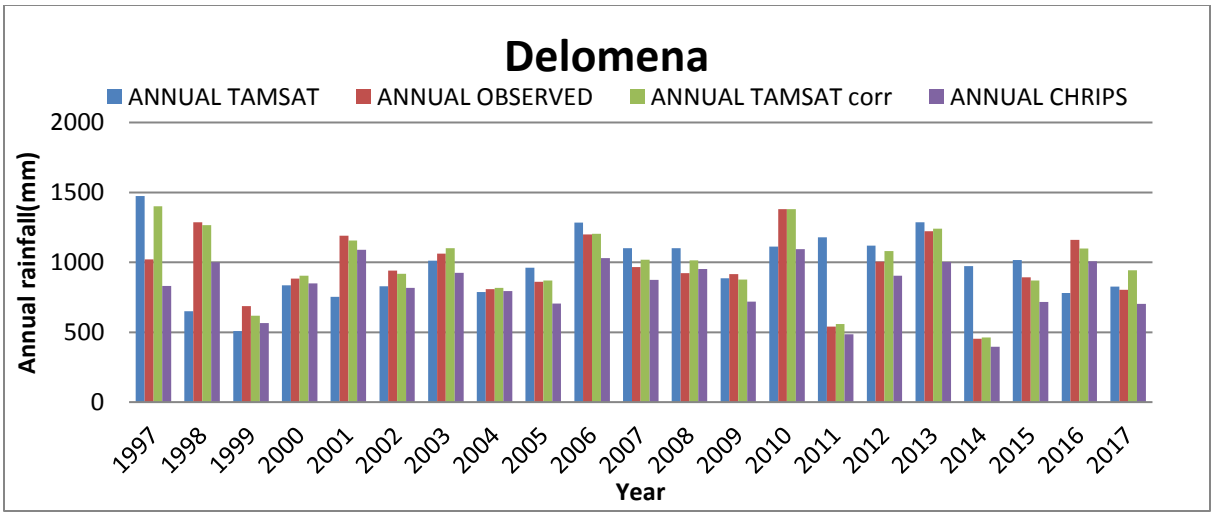
Delomena
ANNUAL TAMSAT
ANNUAL OBSERVED
ANNUAL TAMSAT corr
ANNUAL CHRIPS
Annual rainfall(mm)
2000
1500
1000
500
0
1997
1998
1999
2000
2001
2002
2003
2004
2005
2006
2007
2008
2009
2010
2011
2012
2013
2014
2015
2016
2017
Year

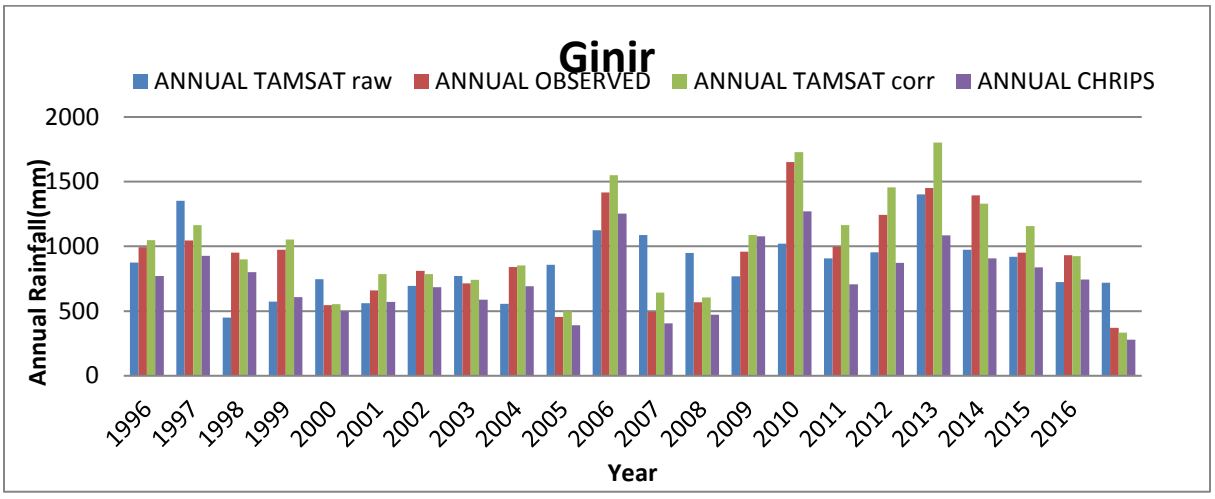
Ginir
ANNUAL TAMSAT raw
ANNUAL OBSERVED
ANNUAL TAMSAT corr
ANNUAL CHRIPS
Annual Rainfall(mm)
2000
1500
1000
500
0
1996
1997
1998
1999
2000
2001
2002
2003
2004
2005
2006
2007
2008
2009
2010
2011
2012
2013
2014
2015
2016
Year

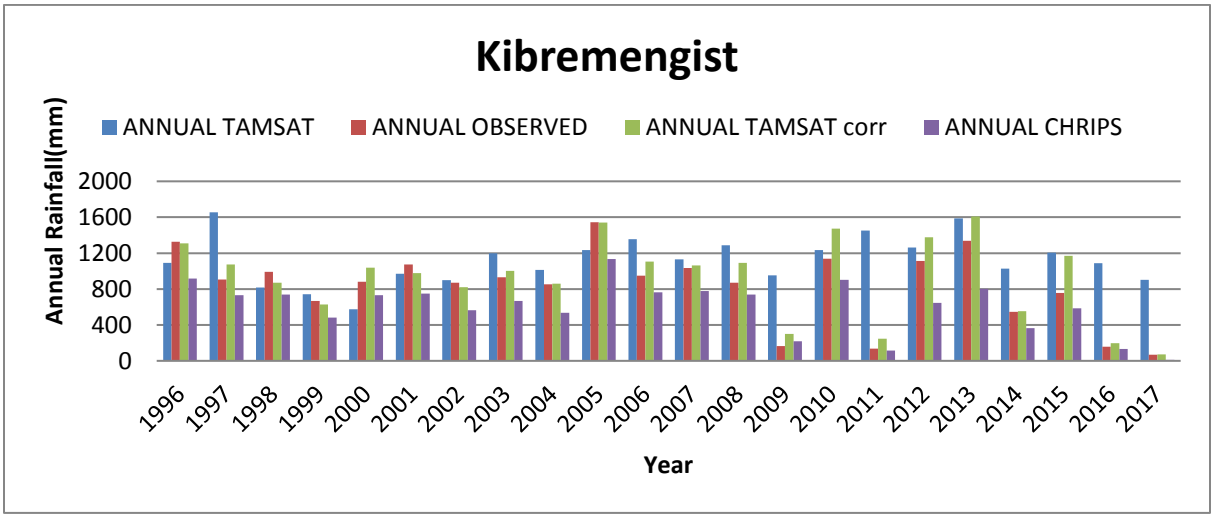
Kibremengist
ANNUAL TAMSAT
ANNUAL OBSERVED
ANNUAL TAMSAT corr
ANNUAL CHRIPS
Annual Rainfall(mm)
2000
1600
1200
800
400
0
1996
1997
1998
1999
2000
2001
2002
2003
2004
2005
2006
2007
2008
2009
2010
2011
2012
2013
2014
2015
2016
2017
Year

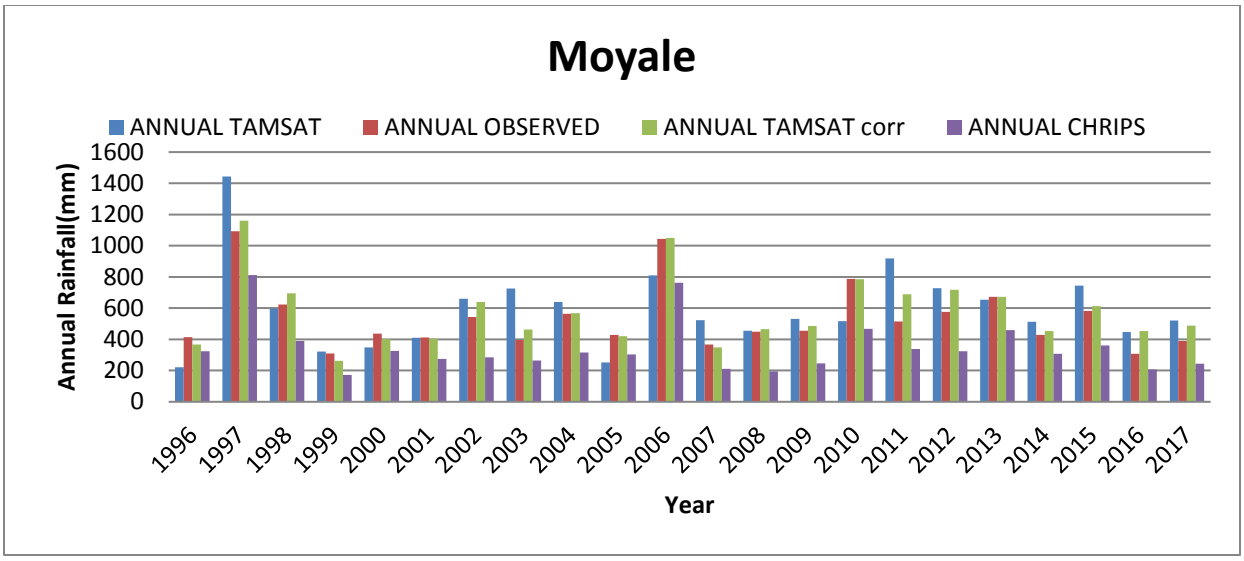
Moyale
ANNUAL TAMSAT
ANNUAL OBSERVED
ANNUAL TAMSAT corr
ANNUAL CHRIPS
Annual Rainfall(mm)
1600
1400
1200
1000
800
600
400
200
0
1996
1997
1998
1999
2000
2001
2002
2003
2004
2005
2006
2007
2008
2009
2010
2011
2012
2013
2014
2015
2016
2017
Year

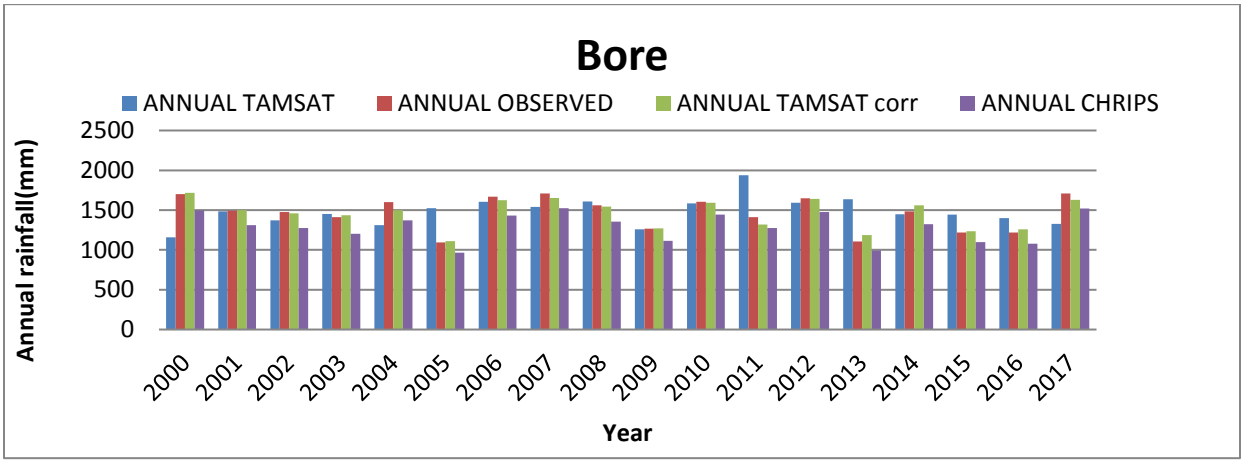
Bore
ANNUAL TAMSAT
ANNUAL OBSERVED
ANNUAL TAMSAT corr
ANNUAL CHRIPS
Annual rainfall(mm)
2500
2000
1500
1000
500
0
2000
2001
2002
2003
2004
2005
2006
2007
2008
2009
2010
2011
2012
2013
2014
2015
2016
2017
Year

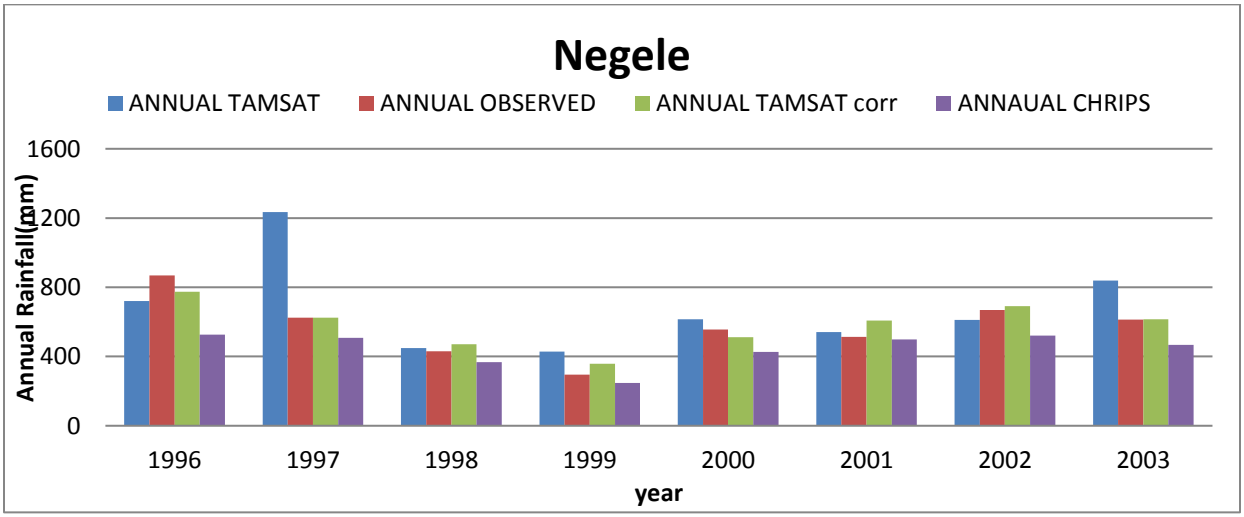
Negele
ANNUAL TAMSAT
ANNUAL OBSERVED
ANNUAL TAMSAT corr
ANNAUAL CHRIPS
Annual Rainfall(mm)
1600
1200
800
400
0
1996
1997
1998
1999
2000
2001
2002
2003
year

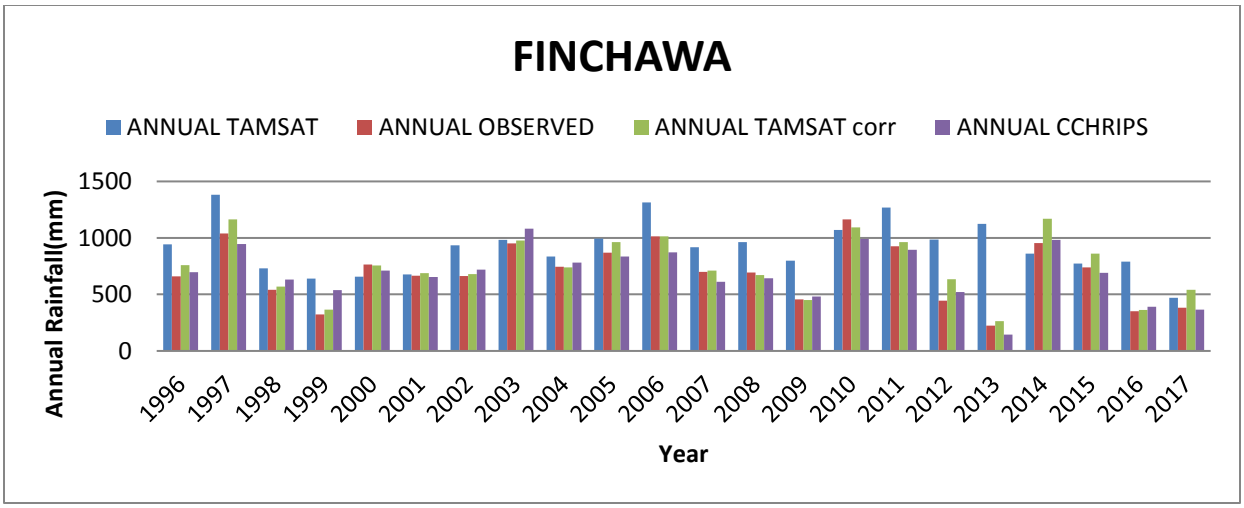

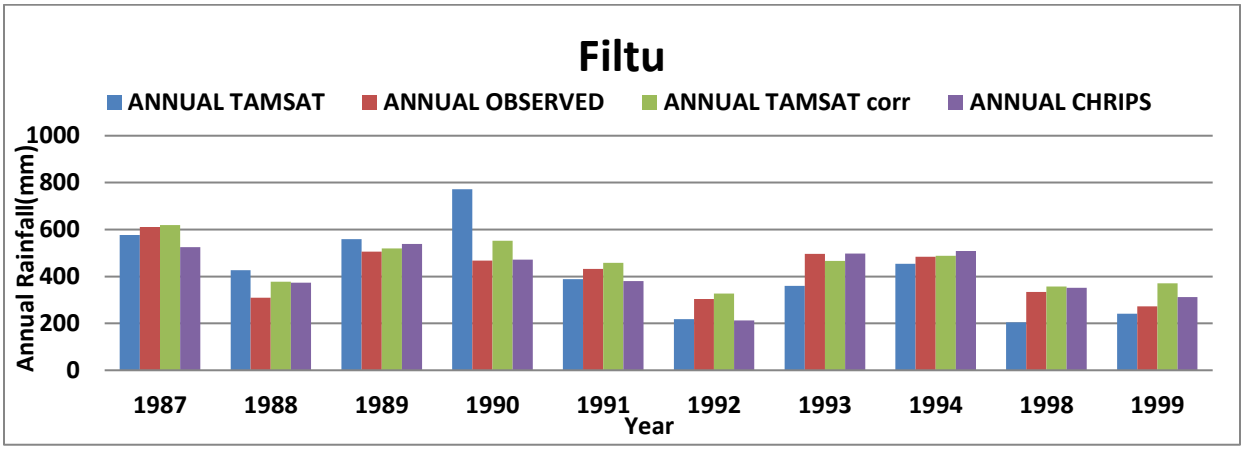

Figure 4-4 Annual rainfall over Genale Dawa obtained from rain gauge data and various satellite rainfall products

Figure 4.5 shows monthly mean rainfall analysis from various satellite rainfall products. The trend of monthly rainfall observed at rain gauges captured by both Bias corrected TAMSAT and CHRIPS satellite rainfall products. The monthly peak rainfall observed by rain gauge was underestimated in the range of 5.77 % to 30 % by CHRIPS for the whole station Stations by CHRIPS. Bias corrected TAMSAT overestimate monthly peak rainfall observed by rain gauge in the range of 0.75% to 3.94%for all stations except three stations; Robe, Bore, and Moyale Stations Which underestimate monthly peak by (2.16%,3.75%, and 5.89%) respectively.

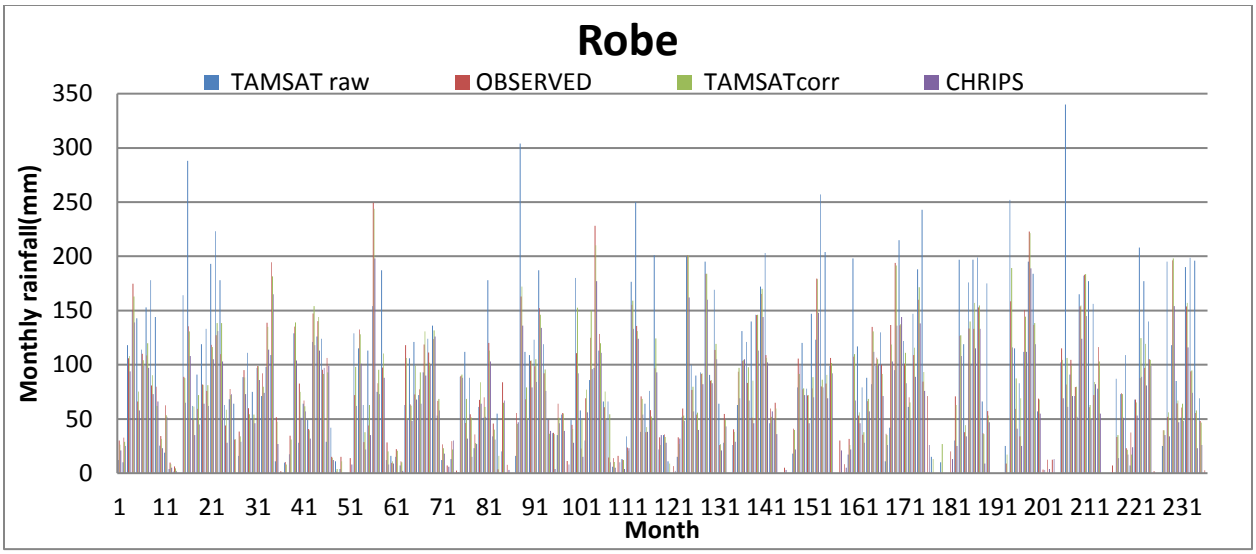
Robe
TAMSAT raw
OBSERVED
TAMSATcorr
CHRIPS
Monthly rainfall(mm)
350
300
250
200
150
100
50
0
1 11 21 31 41 51 61 71 81 91 101 111 121 131 141 151 161 171 181 191 201 211 221 231
Month

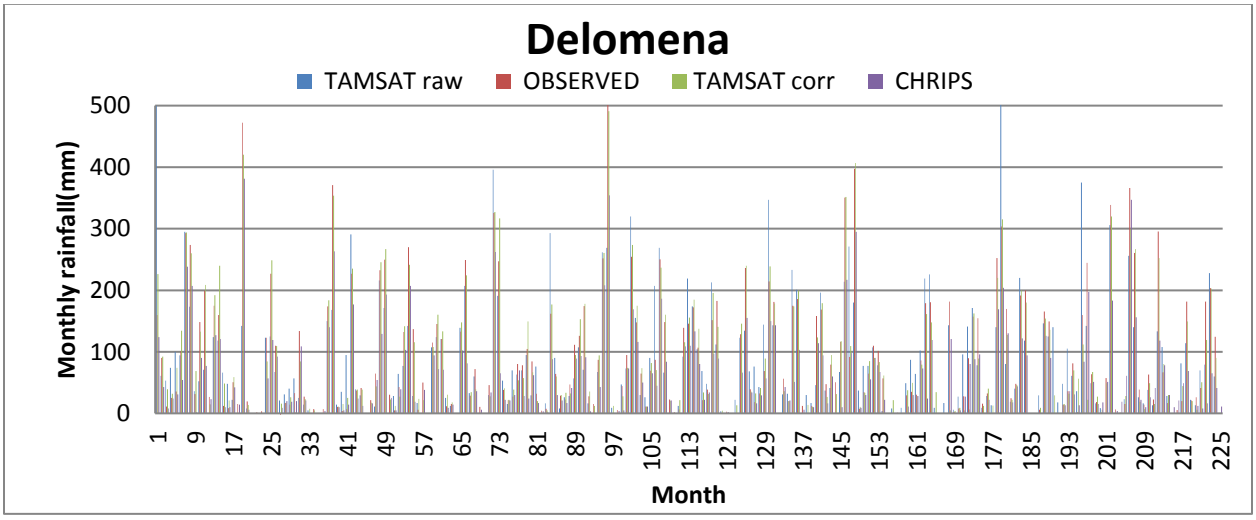
Delomena
TAMSAT raw
OBSERVED
TAMSAT corr
CHRIPS
Monthly rainfall(mm)
500
400
300
200
100
0
1 9 17 25 33 41 49 57 65 73 81 89 97 105 113 121 129 137 145 153 161 169 177 185 193 201 209 217 225
Month

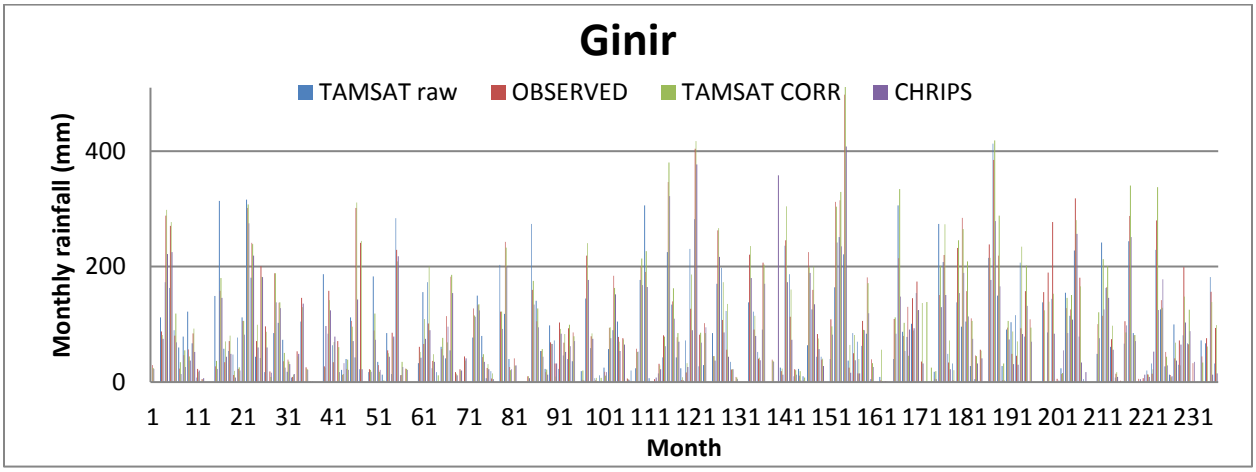
Ginir
TAMSAT raw
OBSERVED
TAMSAT CORR
CHRIPS
Monthly rainfall (mm)
400
200
0
1 11 21 31 41 51 61 71 81 91 101 111 121 131 141 151 161 171 181 191 201 211 221 231
Month

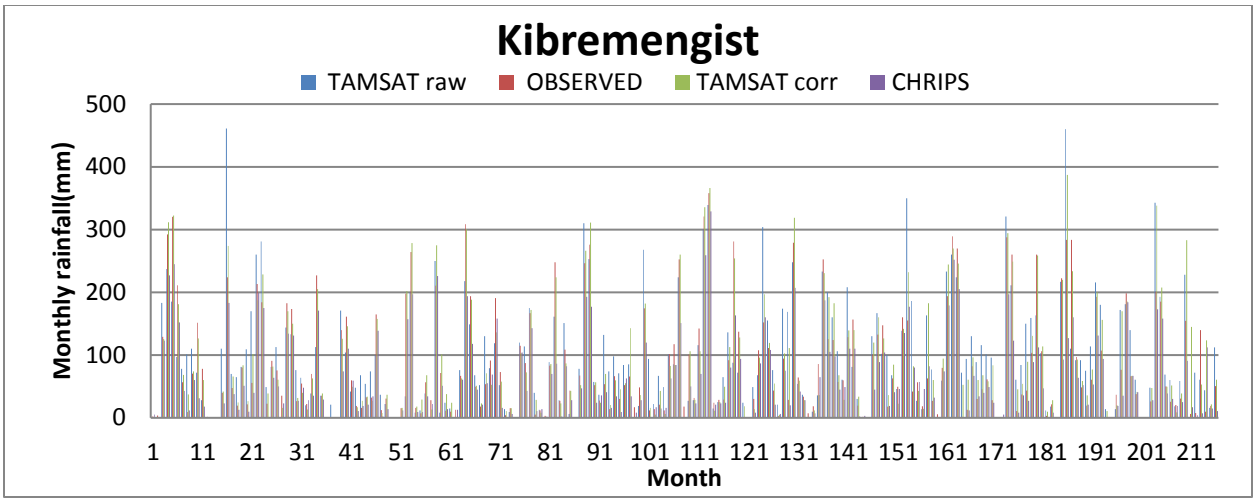
Kibremengist
TAMSAT raw
OBSERVED
TAMSAT corr
CHRIPS
Monthly rainfall(mm)
0
100
200
300
400
500
1 11 21 31 41 51 61 71 81 91 101 111 121 131 141 151 161 171 181 191 201 211
Month

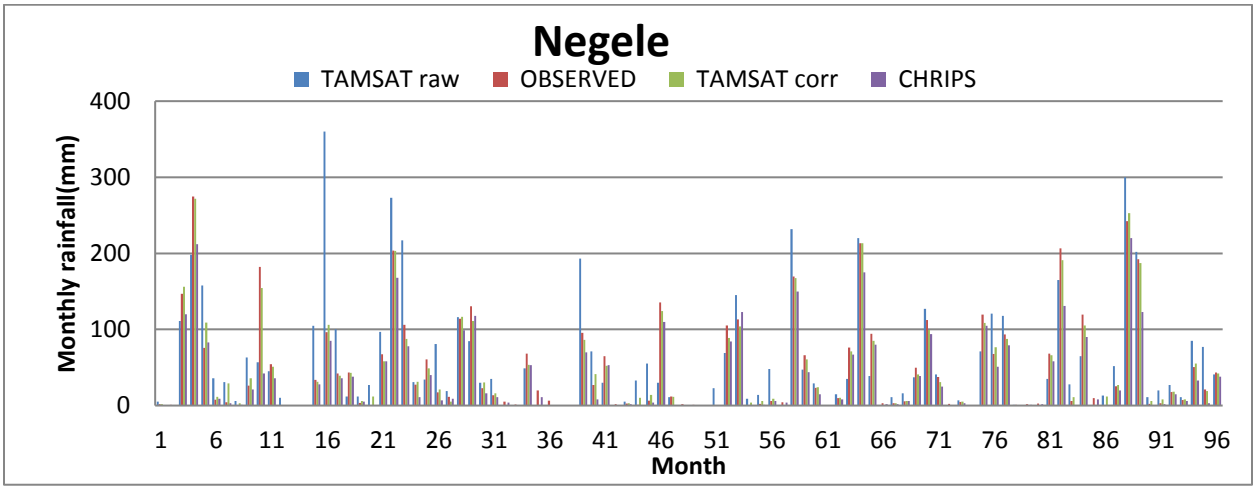
Negele
TAMSAT raw
OBSERVED
TAMSAT corr
CHRIPS
Monthly rainfall(mm)
0
100
200
300
400
1 6 11 16 21 26 31 36 41 46 51 56 61 66 71 76 81 86 91 96
Month

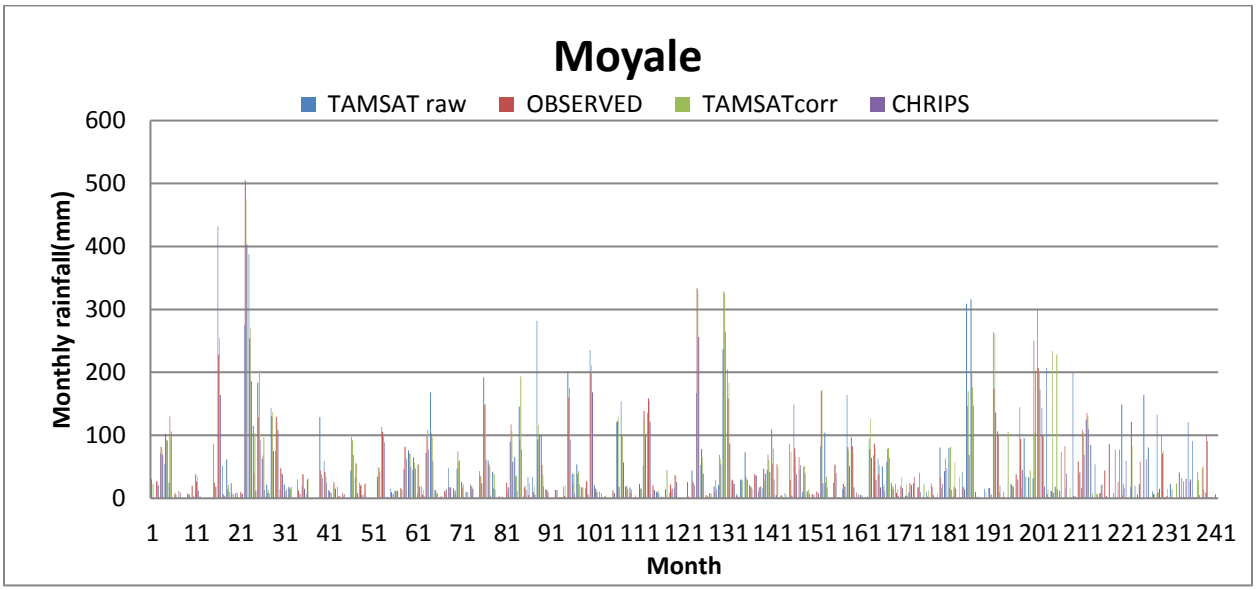
Moyale
TAMSAT raw
OBSERVED
TAMSATcorr
CHRIPS
Monthly rainfall(mm)
0
100
200
300
400
500
600
1 11 21 31 41 51 61 71 81 91 101 111 121 131 141 151 161 171 181 191 201 211 221 231 241
Month

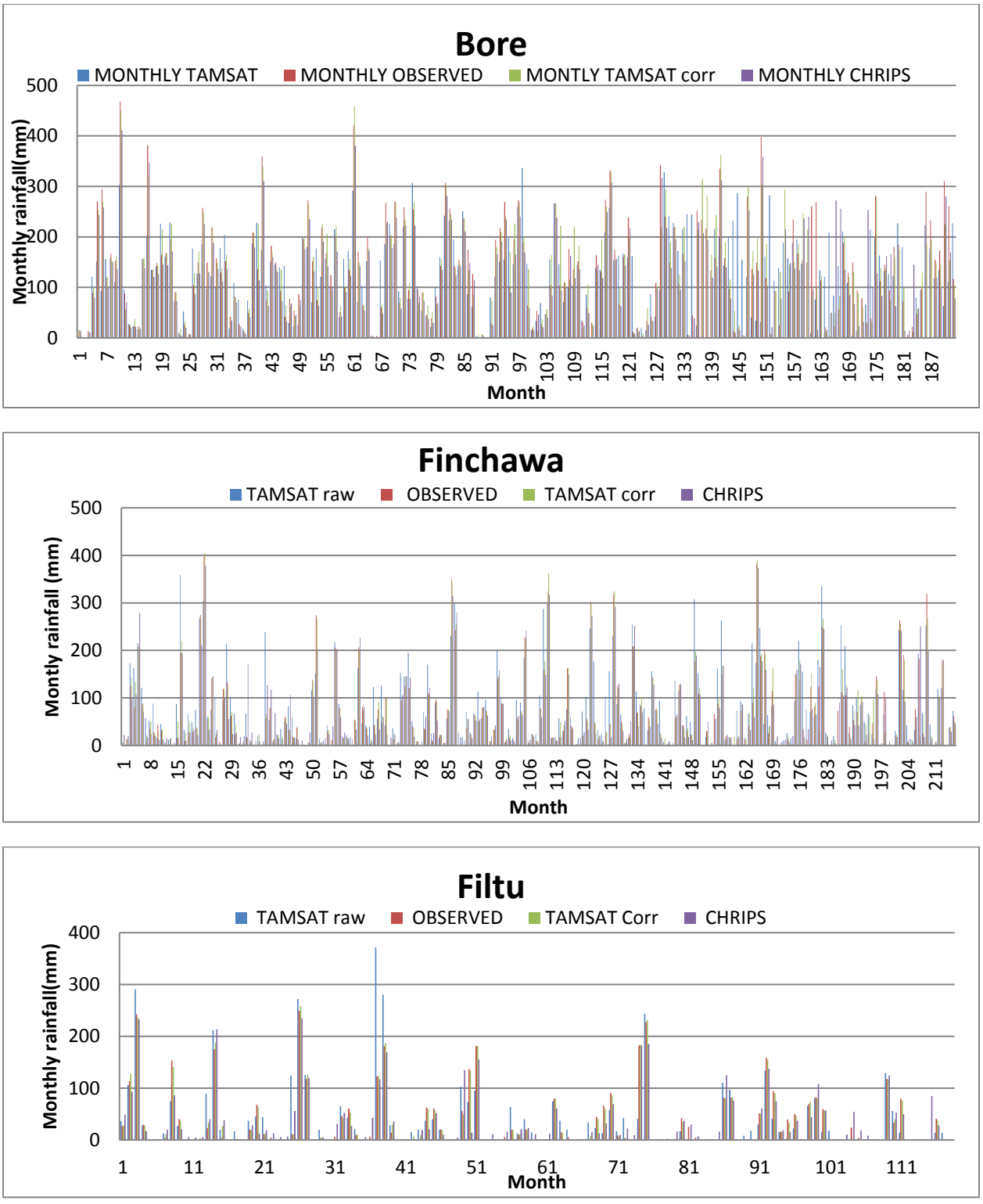

Figure 4-5 Monthly rainfall over Genale Dawa obtained from rain gauge data and various satellite rainfall products

Figure 4.6 presents inter-comparison of mean monthly rainfall data for rainfall estimates. The mean monthly maximum rainfall has the same trend as observed data. The rainfall maximum is in April with a secondary maximum in October for each location and the minimum are in January and July for each location. Compared to rain gauges values, CHRIPS satellite rainfall products underestimated the monthly rainfall in the range 0.84% to28.5 %, While TAMSAT over estimated in the range 0.52% to 30%. The detail is presented in the Appendix table.

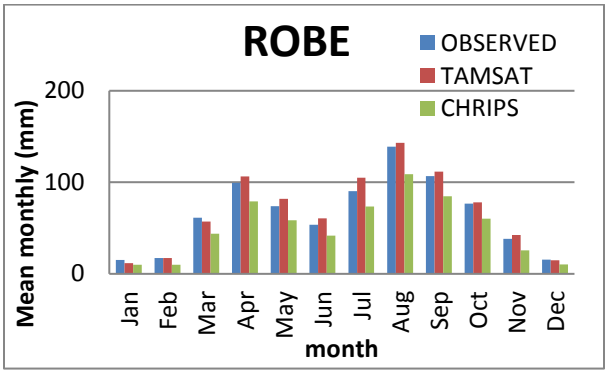

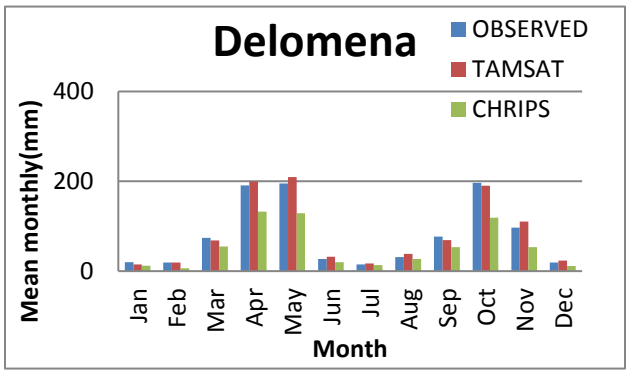

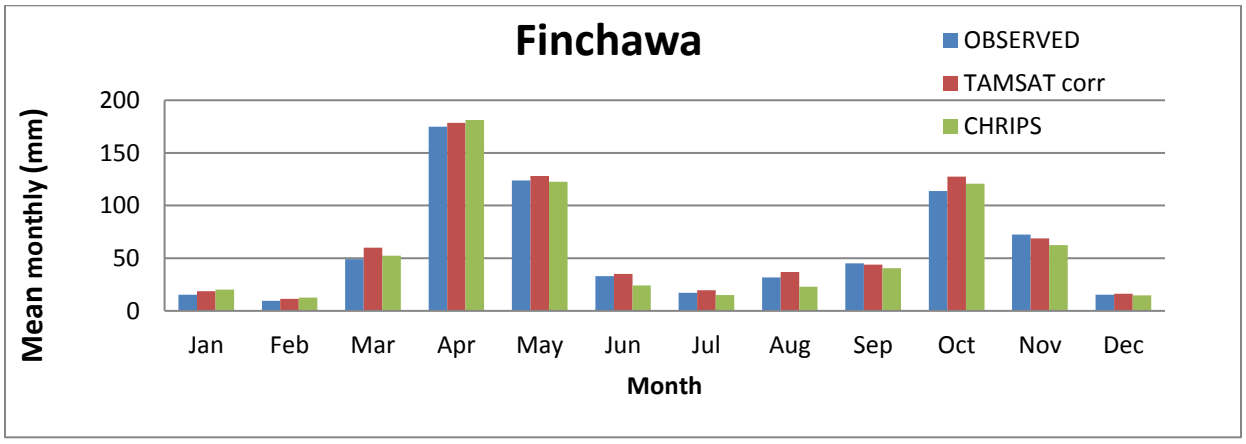

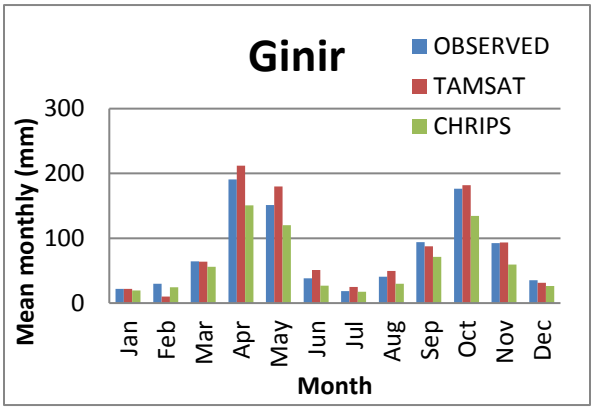

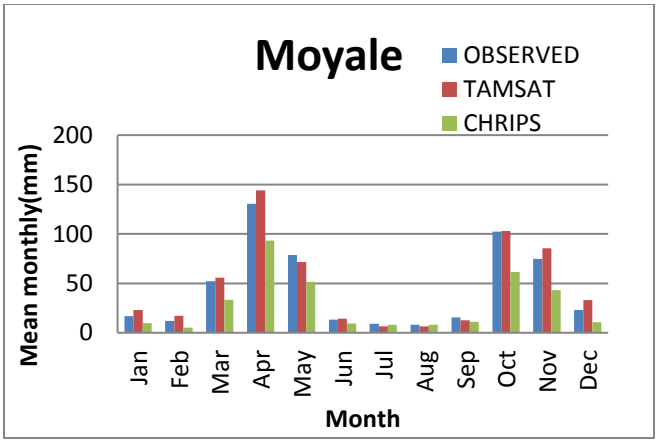

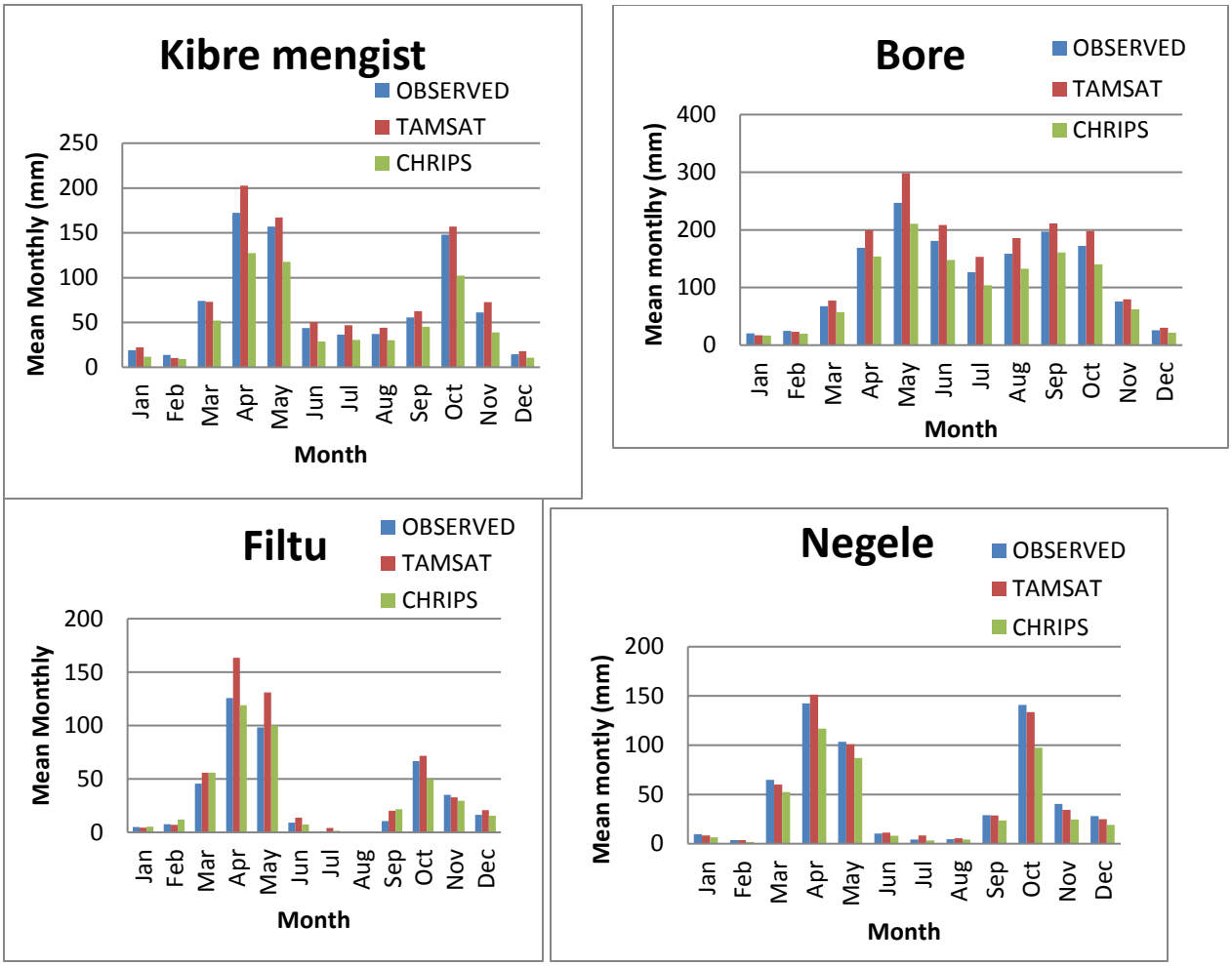

Figure 4-6 Mean monthly rainfall over Genale Dawa obtained from rain gauge data and various satellite rainfall products

Figure 4.7 presents inter-comparison of daily rainfall estimates. The comparison statistics (R = Pearson's correlation coefficient) are given in each plot. Correlations between satellite rainfall values and rain gauge values were very good which ranges (0.8064 – 0.9614) for CHRIPS and (0.827-0.951) for TAMSAT for Selected nine stations. For each station (R = Pearson's correlation coefficient) is presented in the corresponding figure and the detail of other continuous, and categorical evaluation statistics were presented in Appendix

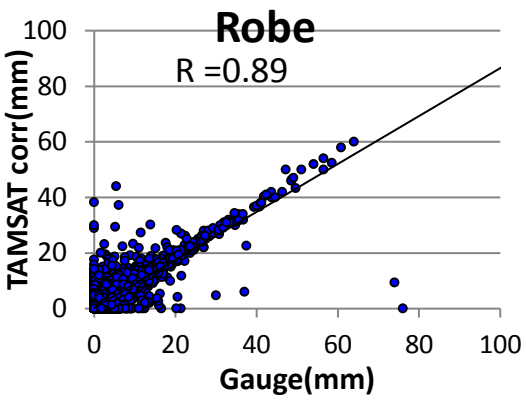
Robe
R =0.89
TAMSAT corr(mm)
Gauge(mm)
0
20
40
60
80
100

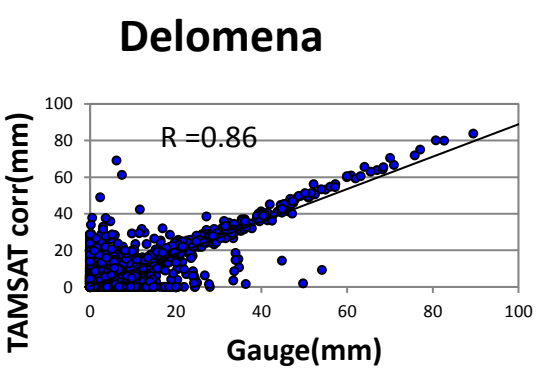
Delomena
R =0.86
TAMSAT corr(mm)
Gauge(mm)
0
20
40
60
80
100

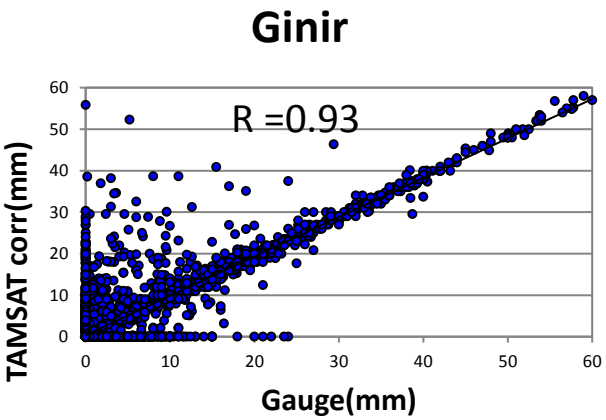
Ginir
R =0.93
TAMSAT corr(mm)
Gauge(mm)
0
10
20
30
40
50
60

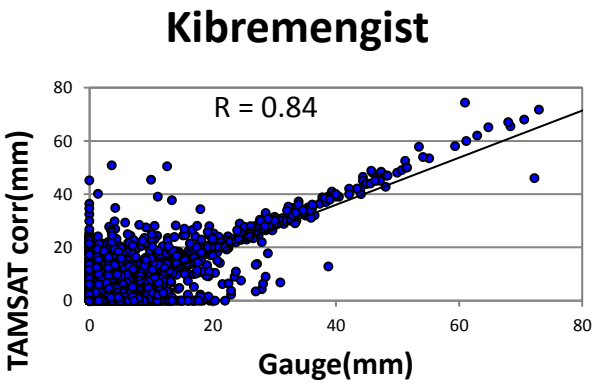
Kibremengist
R = 0.84
TAMSAT corr(mm)
Gauge(mm)
0
20
40
60
80

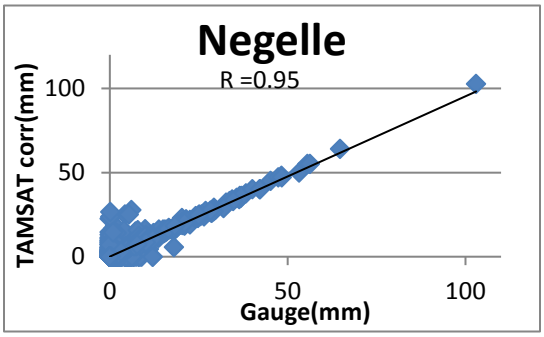
Negelle
R =0.95
TAMSAT corr(mm)
Gauge(mm)
0
50
100

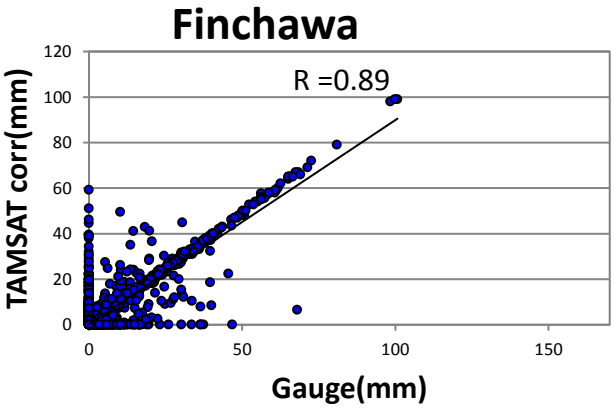
Finchawa
R =0.89
TAMSAT corr(mm)
Gauge(mm)
0
20
40
60
80
100
120
0
50
100
150

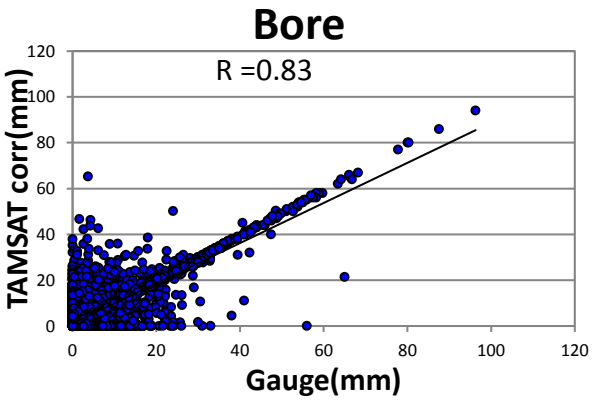
Bore
R =0.83
TAMSAT corr(mm)
Gauge(mm)
0
20
40
60
80
100
120

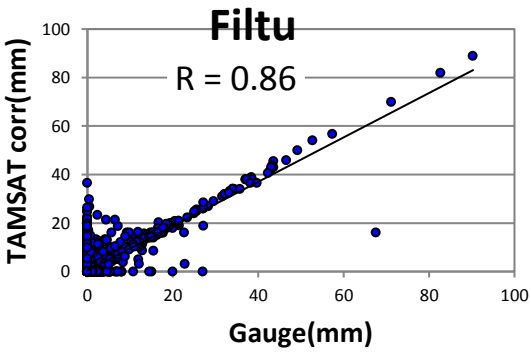
Filtu
R = 0.86
TAMSAT corr(mm)
Gauge(mm)
0
20
40
60
80
100

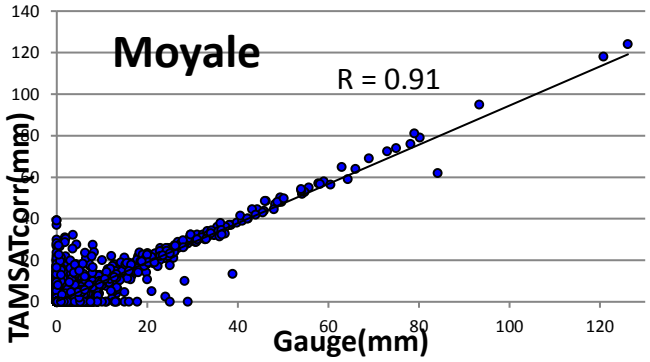
Moyale
R = 0.91
TAMSATcorr(mm)
Gauge(mm)
0
20
40
60
80
100
120
140

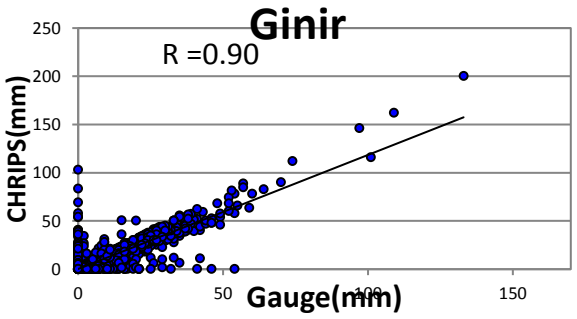
Ginir
R =0.90
CHRIPS(mm)
Gauge(mm)
0
50
100
150
200
250

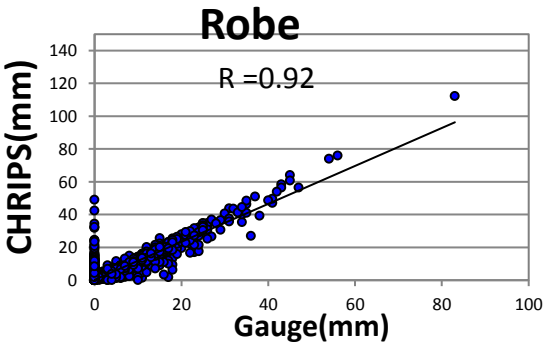
Robe
R =0.92
CHRIPS(mm)
Gauge(mm)
0
20
40
60
80
100
120
140

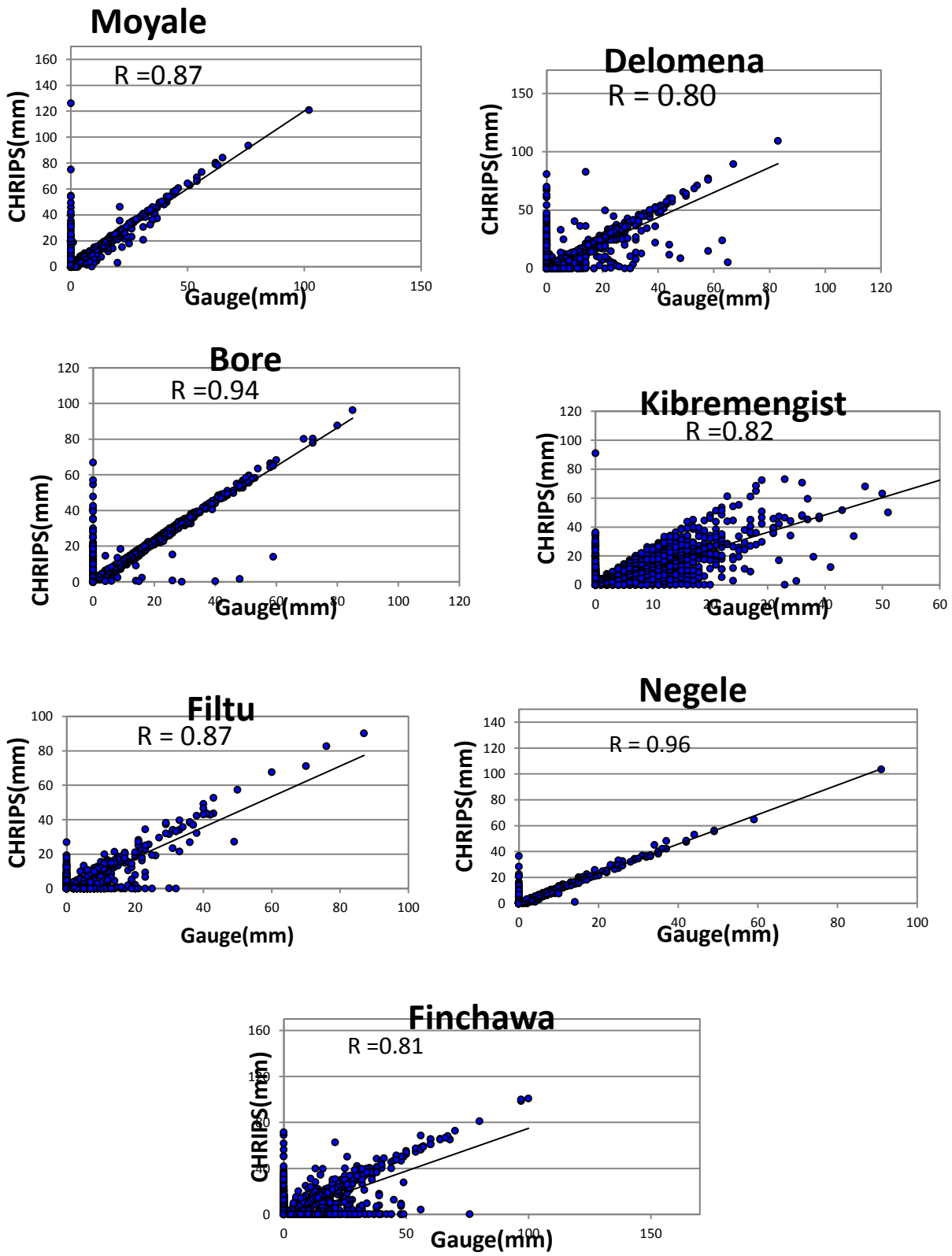

Figure 4-7 Intercomparison of daily rainfall from satellite rainfall products and rain gauge Genale Dawa river basin

The above comparison, especially the daily basis is very important in our case because Arc SWAT uses daily observed rainfall data. Therefore, both CHRIPS and TAMSAT rainfall estimates gave a very good result, and this result also consistent with findings in Eastern parts of Ethiopia (27). There have been subsequent studies that conducted in Ethiopia to evaluate satellite rainfall products in the estimation of rainfall, (54), (27) (18), (20) (55); based on their studies and the result of this study, it is concluded that TAMSAT and CHRIPS are much closer to the actual rainfall fields in Ethiopian basins.

4.5 Model Calibration and Validation

Base flow and surface flow was separated using the automated digital filter methods based on the daily flow data measured at the outlet of the Genale Dawa River Basin. The base flow separation technique indicated that about 29.8% of the total water yield was contributed from the subsurface water source which was less than surface runoff involvement for the total water yield at the outlet of the watershed for CHRIPS product and 29% of the total water yield was contributed from the subsurface water source which was again less than surface runoff involvement for the total water yield at the outlet of the watershed for TAMSAT. The model was run for a period of thirty five years January 1, 1983 to December 31, 2017. However, the first three years of the recording period were used for stabilization of model runs (warm up period). The calibration was performed for a period of six years on daily bases. The general hydrological water balance and hydrological parameters estimated for nine representative stations are presented below in the table.

Table 4-9 **Hydrological water balance ratio and hydrological parameters**

Hydrological water balance ratio and hydrological parameters									
		CHRIPS							
Hydrology (Water balance ratio)	Bore	Delomena	Filtu	Finchawa	Ginir	KibreMeng	Moyale	Negele	Robe
Streamflow/Precip	0.33	0.34	0.32	0.28	0.33	0.35	0.29	0.3	0.34
Base flow/total flow	0.27	0.29	0.28	0.3	0.32	0.27	0.32	0.33	0.3
Surface Run-off/total flow	0.73	0.71	0.72	0.7	0.68	0.73	0.68	0.67	0.7
Percolation/precipitation	0.12	0.12	0.11	0.1	0.12	0.12	0.1	0.1	0.1
Deep recharge/precipitation	0.01	0.01	0.01	0.01	0.01	0.01	0.01	0.01	0.01
ET/precipitation	0.66	0.65	0.67	0.71	0.66	0.64	0.7	0.69	0.65
		TAMSAT							
Hydrology (Water balance ratio)	Bore	Delomena	Filtu	Finchawa	Ginir	KibreMeng	Moyale	Negele	Robe
Streamflow/Precip	0.28	0.3	0.32	0.33	0.33	0.34	0.3	0.29	0.33
Base flow/total flow	0.28	0.27	0.29	0.3	0.31	0.27	0.3	0.29	0.3
Surface Run-off/total flow	0.72	0.73	0.71	0.7	0.69	0.73	0.7	0.71	0.7
Percolation/precipitation	0.12	0.12	0.11	0.12	0.12	0.1	0.12	0.11	0.12
Deep recharge/precipitation	0.01	0.01	0.01	0.01	0.01	0.01	0.01	0.01	0.01
ET/precipitation	0.71	0.69	0.67	0.66	0.66	0.65	0.67	0.71	0.66

			CHRIPS							
	Hydrological parameters	Bore	Delomena	Filtu	Finchawa	Ginir	KibreMeng	Moyale	Negele	Robe
	Average Curve Number	76.22	75.62	75.57	84.86	85.48	86.27	84.73	84.58	78.38
	ET and transpiration	116.2	116.2	121.1	118.6	117.6	116.2	119.4	122.1	117.3
	Precipitation	229.8	229.8	229.8	229.8	229.8	229.8	229.8	229.8	229.8
	Surface run-off	80.42	78.14	75.1	73.32	76.28	80.74	71.92	68.98	86.76
	Lateral Flow	0.1	0.1	0.1	0.1	0.1	0.1	0.1	0.11	3.15
	Return Flow	16.39	18.51	16.02	20.3	18.74	16.04	20.55	20.55	21.74
	Percolation to Shallow aquifer	33.28	35.07	33.7	37.96	35.99	32.96	38.55	38.84	22.88
	Recharge to deep aquifer	1.66	1.78	1.68	1.9	1.8	1.65	1.93	1.94	1.14
	Revaporation from shallow aquifer	15.82	15.82	15.82	15.82	15.82	15.82	15.82	15.82	15.8
			TAMSAT							
	Hydrological parameters	Bore	Delomena	Filtu	Finchawa	Ginir	KibreMeng	Moyale	Negele	Robe
	Average Curve Number	83.36	83.47	87.02	87.16	86.51	86.44	87.08	83.6	83.75
	ET and transpiration	254.3	254.3	254.1	254.1	254.2	254.2	254.2	254	253.8
	Precipitation	630.8	630.8	630.8	630.8	630.8	630.8	630.8	630.8	630.8
	Surface run-off	252.05	254.5	261.63	262.47	259.3	258.77	261.55	260.78	262.14
	Lateral Flow	2.11	2.11	1.96	1.95	1.97	1.98	1.95	2.07	2.06
	Return Flow	96.82	96.37	88.84	88.03	91.03	91.57	88.94	88.49	86.97
	Percolation to Shallow aquifer	121.66	121.21	112.53	111.71	114.7	115.23	112.52	113.34	111.83
	Recharge to deep aquifer	6.08	6.06	5.65	5.59	5.73	5.76	5.63	5.67	5.59
	Revaporation from shallow aquifer	14.07	14.07	14.07	14.07	14.07	14.07	14.07	14.07	14.07

Model parameters were first calibrated manually for the four gauge station (Dawa at Melka Guba, Welmel at Melka Amana, Dimtu near Bore and Genale at Hawlen) which was very time consuming process, followed by automatic calibration using SUFI-2, an auto calibration tool which is embedded in SWAT 2012. The calibration processes considered 18 flow parameters (Table 3.8) and their values were varied iteratively within the allowable ranges until satisfactory agreement between measured and simulated stream flow was obtained. The auto calibration processes significantly improved model efficiency. Table 4.9 illustrates the final calibrated and fitted values. The result from different statistical method of model performance evaluation met the criteria of NSE > 0.5, R^2 > 0.6 and Pbias = ±15%.

The statistical results of the model performance for calibration periods on monthly time steps are summarized in Table 4.10.The calibration results in Table 4.10 show that there is a good agreement between the simulated and measured monthly flows. Percent of error of the observed and simulated monthly flows at the four gauge stations are (2.8 - 8.2) % for CHRIPS product and (-11.6 - 3.6) % for TAMSAT product which is well within the acceptable range of ±15%. Further a good agreement between observed and simulated daily flows are shown by the coefficient of determinations (R^2 =0.84 - 0.88) for CHRIPS and (R^2 =0.71 - 0.95) for TAMSAT and the Nash-Suttcliffe simulation efficiency (NSE=0.78-0.86) for CHRIPS and (NSE=0.7 - 0.92) for TAMSAT thus fulfilled the requirements suggested by Santhi., *et al*. (2001) for R >0.6 and ENS> 0.5.

Validation of the model was carried out using an independent data set for four years from 2004-

2007 without making further adjustments of sensitive parameters. As it can be seen from the Table 4.10 there is good agreement between daily observed and simulated flows at four gauge stations. The percent of error between the observed and simulated daily flow are (-0.82 - 3) % for CHRIPS and (-14 - 0.3) % for TAMSAT. Thus it is found within the tolerable range of ±15%. The coefficient of determinations (R^2) was found to be (0.72 - 0.93) for CHRIPS and (0.81 -0.87) for TAMSAT respectively and Nash-Suttcliffe simulation efficiency (NSE) was (0.7 - 0.95) for CHRIPS and (0.76 -0.88) for TAMSAT respectively. These shows a very good correlation of the simulation results with the observed values. Furthermore, figure 4.8 up to figure 4.11 shows the hydrograph of daily observed and simulated flows.

Generally there is a good fit between measured and simulated output and a slight over estimation of the low flows and under estimation of the peak flows were observed at the validation period. Since the model performed as well in the validation period, as for the calibration period hence, the set of optimized parameters listed in Table 4.11 and Table 4.12 during calibration process for Genale Dawa River Basin can be taken as the representative set of parameters for the basin. Thus, the validation check illustrates the accuracy of the model for simulating time-periods outside of the calibration period. The model performed as good in the validation period (2004-2007), as for the calibration period (1998-2003) at the four gauge stations as indicated in Table 4.9. Hence, the set of optimized parameters used during calibration process can be taken as the representative set of parameter to explain the hydrologic characteristic of the Genale Dawa River Basin and further simulations using SWAT model can be carried out by using these parameters for any period of time.

Table 4-10 Model performance statistics for the Genale Dawa River Basin at Four discharge gauging stations.

		Calibration (1998-2003)				Validation(2004-2007)			
Product	Criteria	Dawa at Melka Guba	Welmel at Melka Amana	Dimtu Nr Bore	Genale at Hawlen	Dawa at Melka Guba	Welmel at Melka Amana	Dimtu Nr Bore	Genale at Hawlen
CHRIPS	R2	0.86	0.84	0.88	0.86	0.83	0.93	0.72	0.97
	NSE	0.84	0.78	0.85	0.86	0.80	0.89	0.7	0.95
	PBIAS	8.2	6.6	4.6	2.8	-0.82	3	0.7	1.2
	RSR	0.42	0.51	0.38	0.38	0.34	0.28	0.55	0.13
TAMSAT	R2	0.95	0.79	0.81	0.71	0.87	0.83	0.88	0.81
	NSE	0.92	0.73	0.8	0.7	0.83	0.77	0.88	0.76
	PBIAS	-11.5	3.6	2	-4	-4.8	0.3	-2.3	-17.4
	RSR	0.27	0.52	0.44	0.55	0.4	0.42	0.35	0.49

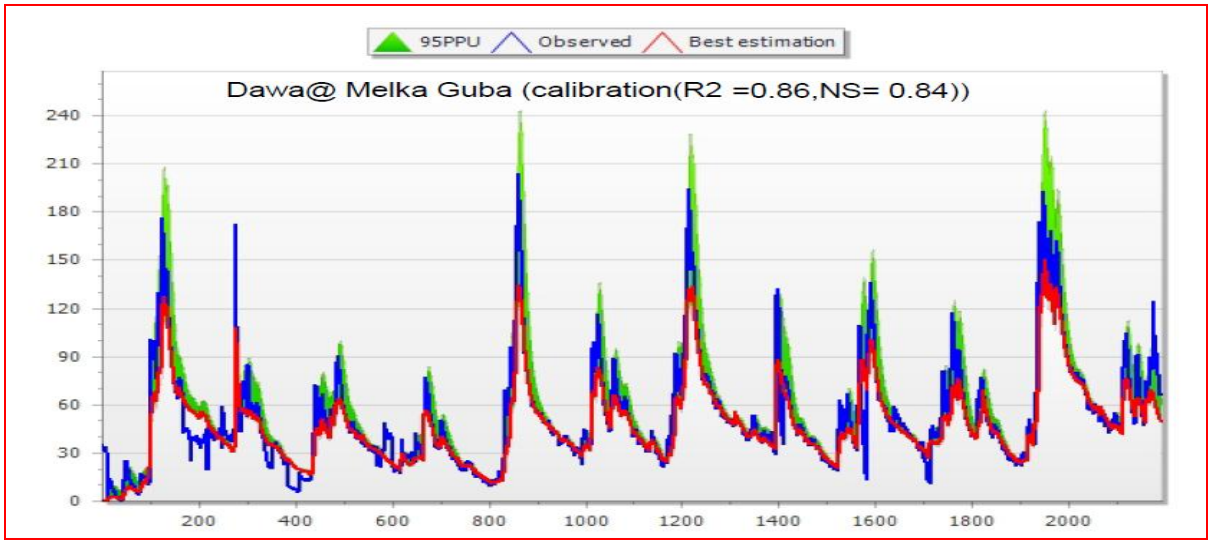
95PPU
Observed
Best estimation
Dawa@ Melka Guba (calibration(R2 =0.86,NS= 0.84))
240
210
180
150
120
90
60
30
0
200
400
600
800
1000
1200
1400
1600
1800
2000

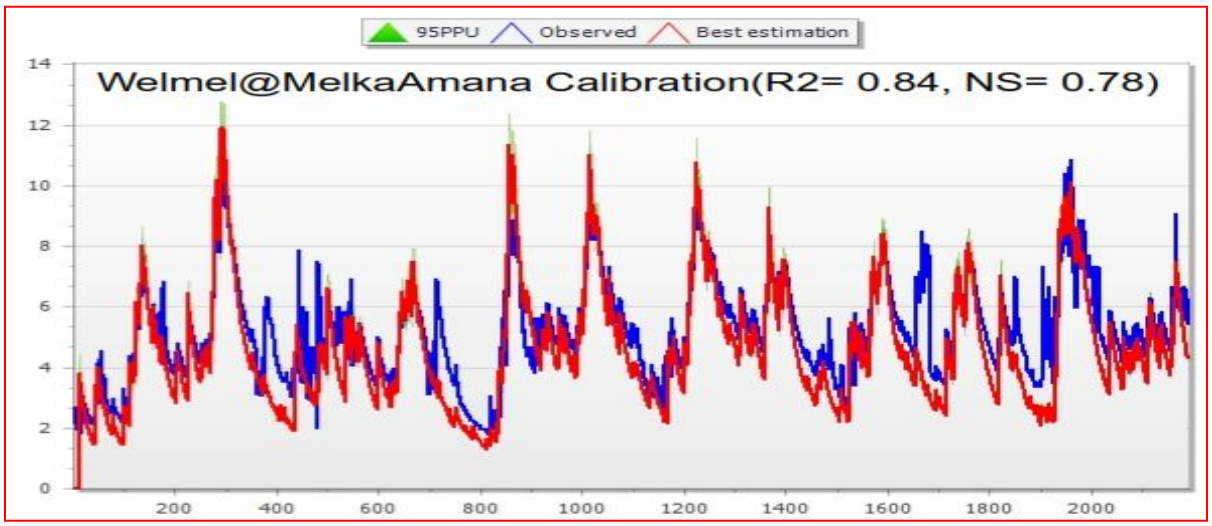
95PPU
Observed
Best estimation
Welmel@MelkaAmana Calibration(R2= 0.84, NS= 0.78)
14
12
10
8
6
4
2
0
200
400
600
800
1000
1200
1400
1600
1800
2000

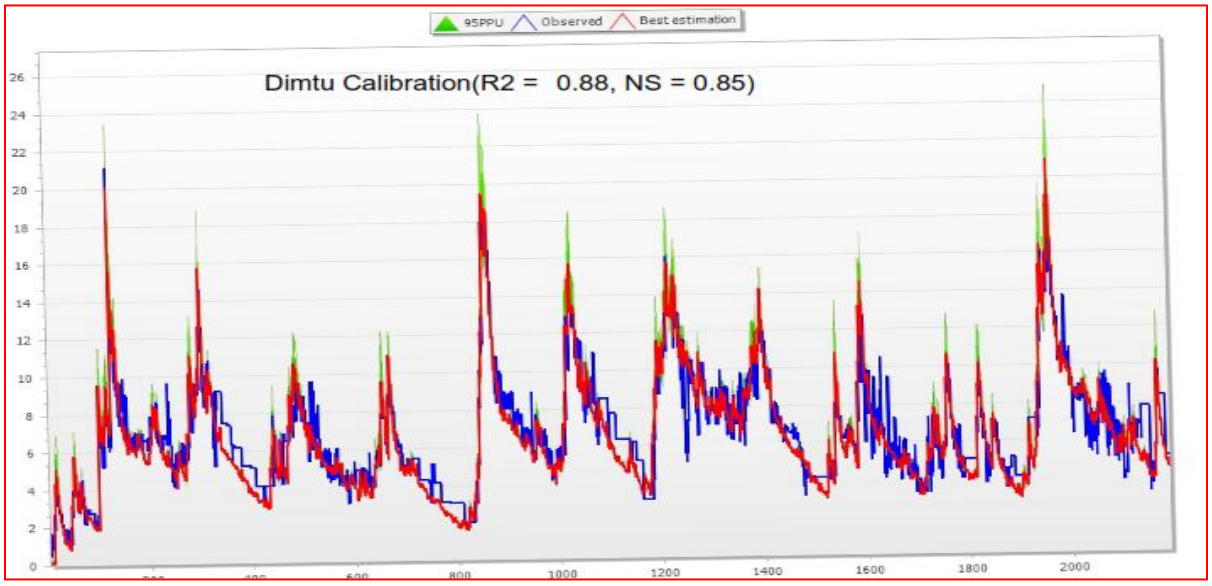
95PPU
Observed
Best estimation
Dimtu Calibration(R2 = 0.88, NS = 0.85)
26
24
22
20
18
16
14
12
10
8
6
4
2
0

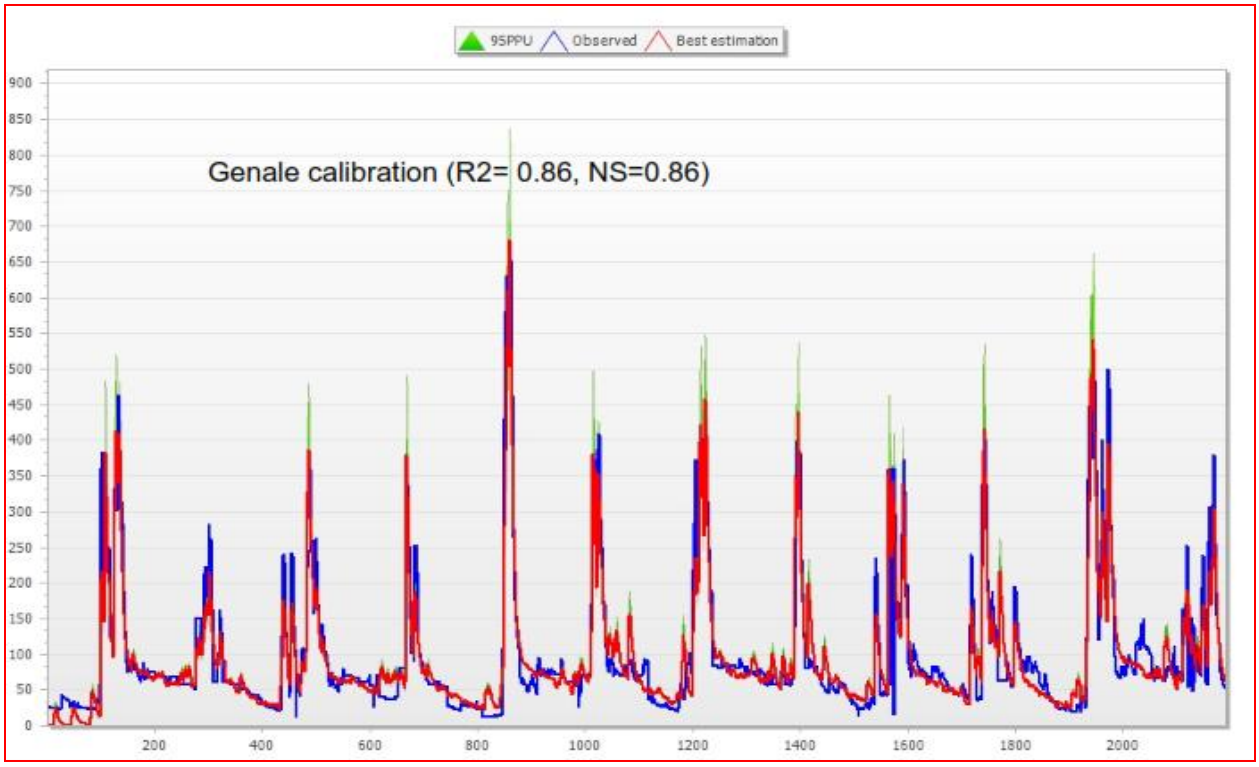

Figure 4-8 Calibration of model for CHRIPS Rainfall product

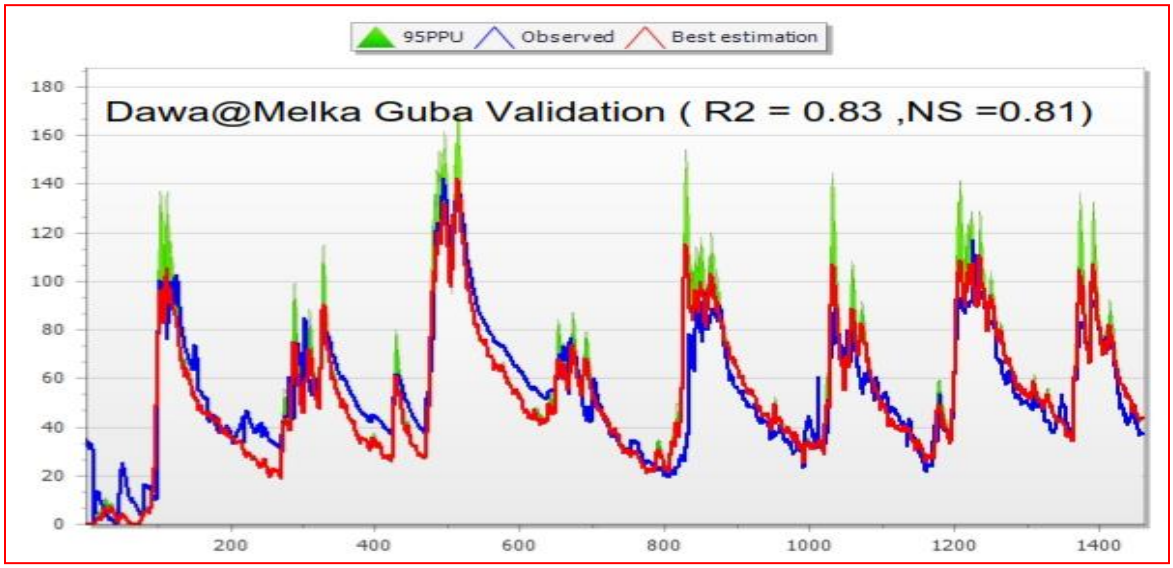

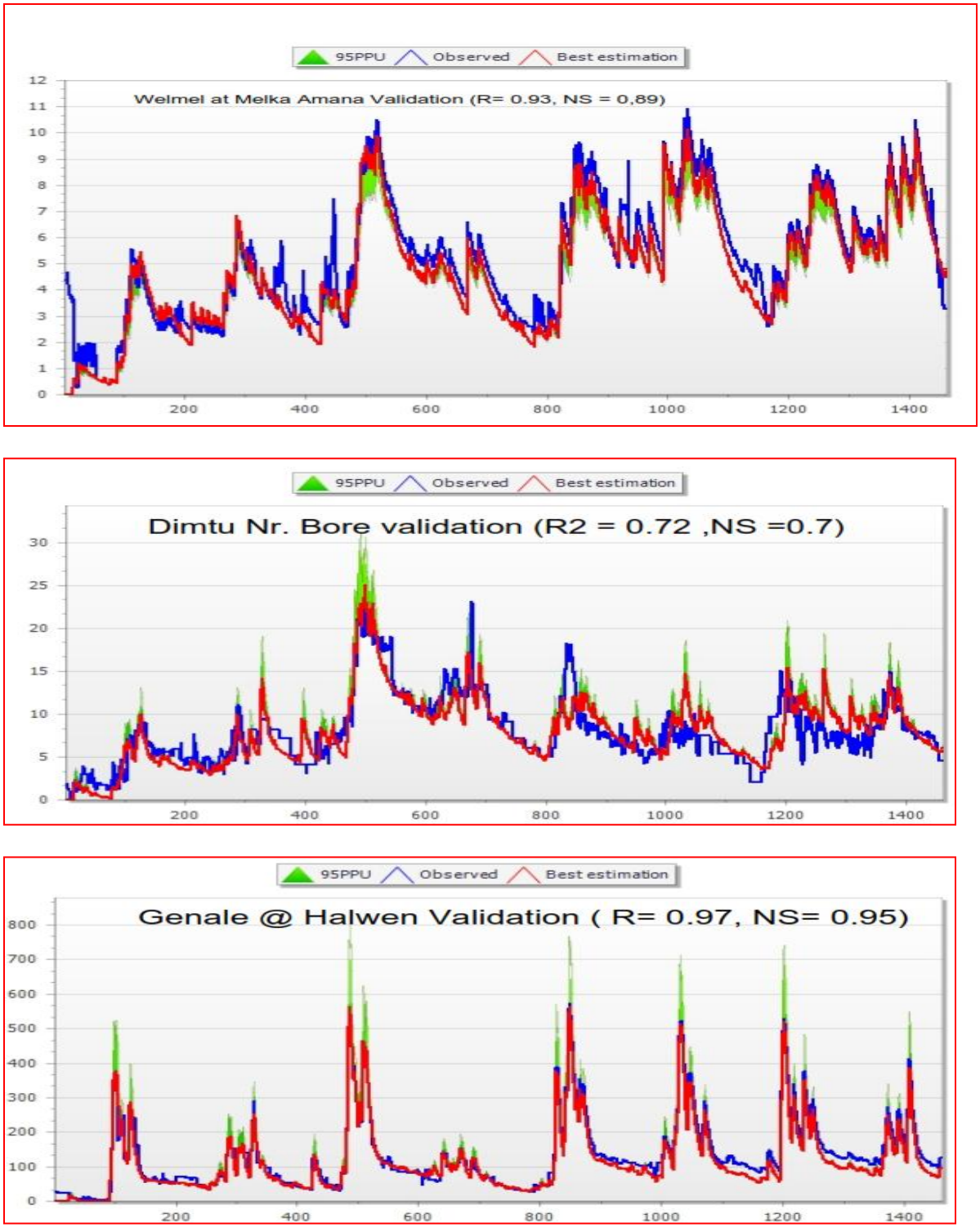

Figure 4-9 Validation of model for CHRIPS Rainfall product

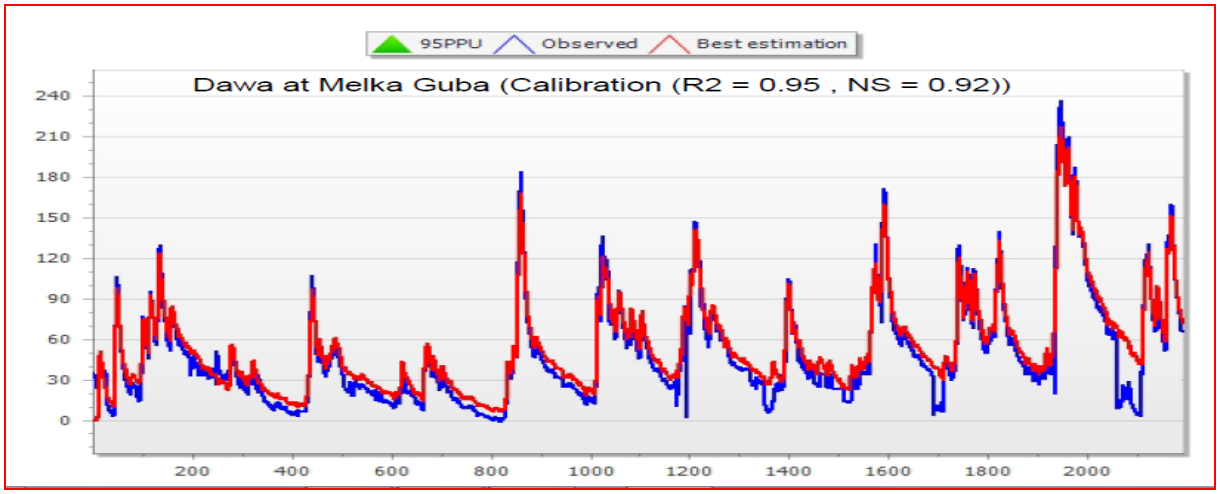
95PPU
Observed
Best estimation
Dawa at Melka Guba (Calibration (R2 = 0.95 , NS = 0.92))
240
210
180
150
120
90
60
30
0
200
400
600
800
1000
1200
1400
1600
1800
2000

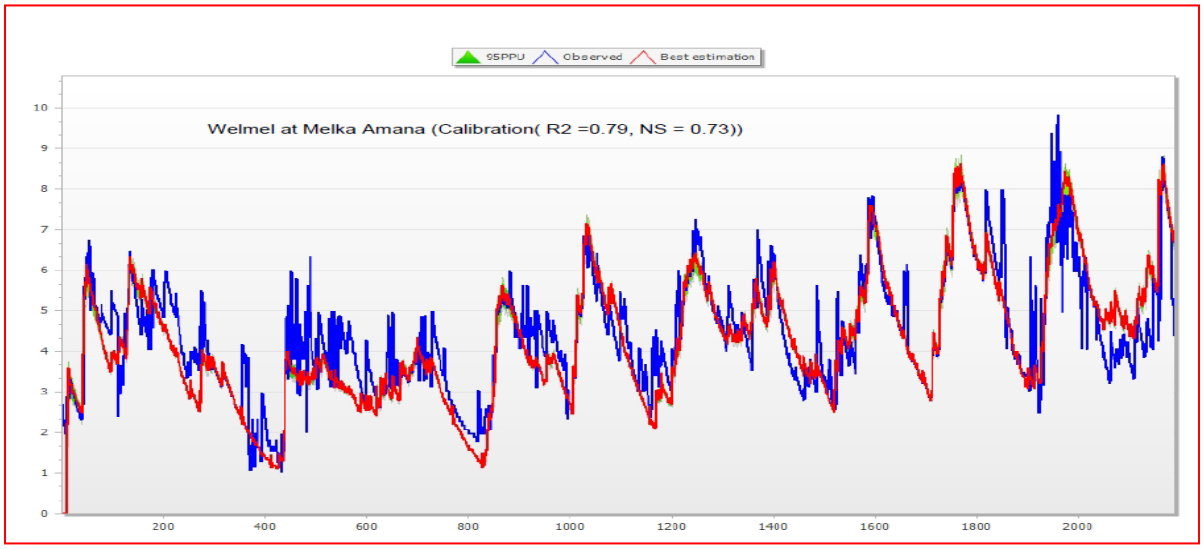
95PPU
Observed
Best estimation
Welmel at Melka Amana (Calibration(R2 =0.79, NS = 0.73))
10
9
8
7
6
5
4
3
2
1
0
200
400
600
800
1000
1200
1400
1600
1800
2000

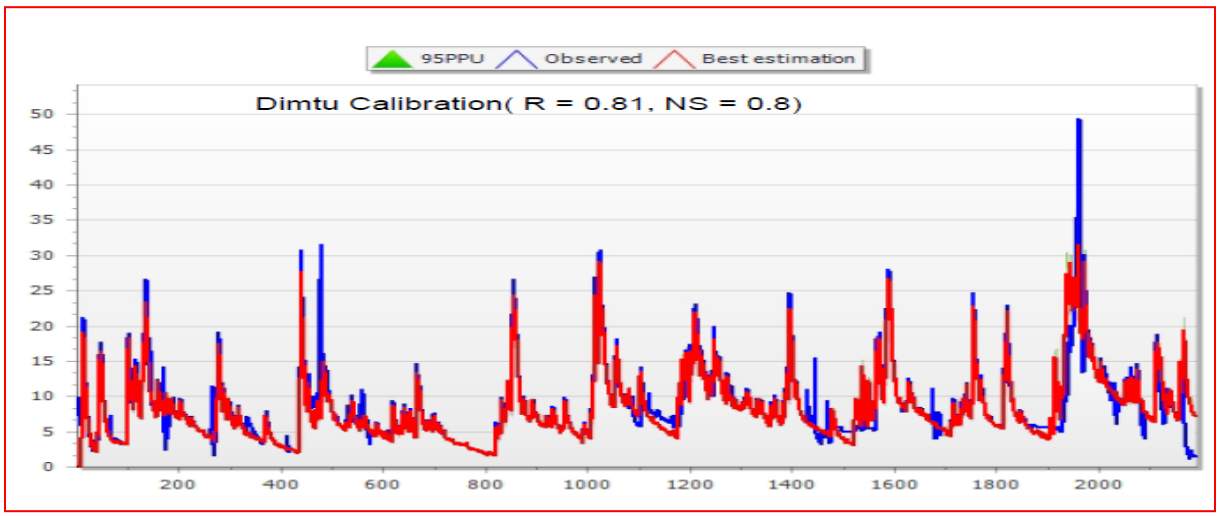
95PPU
Observed
Best estimation
Dimtu Calibration(R = 0.81, NS = 0.8)
50
45
40
35
30
25
20
15
10
5
0
200
400
600
800
1000
1200
1400
1600
1800
2000

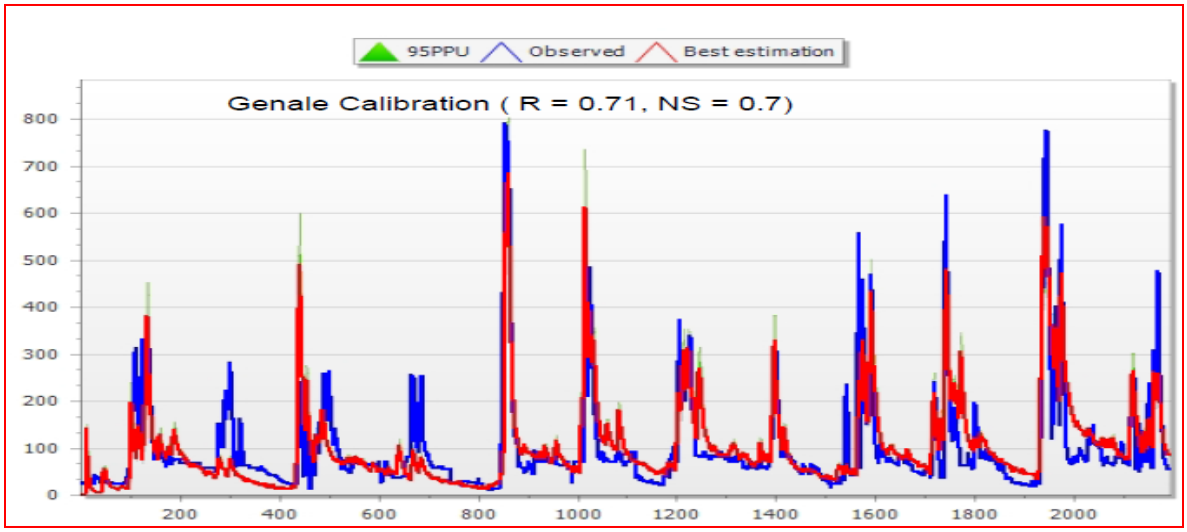

Figure 4-10 calibration of model for TAMSAT Rainfall product

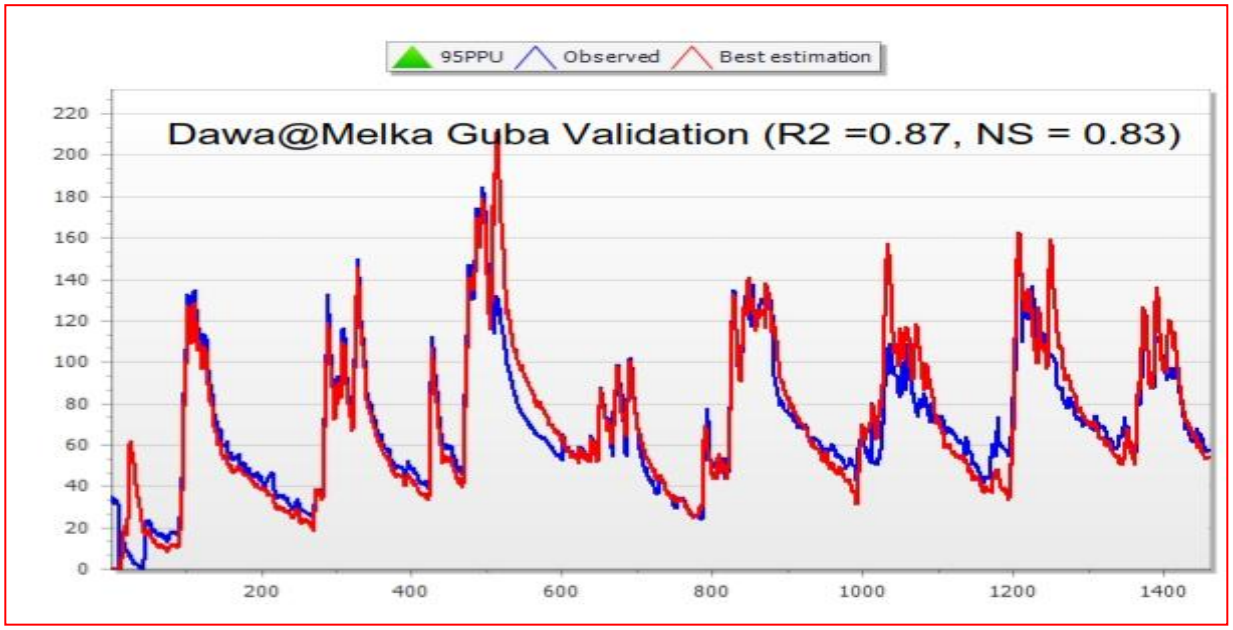

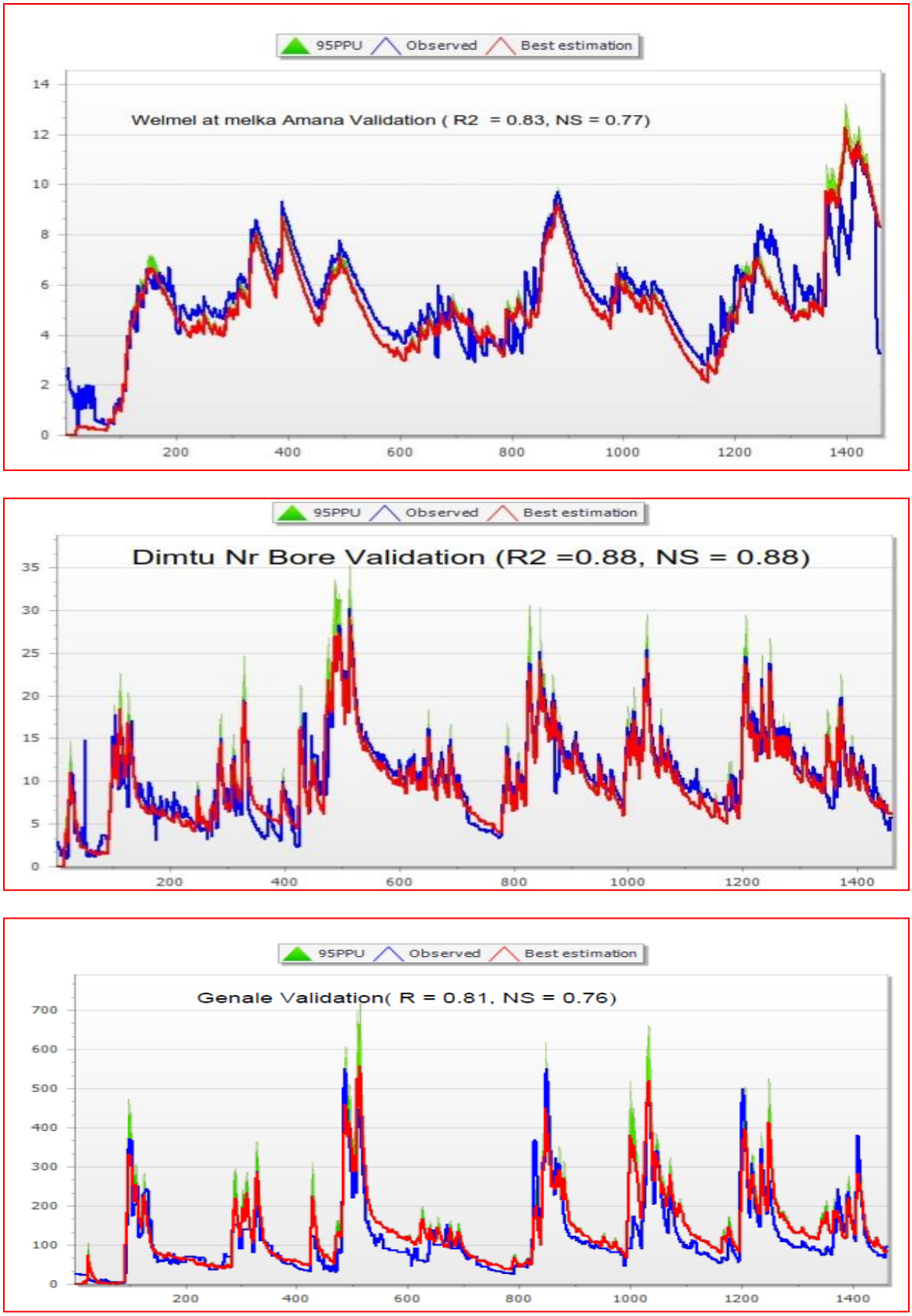

Figure 4-11 Validation of model for TAMSAT Rainfall product

4.6 Sensitivity Analysis

Sensitivity analysis is the process of identifying the model parameters that exert the highest influence on model calibration or on model predictions. Eighteen parameters were used for the sensitivity analysis with the category of sensitivity ranging from very high to small or negligible. Among the sensitive flow parameters the ground water parameters were found to be the most sensitive. Deep aquifer percolation fraction; Rchrg_Dp, Base flow alpha factor [days]; Alpha_Bf, Threshold water depth in the shallow aquifer for flow [mm]; Gwqmn, Soil evaporation compensation factor; Esco, Initial curve number (II) value; Cn2, Soil depth [mm]; Sol_Z, Threshold water depth in the shallow aquifer for "revap" [mm]; Revapmin, Channel effective hydraulic conductivity [mm/hr]; Ch_K2, Available water capacity [mm water / mm soil]; Sol_Awc, Maximum canopy storage [mm]; Canmx and Surface runoff lag time [days]; Surlag were found to be the most effective hydrologic parameters for the simulation of stream flow. Sensitive flow parameters, relative sensitivity values, parameter ranking and their category were presented in the Table 5. A brief description of each hydrologic parameter is listed in the SWAT model user's manual (Neitsch *et al*., 2004).

Table 4-11 Sensitivity analysis result

Parameter	Rank	Mean relative sensitivity	Category of Sensetivity
R__CN2.mgt	1	1.06	Very High
V__ALPHA_BNK.rte	2	0.689	Very High
V__CH_K2.rte	3	0.319	High
V__SOL_AWC(..).sol	4	0.23	High
V__GWQMN.gw	5	0.16	High
V__ALPHA_BF.gw	6	0.132	High
V__HRU_SLP.hru	7	0.127	High
V__EPCO.hru	8	0.121	High
V__REVAPMN.gw	9	0.106	High
V__SOL_K(..).sol	10	0.097	Medium
V__SURLAG.hru	11	0.081	Medium
V__SLSUBBSN.hru	12	0.072	Medium
V__CANMX.hru	13	0.067	Medium
V__CH_N2.rte	14	0.062	Medium
V__ESCO.hru	15	0.034	Medium
V__GW_REVAP.gw	16	0.005	Small
V__RCHRG_DP.gw	17	0.004	Small
V__GW_DELAY.gw	18	0.002	Small

4.7 Dotty plots

Dotty plots command show the dotty plots of all parameters. These are plots of parameter values vs objective function. The main purpose of these graphs is to show the distribution of the sampling points and to give an idea of parameter sensitivity. Dotty plots for welmel watershed is shown as an example in Figure 4-14. The X-axis ranges of calibration parameters whereas, the Y-axis is the objective function (NS)

1:R__CN2.mgt

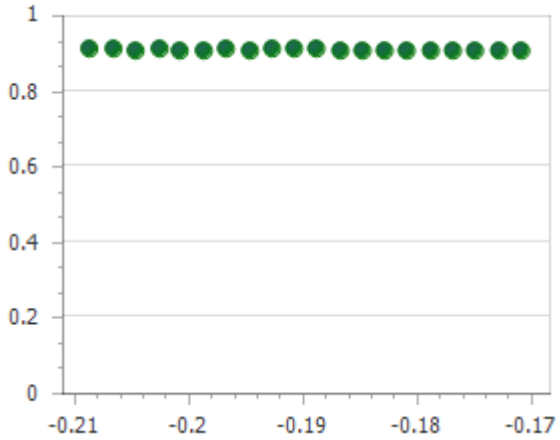

2:V__ALPHA_BF.gw

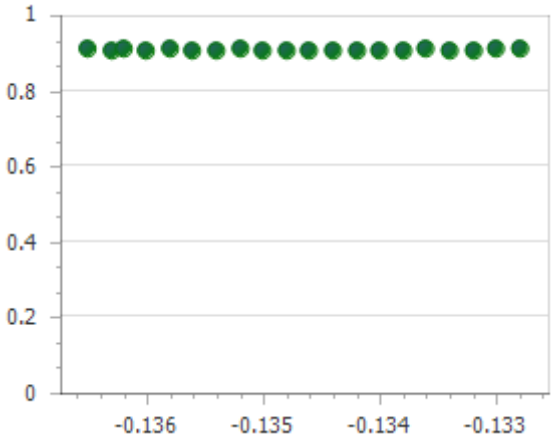

3:V__GW_DELAY.gw

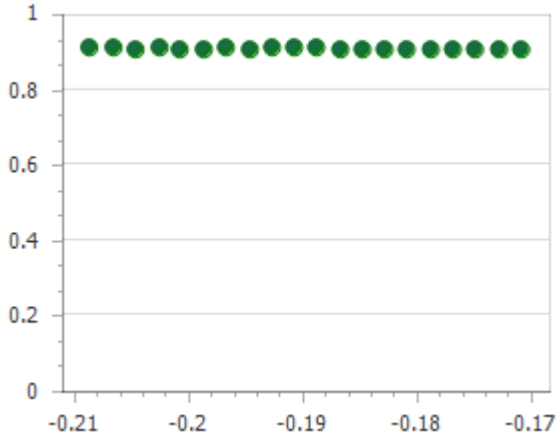

4:V__GWQMN.gw

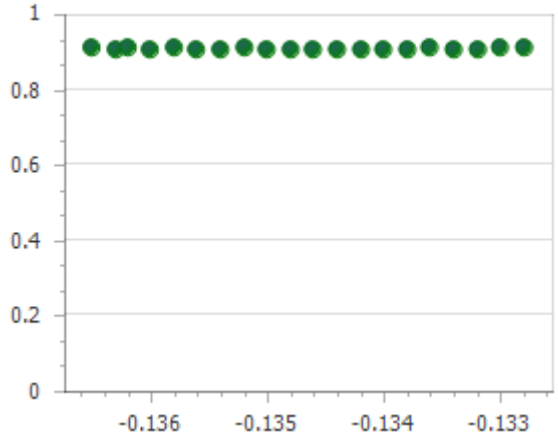

5:V__REVAPMN.gw

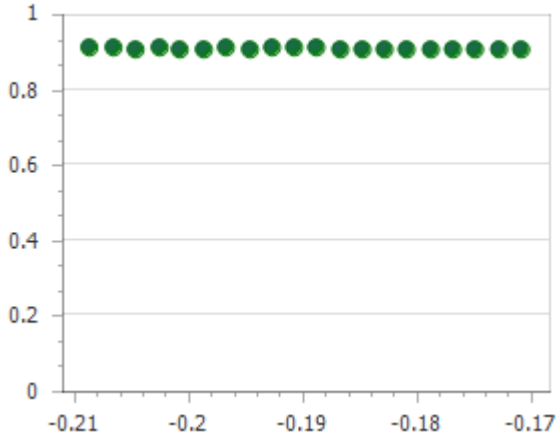

6:V__GW_REVAP.gw

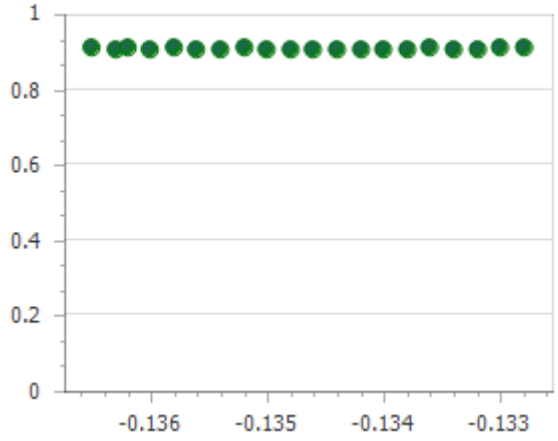

7:V__RCHRG_DP.gw

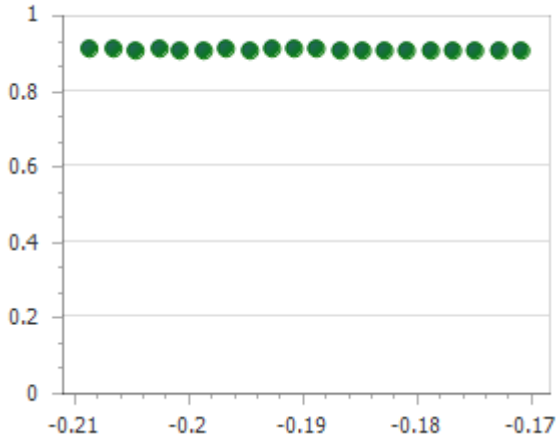

8:V__SURLAG.hru

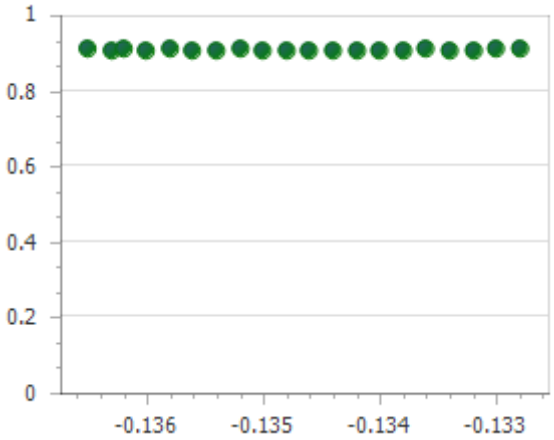

9:V__EPCO.hru

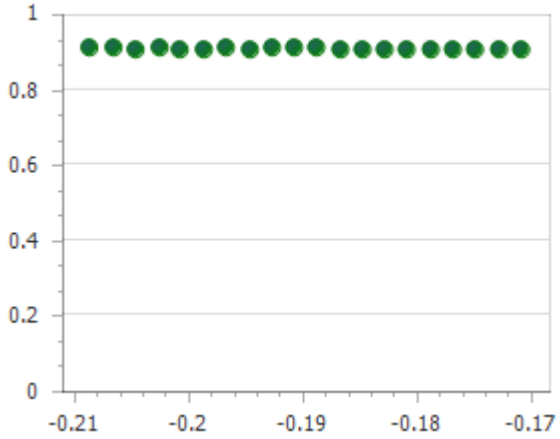

10:V__ESCO.hru

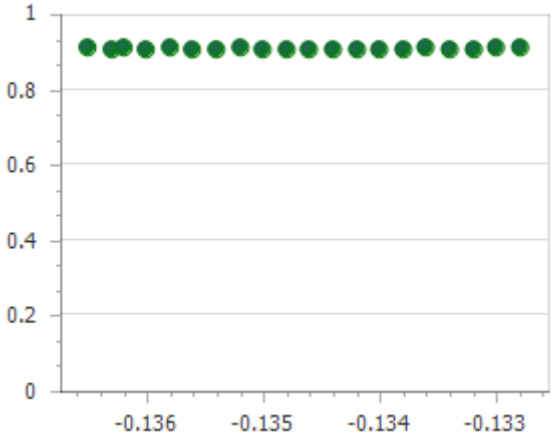

11:V__HRU_SLP.hru

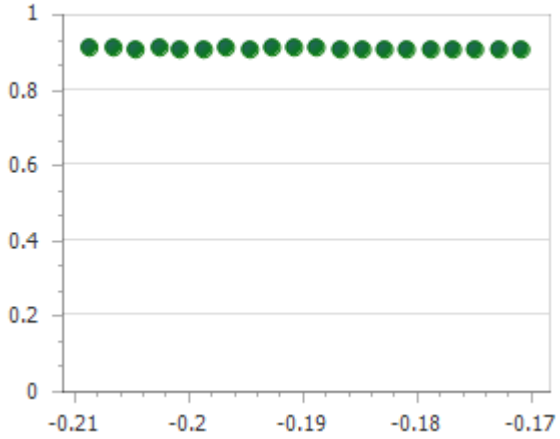

12:V__SLSUBBSN.hru

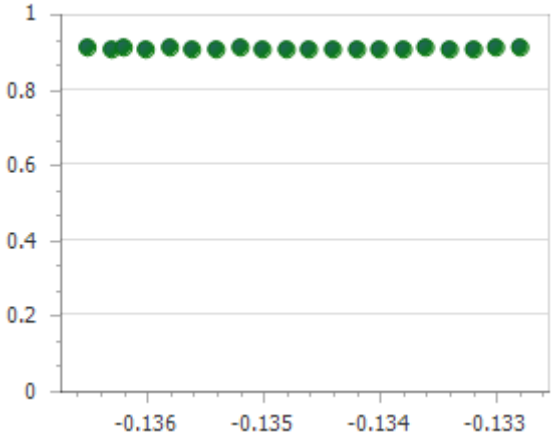

13:V__ALPHA_BNK.rte

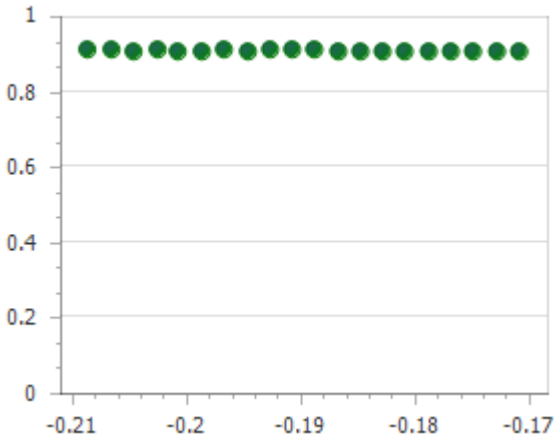

14:V__CH_K2.rte

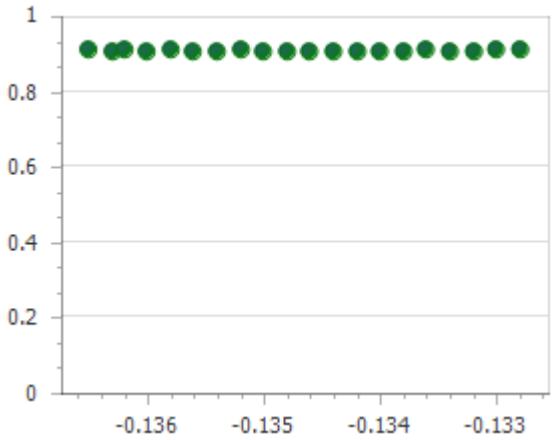

15:V__CH_N2.rte

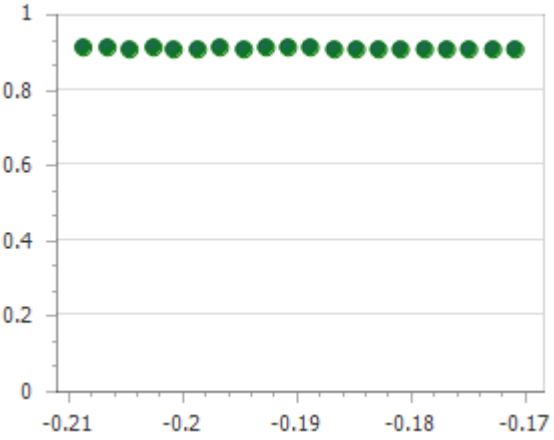

16:V__SOL_AWC(..).sol

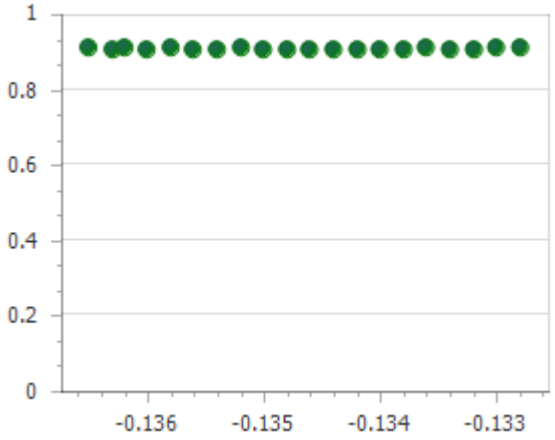

17:V__SOL_K(..).sol

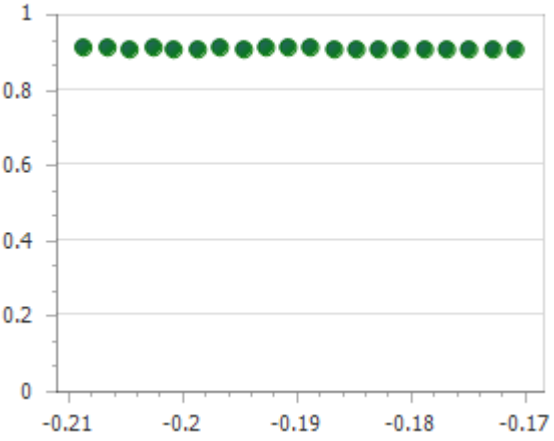

18:V__CANMX.hru

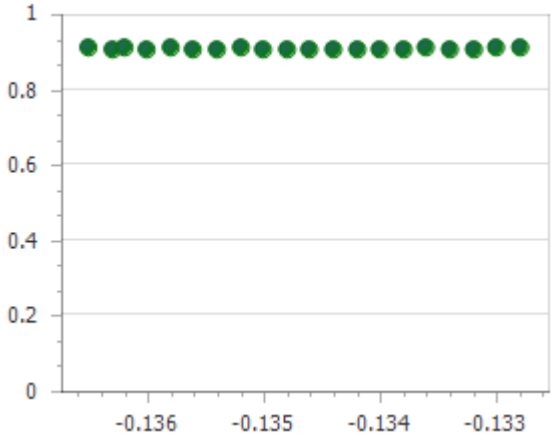

Figure 4-12 Dotty plot for Welmel Watershed

4.8 Global sensitivity Analysis

The global sensitivity of stream-flow parameters has been calculated using Latin hypercube regression systems. The parameters have given ranks for their sensitivity to the model calibration for both procedures. The most sensitive parameters recorded after sensitivity analysis for daily calibration in SUFI-2 procedures are shown in Table VII. Out of 18 selected parameters, the curve number, available water capacity, average slope steepness, saturated hydraulic conductivity, groundwater evaporation coefficient, threshold water depth in the shallow aquifer for flow, and base flow alpha-factor were identified as being parameters to which the flow has medium to high sensitivity. New sensitive parameters that can affect flow are Manning's "n" value for the main channel (CH_N2) were getting. The ranking of the parameters was different at various outlets where sensitivity test was carried out. However, the curve number (CN2) was the main sensitivity parameter for all outlets.

After calibration best parameters are found Best_par.txt in Sufi-2. This file shows the" best parameter" values as well as their ranges. These are the parameters, which gave the best objective function values in the current iteration. The fitted value of these best parameters can explain the mineral characteristics of the sub-basin. For Dawa at Melka Guba, Welme at Melka Amana, Dimtu Nr. Bore and Genale at Halwen; since base flow is over estimated manual calibration is needed increase, Sol-AWC close 0.4m/m, decrease ESCO close 0.002 to increase soil Evapo-transpiration which shows properties of vegetation land before calibration was done in SWAT-CUP. Soil saturated hydraulic conductivity (mm/hr) is all kept 5 for reach along Genale Dawa mainline. All 18 parameters are estimated for the four Sub-basins in Genale Dawa basin. Groundwater flows into the main channel increases when ALPHA_BF increases.
The manning coefficient of the main channel (CH_N2) rules the velocity of the flow in the reaches. If the CH_N2 value gets higher, the velocity is reduced and the simulated flow will become lagged compared to the measured flow. This can be attributed to the decreasing channel velocity with higher values of CH_N2, introducing a lag in the daily model output.
Soil saturated conductivity (SOL_K) of the sub-basin is found to be in the range of 4 to 6 mm/h. To account for different soils' ability to infiltrate, NRCS has divided soils into four hydrologic soil groups (HSGs). So HSG Group B fits the sub-basin soil group because these soils have a moderate rate of water transmission (final infiltration rate of 3.81 to 7.62mm./h). Soils with moderate infiltration rates when thoroughly wetted. These consist chiefly of soils that are moderately deep to deep, moderately well-drained to well-drained with moderately fine to moderately coarse textures. As we can see from hydrological water balance, flow is surface flow dominated. Hence, it is the best idea to find what is the dominant parameter that affects surface flow to be highest? The average value of CN of the sub-basin lies between 75.57 and 86.22 for CHRIPS and 83.36 and 87.16 for TAMSAT model. The value of saturated soil conductivity can also affect groundwater flow. Consequently, this maximum value of CN2 and moderate conductivity SOL_K indicates flow to be surface flow dominated.

As the value of ESCO is very small means evaporative demand for soil layer is very high for each watershed.

Table 0-12 Global sensitivity result of model for CHRIPS

CHRIPS									
		CALIBRATION				VALIDATION			
	Parameter	Dawa at Melka Gub	Welmel at Melka Amar	Dimtu Nr. Bore	Genale at Halwen	Dawa at Melka Guba	Welmel at Melka Amana	Dimtu Nr. Bore	Genale at Halwen
No		Fitted valule	Fitted valule	Fitted valule	Fitted valule	Fitted valule	Fitted valule	Fitted valule	Fitted valule
1	R__CN2.mgt	-0.25882	-0.205904	-0.15879	-0.204528	-0.147022	-0.199617	-0.208489	-0.143078
2	V__ALPHA_BF.gw	-0.143054	-0.133874	-0.136296	-0.134792	-0.140229	-0.13115	-0.136541	-0.126553
3	V__GW_DELAY.gw	201.901917	200.030853	194.975327	193.072952	201.024582	201.14035	193.452194	196.564667
4	V__GWQMN.gw	7471.821777	7154.966797	8248.732422	8534.6875	6964.106445	7799.654297	8436.644531	8022.041992
5	V__REVAPMN.gw	313.113251	325.381195	357.502869	334.152069	317.648712	308.033417	346.052673	344.768768
6	V__GW_REVAP.gw	0.125215	0.125489	0.123269	0.123855	0.125006	0.124943	0.123909	0.124174
7	V__RCHRG_DP.gw	0.151224	0.148676	0.002932	-0.001996	0.162938	0.12985	0.008455	0.06271
8	V__SURLAG.hru	-8.536234	-7.862199	-9.281226	-9.51854	-8.180043	-9.056177	-9.357737	-8.85037
9	V__EPCO.hru	0.978934	0.977925	0.975761	0.976105	0.978781	0.979018	0.975936	0.976558
10	V__ESCO.hru	0.129072	0.09434	0.110166	0.095725	0.104186	0.102712	0.098489	0.092718
11	V__HRU_SLP.hru	0.077476	0.071012	0.075379	0.077521	0.068246	0.081357	0.077438	0.077179
12	V__SLSUBBSN.hru	195.989807	196.228668	196.368637	196.341202	196.271271	196.147827	196.344055	196.387436
13	V__ALPHA_BNK.rte	0.009867	0.009405	0.010638	0.010806	0.00987	0.01015	0.010558	0.010121
14	V__CH_K2.rte	499.736359	500.380554	505.132721	505.031891	499.930939	501.068909	504.080078	502.844574
15	V__CH_N2.rte	0.174226	0.17482	0.173822	0.173764	0.173989	0.173773	0.173871	0.173974
16	V__SOL_AWC().sol	0.509268	0.507489	0.503922	0.503885	0.50717	0.507993	0.504511	0.505457
17	V__SOL_K().sol	261.55011	262.147675	261.937653	262.205231	261.601349	261.447388	262.267487	262.218536
18	V__CANMX.hru	8.765289	8.781962	8.78324	8.764662	8.756018	8.750915	8.77949	8.783543

Table 4-13 Global sensitivity result of model for TAMSAT

		TAMSAT							
		CALIBRATION				VALIDATION			
	Parameter	Dawa at Melka Gub	Welmel at Melka Amar	Dimtu Nr. Bore	Genale at Halwen	Dawa at Melka Guba	Welmel at Melka Amana	Dimtu Nr. Bore	Genale at Halwen
No		Fitted valule	Fitted valule	Fitted valule	Fitted valule	Fitted valule	Fitted valule	Fitted valule	Fitted valule
1	R__CN2.mgt	-0.204528	-0.143078	-0.186703	-0.208489	-0.204528	-0.15879	-0.208489	-0.204528
2	V__ALPHA_BF.gw	-0.134792	-0.126553	-0.134015	-0.136541	-0.134792	-0.136296	-0.136541	-0.134792
3	V__GW_DELAY.gw	193.072952	196.564667	193.768234	193.452194	193.072952	194.975327	193.452194	193.072952
4	V__GWQMN.gw	8534.6875	8022.041992	8485.666016	8436.644531	8534.6875	8248.732422	8436.644531	8534.6875
5	V__REVAPMN.gw	334.152069	344.768768	344.069244	346.052673	334.152069	357.502869	346.052673	334.152069
6	V__GW_REVAP.gw	0.123855	0.124174	0.12392	0.123909	0.123855	0.123269	0.123909	0.123855
7	V__RCHRG_DP.gw	-0.001996	0.06271	-0.003489	0.008455	-0.001996	0.002932	0.008455	-0.001996
8	V__SURLAG.hru	-9.51854	-8.85037	-9.445448	-9.357737	-9.51854	-9.281226	-9.357737	-9.51854
9	V__EPCO.hru	0.976105	0.976558	0.976189	0.975936	0.976105	0.975761	0.975936	0.976105
10	V__ESCO.hru	0.095725	0.092718	0.095265	0.098489	0.095725	0.110166	0.098489	0.095725
11	V__HRU_SLP.hru	0.077521	0.077179	0.077355	0.077438	0.077521	0.075379	0.077438	0.077521
12	V__SLSUBBSN.hru	196.341202	196.387436	196.383896	196.344055	196.341202	196.368637	196.344055	196.341202
13	V__ALPHA_BNK.rte	0.010806	0.010121	0.010463	0.010558	0.010806	0.010638	0.010558	0.010806
14	V__CH_K2.rte	505.031891	502.844574	504.807922	504.080078	505.031891	505.132721	504.080078	505.031891
15	V__CH_N2.rte	0.173764	0.173974	0.173809	0.173871	0.173764	0.173822	0.173871	0.173764
16	V__SOL_AWC().sol	0.503885	0.505457	0.50469	0.504511	0.503885	0.503922	0.504511	0.503885
17	V__SOL_K().sol	262.205231	262.218536	262.288239	262.267487	262.205231	261.937653	262.267487	262.205231
18	V__CANMX.hru	8.764662	8.783543	8.772571	8.77949	8.764662	8.78324	8.77949	8.764662

5. CONCLUSIONS and RECOMMENDATIONS

5.1. Conclusion

The study "Evaluation of the performance of high-resolution Satellite rainfall product for stream flow simulation was conducted as a case study of Genale Dawa River basin. The basin can be provided as a good example where the use of satellite-derived precipitation could be beneficial. To overcome limitation of lacking sufficient station data, this research study uses some of the available globally gridded high resolution precipitation datasets to simulate runoff using SWAT model. Two satellite precipitation products (CHRIPS and TAMSAT) were selected for this evaluation.

The products were evaluated and compared on daily, monthly and annual time scales against the ground precipitation measurements through visual assessment of plots and by using some statistical methods such as Nash-Sutcliffe Coefficient of Efficiency, root mean square difference, estimation bias, and correlation coefficients and so on.

The comparison results of rainfall magnitudes from satellite rainfall products and rain gauges revealed that the CHRIPS and bias corrected TAMSAT rainfall estimates gave relatively accurate result compared to rain gauge rainfall estimates at daily scale. Comparing CHRIPS and bias corrected TAMSAT, the former shows better result. The result revealed that, in this region, correlations between satellite rainfall values and rain gauge values were good (R Values are ranging from 0.72 to 0.96) for different selected stations.

On comparison of monthly datasets, the trend is totally captured while the magnitude shows under estimation from 5.7% to 30% by CHRIPS product and shows small over estimation from 0.75% to 3.4% for TAMSAT product. On the basis of annual comparison our result showed that tend correctly captured and CHRIPS shows small under estimation while TAMSAT shows small over estimation. Our results reveal that the utility of satellite rainfall products as input to SWAT for daily stream flow simulation strongly depends on the product type.

Simulation from both rainfall inputs showed the trend of observed hydrograph. Simulation based on CHRIPS and TAMSAT showed consistent and modest skills in their simulations. Overall, the results indicate that although some uncertainties exist in these gridded datasets (CHRIPS & TAMSAT), the appliance of these gridded data prove useful for hydrological studies within the absence of station data. When comparing simulation from both inputs, R^2 ranges from 0.72 to 0.97 for CHRIPS and from 0.71 to 0.95 for TAMSAT during calibration and validation. The NS ranges from 0.7 to 0.95 for CHRIPS and from 0.7 to 0.92 for TAMSAT. It strongly indicates the raising potential of the predictive accuracy of the satellite rainfall products in reproducing hydrological features. The SWAT model also proves to be a good tool in such a modeling approach. In all cases the bias corrected TAMSAT shows better results compared to CHRIPS.

5.2. Recommendations

On the basis of our analysis, we recommend that the hydrologists, Decision makers and stakeholders Should consider the use of satellite data in areas where the rain gauge distribution are highly sparse and practically impossible due to physical features which might provide installations of rain gauges are difficult. Even though the spatial resolution may be higher, the different sources of errors in these datasets need further investigation and much more work is needed to that end. Nevertheless, the usefulness and suitability of applying these gridded products have been highlighted and it is promising that in areas where there is the paucity of station observations, these gridded products can be used well for applications of rainfall-runoff modeling. The other thing which is highly recommended is that the weather stations should be improved both in quality and quantity to improve the performance of the model. Hence, it is highly recommended to establish good meteorological stations and to have a high quality of streamflow data.

Remote sensing of precipitation is a growing field of science and needs to be evaluated. New satellites are being launched that are specialized in measuring precipitation. Our country Ethiopia also starts anticipating operational earth observing satellite. More work is also being done to improve the algorithms of the estimates. Hence, there will be continuous improvement of remotely-sensed estimates. Thus, continuous evaluation of these products is needed especially in complex climates.

Neither the satellite data nor the rain gauge data are sufficient to understand the climatology of a basin; they should be used in combination. Similar studies must be performed with more meteorological data covering the whole country. In the rainfall-runoff modeling the evapotranspiration and snowmelt data can be included to observe the performance of the model for all seasons and to estimate the annual water potential of a basin.

The SWAT model performed well in simulating the daily flow of the Genale Dawa river basin. Therefore, the calibrated parameter values can be considered for further hydrologic simulation of the basin and the model can be taken as a potential tool for simulation of the hydrology of ungauged watershed in mountainous areas of Ethiopia which behave hydro-meteorologically similar with Genale Dawa river basin.

REFERENCE

1. *Validation of new satellite rainfall products over the upper blue nile basin .* **Getachew Tesfaye Ayehu, Tsegaye Tadesse,Berhan Gessesse,Tufa Dinku.** 2018, Atmospheric MeasurementTechniques, pp. 1-16.

2. *Validation of satellite rainfall products over East Africa's complex topograpy.* **T. Dinku, P. Ceccato , E. Grover-Kopec , M. Lemma , S. J. Connor & C. F.** 2006, International Journal of Remote Sensing, pp. 2-25.

3. *Assessment of the Performance of Satellite-Based Rainfall product overupper Blue Nile river basin.* **Chad Furl, Dawit Ghebreyesus and Hatim O. Sharif.** 2018, Geosciences, pp. 1-18.

4. *Evaluation of High-Resolution Satellite Rainfall Products through Streamflow.* **Menberu M. Bitew and Mekonnen Gebremichael, Lula T. Ghebremichae , Yared A. Bayissa.** 2011, Journal of Hydrometrology, pp. 2-15.

5. *A Quasi-Global Precipitation Time Series for Drought Monitoring.* **Chris C. Funk, Pete J. Peterson, Martin F. Landsfeld, Diego H. Pedreros,James P. Verdin, James D. Rowland, Bo E. Romero, Gregory J. Husak,Joel C. Michaelsen, and Andrew P. Verdin.** 2014, USGS, pp. 1-12.

6. *Performance of High Resolution Satellite Rainfall Products over Data Scarce Parts of Eastern Ethiopia.* **Shimelis B. Gebere, Tena Alamirew , Broder J. Merkel.** 2015, remote sensing, pp. 1-25.

7. *Assessment of satellite rainfall products for streamflow simulation.* **Gebremichael, M. M. Bitew and M.** 2011, Hydrology and Earth Sciences, pp. 1-9.

8. *A comparison of precipitation in - situ measurements and model predictions over the Baltic Sea Area.* **Clemens, M. and Bumke, K.** 2001, hydrology, Oceans and Atmosphere, pp. 5-6.

9. *Model sensitivity to rainfall representation: the representative elementary watershed.* **Haile, A, T., Rientjes, T.,and Reggiani, P.** 2009, Water Resource Research, pp. 1-5.

10. *Evaluating the streamflow simulation capability of PERSIANN-CDR daily rainfall products in two river basins on the Tibetan Plateau.* **Xiaomang Liu, Tiantian Yang, Koulin Hsu, Changming Liu, and Soroosh Sorooshian.** 2017, Hydrology and Earth System Science, pp. 1-2.

11. *The estimation of monthly rainfall from satellite data.* **Barrett, E. C.** 1970, Mon. Wea. Rev., 98, pp. 322-327.

12. *Spatially Distributed Modeling of Storm Runoff and Non-Point Source Pollution Using Geographic Information Systems (GIS).* **Francisco Olivera, David R. Maidment and Randall J. Charbeneau.** s.l. : The University of Texas at Austin, 1996.

13. *A two-parameter climate elasticity of streamflow index to assess climate change effects on annual streamflow.* **Fu G, C. S.** s.l. : Water Resources Research, 2007.

14. *A water balance model of the upper Blue Nile in Ethiopia. Hydrological Sciences.* **Conway, D.** s.l. : Geographical Journal, 1997.

15. *An experimental investigation of partial area contributions .* **Ragan, R.M.** 1968, Int.Assoc. of Science Hydrology, pp. 241-251.

16. *Recent advances in the modeling of hydrological systems.* **O"Connell, P.E.** 1991, Kluwer, Dordrecht, pp. 3-30.

17. *Applied Hydrology.* **Chow, V. T., Maidment, D. R. & Mays, L. W.** 1988, s.l.:McGraw-Hill Book Company, pp. 1-45.

18. *Evaluation of Satellite-Based Rainfall Estimates and Application to Monitor Meteorological Drought for the Upper Blue Nile Basin, Ethiopia.* **Yared Bayissa, Tsegaye Tadesse,Getachew B. Demisse,Andualem Shiferaw.** 2017, Remote Sensing, pp. 1-18.

19. *Comparison and validation of eight satellite rainfall products over the rugged topography of Tekeze-Atbara Basin at different spatial and temporal scales.* **Tesfay G. Gebremicael, Yasir A. Mohamed1, Pieter van der Zaag,Amdom G.Berhe5, Gebremedhin G. Haile, Eyasu Y. Hagos, Mulubrhan K. Hagos.** 2017, Journal of Hydrology and Earth System Science, pp. 1-31.

20. *Investigation of Discrepancies in Satellite Rainfall Estimates over Ethiopia.* **MATTHEW P. YOUNG, CHARLES J. R. WILLIAMS, J. CHRISTINE CHIU, AND ROSS I. MAIDMENT.** 2014, J O U R N A L O F H Y D R O M E T E O R O L O G Y, pp. 2347-2368.

21. *Evaluation of satellite rainfall estimates over the Lake Tana basinat the source region of the Blue Nile River.* **Ayele Almaw Fenta, Hiroshi Yasuda, Katsuyuki Shimizu,Yasuomi Ibaraki, Nigussie Haregeweyn, Takayuki Kawai,Ashebir Sewale Belay, Dagnenet Sultan, Kindiye Ebabu.** 2018, Athmospheric Research, pp. 1-36.

22. *VALIDATION OF THE CHIRPS SATELLITE RAINFALL ESTIMATE OVER EAST AFRICA.* **Dinku, Tufa.** 2016, International Research Institute for Climate and Society(IRI), p. 1.

23. *Validation of satellite rainfall products over East Africa's complex topography.* **T. Dinku, P. Ceccato , E. Grover-Kopec , M. Lemma , S. J. Connor & C. F.Ropelewski.** 2006, International Journal of Remote Sensing, pp. 1503-1526.

24. *Evaluation of High-Resolution Multisatellite and Reanalysis Rainfall Products over East Africa.* **Dejene Sahlu, Semu A. Moges, Efthymios I. Nikolopoulos,Emmanouil N. Anagnostou, and Dereje Hailu.** 2017, Hindawi Advances in Meteorology, pp. 1-15.

25. *Performance of satellite-based and GPCC 7.0 rainfall products in an extremely data-scarce country in the Nile Basin.* **Mohammed Basheer, Nadir Ahmed Elagib.** 2019, Atmospheric Research.

26. *Evaluation of multiple climate data sources for managing environmental resources in East Africa.* **Solomon Hailu Gebrechorkos, Stephan Hülsmann, and Christian Bernhofer.** 2018, Hydrology and Earth System Science.

27. *Statistical Evaluation of High Resolution Satellite Precipitation Products in Arid and Semi-Arid Parts of Ethiopia: A Note for Hydro-meteorological Applications.* **Gella, Getachew Workineh.** 2019, Water and Environment Journal, p. 86.

28. *Hydrological model selection for CFCAS project, Assessment of water resource risk and vulnerability to change in climate condition, University of Western Ontario.* **Cunderlik, J.** 2003.

29. *Large area hydrologic modeling and assessment, part I: Model development.* **Arnold, J.G., Srinivasan, R., Muttiah, R.S. and Williams, J.R.** 1998, Journal of American Water Resources Association, pp. 73-89.

30. *Soil and Water Assessment Tool, Theoretical documentation: Version 2005.* **Neitsch, S.L., Arnold, J.G., Kiniry, J.R., and Williams, J.R.** 2005, Temple, TX. USDA Agricultural Research Service and Texas A & M Black land Research Centre.

31. *GIS-Based Surface Runoff Modeling and Analysis of Contributing Factors; a Case study of the Nam Chun watershed, Thailand. M.Sc Thesis, ITC, the Netherlands.* **Solomon, H.** 2005.

32. *A comprehensive surface- groundwater flow model.* **Arnold, J. G., Allen. P. M. and Bernhardt. G.** 1993, Journal of Hydrology, pp. 47-69.

33. *SWAT model application in a data scarce tropical complex catchment in Tanzania.* **Ndomba, P.** 2002, Physics and chemistry of the Earth.

34. *The Soil and Water Assessment Tool: Historical Development, Applications, and Future Research Direction.* **Gassman, P. W., Reyes. M. R., Green. C. H., Arnold. J. G.** 2007, American Society of Agricultural and Biological Engineers.

35. *Predicting Rainfall and Runoff Through Satellite Soil Moisture Data and SWAT Modelling for a Poorly Gauged Basin in Iran.* **Majid Fereidoon, Manfred Koch and Luca Brocca.** 2019, water.

36. *Runoff simulation by SWAT model using high-resolution gridded precipitation in the upper Heihe River Basin, Northeastern Tibetan Plateau.* **Hongwei Ruan, Songbing Zou, Zhentao Cong, Yuhan Wang, Zhenliang Yin, Zhixiang Lu, Fang Li, Baorong Xu.** 2016, Hydrology and Earth System Science.

37. *Spatial delineation of soil erosion vulnerability in the Lake Tana Basin, Ethiopia.* **Setegn, S., Srinivasan, R., Dargahi, B. and Melesse, A.** 2009, Hydrological Processes.

38. *Prediction of sediment inflow for Legedadi reservoir using SWAT watershed and CCHE1D sediment transport models.* **Gessese, A.** 2008, Faculty of Technology, Addis Ababa University.

39. *Assessiment of Surface Runoff Generation and Soil Erosion Rates for a Small Watershed in Awash River Basin.* **Bewket, Tibebe and.** 2011, Journal of Hydology.

40. *Evaluation of the ArcSWAT Model in Simulating Catchment Hydrology: In Weyib River Basin, Bale Mountainous Area of Southeastern Ethiopia.* **Sarma, Abdulkerim B. Serur and Arup K.** 2016, International Journal of Innovative and Emerging Research in Engineering.

41. *SWAT-Modeling of the Impact of future Climate Change on the Hydrology and the Water Resources in the Upper Blue Nile River Basin, Ethiopia.* **Cherie, Manfred Koch · Netsanet.** 2013, ICWRER.

42. *Evaluation of the Climate Forecast System Reanalysis,Weather Data for Watershed Modeling in Upper Awash Basin, Ethiopia.* **Mesfin Benti Tolera, Il-Moon Chung ,and Sun Woo Chang.** 2018, Water.

43. *Calibration and validation of SWAT model and estimation of water balance components of Shaya mountainous watershed, Southeastern Ethiopia.* **A. A. ShawuL, T. Alamirew, and M. O. Dinka.** 2013, Hydrology and Earth System Science.

44. *Comparing Bias Correction Methods Used in Downscaling Precipitation and Temperature from Regional Climate Models: A Case Study from the Kaidu River Basin in Western China.* **Min Luo, Tie Liu , Fanhao Meng , Yongchao Duan , Amaury Frankl ,Anming Bao and Philippe De Maeyer.** 2018, Water.

45. *Comparing bias correction methods in downscaling meteorological variables for a hydrologic impact study in an arid area in China.* **G. H. Fang, J. Yang, Y. N. Chen, and C. Zammit.** 2015, Hydrology and Earth System Science.

46. *Downscaling from GC precipitation: A benchmark for dynamical and statistical downscaling methods.* **Schmidli, J., Frei, C., and Vidale, P. L.** 2006, International Journal of Climatology.

47. *A Stochastic Model for weather Data Generation. .* **Danuso, F. , Climak.** 2002, Italian Journal of Agronomy , pp. 67-68.

48. *Erosion/Productivity Impact Calculator.* **Sharpley, A.N. and Williams, J.R., eds.** 1990, Model Documentation. U. S. Department of Agriculture Technical Bulletin , p. 1.

49. *Investigating the performance of satellite and reanalysis rainfall products at monthly timescales across different rainfall regimes of Ethiopia.* **Estifanos Lemma, Shruti Upadhyaya & RAA J Ramsankaran.** 2019, International Journal of Remote Sensing, pp. 9-10.

50. *Evaluating the use of ‘‘goodness-of-fit’’ measures in hydrologic and hydroclimatic model validation.* **Legates, D.R., McCabe G.J.,.** 1999, Water Resources Res, pp. 233-241.

51. *SWAT: MODEL USE, CALIBRATION, AND VALIDATION .* **J. G. Arnold, D. N. Moriasi, P. W. Gassman, K. C. Abbaspour, M. J. White,R. Srinivasan, C. Santhi, R. D. Harmel, A. van Griensven,M. W. Van Liew, N. Kannan, M. K. Jha.** 2012, American Society of Agricultural and Biological Engineers , p. 1493.

52. *SWAT-CUP Calibration and Uncertainty Programs for SWAT.* **K.C. Abbaspour, M. Vejdani, S. Haghighat.** 2015, NA User Manual, Department of Systems Analysis, Integrated Assessment and Modelling (SIAM), Eawag. Swiss Federal Institute of Aquatic Science and Technology, Duebendorf, Switzerland , p. 1599.

53. *SWAT-CUP for Calibration of Spatially Distributed Hydrological Processes and Ecosystem Services in a Vietnamese River Basin Using Remote Sensing.* **Lan T. Ha, Wim G.M. Bastiaanssen, Ann van Griensven, Albert I.J.M. van Dijk and Gabriel B.Senay.** 2017, Hydrologyand Earth System Science, p. 6.

54. *Validation of new satellite rainfall products over the Upper Blue Nile Basin, Ethiopia.* **Getachew Tesfaye Ayehu, Tsegaye Tadesse, Berhan Gessesse, and Tufa Dinku.** 2018, Atmospheric. Measurement. Techniques.

55. *Combined use of satellite estimates and rain gauge observations to generate high-quality historical rainfall time series over Ethiopia.* **Tufa Dinku, Kinfe Hailemariam, Ross Maidment, Elena Tarnavskyc and Stephen Connord.** 2013, INTERNATIONAL JOURNAL OF CLIMATOLOGY.

56. *Hydrodynamic modeling with SWAT for predicting dynamic behavior of pesticides .* **Holvoet, K., van Griensven, A., Seuntjens P. and Vanrolleghem, P.A.** 2004, Water and Environment Management Series, Young Scientist, pp. 21-22.

57. *River flow forecasting through conceptual models part I: A discussion of principles.* **Nash, J. E.** 1970, Journal of Hydrology, pp. 282-290.

58. *Validation of the SWAT model on a large river basin with point and nonpoint sources.* **Santhi, C., Arnold, J.G., Williams, J.R., Dugas, W.A., Srinivasan, R. and Hauck, L.M.** 2001, Journal of the American Water Resources Association, p. 37.

59. *Evaluating the SWAT Model for Hydrological Modeling in the Xixian Watershed and a Comparison.* **Li, Peng Shi · Chao Chen · Ragahavan Srinivasan. Xuesong Zhang · Tao Cai · Xiuqin Fang · Simin Qu.Xi Chen · Qiongfang.** 2011, Water Resources Management.

60. *Investigating the performance of satellite and reanalysis rainfall products at monthly timescales across different rainfall regimes of Ethiopia.* **Estifanos Lemma, Shruti Upadhyaya & RAA J Ramsankaran.** 2019, International Journal of Remote Sensing, pp. 9-10.

61. *Evaluation of Climate change impacts on hydrology of selected catchments of Abbay Basin.* **Belay, H.** 2011, Hydrology and Earth System Science , p. 10.

62. *Temporal and spatial changes of rainfall and streamflow in the Upper Tekeze–Atbara river basin, Ethiopia.* **Tesfay G. Gebremicael, Yasir A. Mohamed, Pieter v. Zaag, and Eyasu Y. Hagos.** s.l. : Hydrology and Earth system science, 2017, Hydrology and Earth System Sceince, pp. 2-17.

63. *Evaluation of the ArcSWAT Model in Simulating Catchment Hydrology: In Weyib River Basin, Bale Mountainous Area of Southeastern Ethiopia.* **Sarmab, Abdulkerim B. Serura and Arup K.** s.l. : Journal of American metrology, 2016, International Journal of Innovative and Emerging Research in Engineering.

64. *Evaluation of High-Resolution Satellite Precipitation Products over Very Complex Terrain in Ethiopia.* **Feyera A. Hirpa, Mekonnen Gebremichael, Thomas Hopson.** 2009, Journal of Applied Meteorology and Climatology, pp. 1-9.

65. *Comparison of rainfall estimations by TRMM 3B42, MPEG and CFSR with ground-observed data for the Lake Tana basin in Ethiopia.* **A. W. Worqlul1, , B. Maathuis, A. A. Adem, S. S. Demissie, S. Langan, T. S. Steenhuis.** 2014, Hydrology and Earth System Science, pp. 1-11.

APPENDIX

Table A-0-1 Intercomparison of Annual Rainfall From Different Products

Robe	Year	1996	1997	1998	1999	2000	2001	2002	2003	2004	2005	2006	2007	2008	2009	2010	2011	2012	2013	2014	2015	2016	2017
	TAMSAT	1044.5	1514	808.8	723	860	768	711	1092	805	920.5	1096.6	1071	1125	870	1128	1169	1037	1362	916	1127.8	797.1	
	OBSERVED	895.5	896.2	929.6	875.5	773.8	819.1	648.9	891.4	884.1	675.8	985.4	916.5	827.7	848.6	1067.1	769.2	855.3	978.9	532.6	768.8	574.3	
	TAMSAT C	871.0382	970.1816	871.2112	821.8236	775.7257	846.5106	630.6247	894.3837	886.3656	693.6739	975.658	954.3731	809.5156	703.6398	1030.213	792.799	976.2828	966.2824	559.1147	724.6907	577.0752	
	CHRIPS	752	748	737	683	604	629	510	697	686	591	835	768	700	567	845	585	664	722	428	557	27	
Delomena	Year	1997	1998	1999	2000	2001	2002	2003	2004	2005	2006	2007	2008	2009	2010	2011	2012	2013	2014	2015	2016	2017	
	TAMSAT	1475	650.9	508	835	754	828	1012	788	961.6	1283.2	1102	1100	886	1112	1179	1119	1286	972	1016.4	781	825.8	
	Observed	1020.9	1286.3	685.978	883.5	1191.1	940.2	1062.6	807.5	861.7	1199	965.9	921.6	914.9	1380.5	540.5	1004.6	1222	452.3	891.7	1160	804.1	
	TAMSAT	1401.275	1265.044	617.424	905.142	1156.477	916.987	1100.014	817.685	870.218	1203.906	1019.593	1013.177	877.3008	1380.083	558.049	1081.465	1241.254	462.067	868.749	1098.193	943.955	
	CHRIPS	731	901	466	649	790	517	624	495	605	829	674	652	518	893	285	704	803	296	616	908	302	
Ginir	Year	1996	1997	1998	1999	2000	2001	2002	2003	2004	2005	2006	2007	2008	2009	2010	2011	2012	2013	2014	2015	2016	2017
	TAMSAT	874.2	1353	450.6	573	746	560	694	771	555	857.8	1125.3	1088	948	769	1020	907	953	1403	974	918.4	725	718.8
	OBSERVED	994.9	1046.3	952.1	975.1	546.4	659.9	811.5	713.6	840.6	454.8	1417.3	494.1	567.9	960.3	1650.6	996.4	1243.5	1450.1	1394.6	951.9	931.2	370.6
	TAMSAT c	1048.218	1164.59	900.9598	1052.573	553.043	786.788	785.245	742.393	852.446	498.3757	1550.803	642.201	604.631	1087.188	1727.977	1163.932	1456.815	1803.149	1330.067	1157.777	924.814	333.26
	CHRIPS	770	926	801	607	500	570	684	589	691	390	1253	406	473	1078	1271	708	873	1086	906	838	745	280
Kibremen	Year	1996	1997	1998	1999	2000	2001	2002	2003	2004	2005	2006	2007	2008	2009	2010	2011	2012	2013	2014	2015	2016	2017
	TAMSAT	1091	1656	818.5	740.9	575	972	900	1200	1014	1235.3	1354.7	1131	1288	952	1233	1451	1264	1588	1026	1206.1	1088	902
	OBSERVED	1325.3	907.6	993.4	668.3	879.6	1072.7	871.5	929.4	853.4	1545.9	947.3	1034.7	870.6	164.4	1137.2	134.8	1113.1	1336.9	547	756.2	157.6	69.5
	TAMSAT (	1307.533	1072.891	869.02	628.52	1038.241	978.46	819.199	1003.236	858.166	1541.82	1105.708	1063.088	1090.936	300.135	1473.682	244.974	1375.014	1608.588	552.043	1169.731	197.624	72.604
	CHRIPS	916	732	740	483	731	750	563	668	536	1136	762	778	739	217	901	113	645	803	365	584	134	11
Moyale	Year	1996	1997	1998	1999	2000	2001	2002	2003	2004	2005	2006	2007	2008	2009	2010	2011	2012	2013	2014	2015	2016	2017
	TAMSAT	222	1443	597.5	321	349	410	661	726	639	253	810.5	523	455	531	516	919	728	654	513	744.2	446	520.7
	OBSERVED	414.9	1092.1	622.3	309	436	412.6	544	394.9	563.8	427.9	1043.7	366.2	448.4	456.1	787.7	515.6	575.8	673	427.7	582.3	307.9	389.2
	TAMSAT	367.4187	1159.614	695.2863	262.51	402.356	404.484	638.978	463.4799	567.804	420.854	1049.347	348.054	464.725	486.479	785.069	689.061	716.963	672.521	453.3047	612.187	452.88	487.673
	CHRIPS	323	812	389	173	325	274	285	265	315	304	762	212	195	247	467	338	324	460	307	361	207	244
Bore	Year	2000	2001	2002	2003	2004	2005	2006	2007	2008	2009	2010	2011	2012	2013	2014	2015	2016	2017				
	TAMSAT	1157	1484	1370	1453	1310	1523	1602.6	1540	1609	1258	1584	1937	1593	1637	1447	1441.8	1401	1325.7				
	OBSERVED	1701.4	1491	1477.4	1410.4	1599.7	1093.8	1667.9	1708.1	1558.5	1265.9	1605.2	1412.9	1647.7	1107.3	1483.8	1220	1216.8	1710.5				
	TAMSATC	1717.76	1500	1460	1435.9	1498.503	1108.572	1626.018	1653.048	1543.947	1272.223	1590.68	1320	1641.767	1184.717	1561.815	1232.796	1259.048	1626.524				
	CHRIPS	1495	1310	1275	1203	1372	967	1432	1524	1357	1112	1445	1274	1474	994	1322	1098	1078	1520				
FINCHAWA	Year	1996	1997	1998	1999	2000	2001	2002	2003	2004	2005	2006	2007	2008	2009	2010	2011	2012	2013	2014	2015	2016	2017
	TAMSAT	944.3	1381	731.7	640	657	678	936	984	835	994.2	1314.4	917	962	798	1071	1268	985	1123	860	772.5	791	471
	OBSERVED	659.7	1040	541.1	322.1	763.6	665.8	661.7	952	745.4	870.7	1012.7	699.7	693.9	456.5	1162.9	925.3	443.7339	224.4	954	740	350.9	382.3
		759.151	1165.187	570.097	366.541	756.696	688.317	680.549	976.472	737.96	962.361	1012.908	710.122	671.19	450.295	1093.375	962.418	634.278	262.136	1169.108	862.372	363.148	540.692
	CHRIPS	698	946	633	537	712	655	719	1081	781	836	871	612	644	482	990	895	521	144	984	691	391	365
NEGELE	Year	1996	1997	1998	1999	2000	2001	2002	2003														
	TAMSAT	719.7	1234	448.7	428	616	541	611	839														
	OBSERVED	869.2415	624.848	430.845	294.914	556.629	513.752	667.934	613.025														
	TAMSAT C	774.9	624	471.6	358.8	512.3	606.9	691.5	615.4														
	CHRIPS	527	507	368	247	427	498	520	468														
Filtu	YEAR	1987	1988	1989	1990	1991	1992	1993	1994	1998	1999												
	TAMSAT	576.1	427.2	559	771.7	388.4	217.4484	360.1	453.6	204.2	241												
	OBSERVED	610.2	309.5	505.3	467.8	432.1	303.3	496.4	484	333.4	271.9												
	TAMSATcc	618.61	377.913	520.093	551.758	458.211	327.373	466.381	488.633	357.599	370.098												
	CHRIPS	525	374	539	472	380	213	498	509	352	312												

Table A-0-2 Inter comparison Annual total mean and standard deviation for different rainfall product

		MEAN				STANDARD DEVIATION			
No	Station	TAMSAT	OBSERVED	TAMSAT CORR	CHRIPS	TAMSAT	OBSERVED	TAMSAT CORR	CHRIPS
1	Robe	997.4429	829.252381	825.2944359	635	209.5104327	134.0675077	136.8326024	173.8266
2	Delomena	974.9952	961.756095	990.3837087	631.3333	231.7133152	234.4278381	250.7336612	192.7305
3	Ginir	862.9136	928.35	1007.602092	747.5	243.8591675	346.1494692	394.1074527	269.2529
4	Kibre mengist	1122.114	832.563636	925.9642279	604.8636	263.6246579	403.6258753	438.3301096	284.6547
5	Moyale	590.0864	535.959091	572.7749272	344.9545	261.1654707	208.4834027	220.1880486	162.0319
6	Bore	1481.839	1465.46111	1457.406555	1291.778	165.3412815	211.2870187	182.7354827	184.2276
7	Negele	679.675	571.398562	581.925	445.25	261.5759749	170.0249531	130.6930291	96.35315
8	Finchawa	914.2773	694.019722	745.2442278	690.3636	226.380331	257.1654248	259.9904773	229.0428
9	Filtu	419.8748	421.39	453.6668993	417.4	180.3657098	111.085217	94.60270376	107.8478

Table 0-3 Inter comparison Annual total rainfall from different rainfall product

No	Station	TAMSAT	OBSERVED	TAMSAT CORR	CHRIPS	OBS-TAMSAT raw	OBS-TAMSAT cor	OBS-CHRIPS
1	Robe	20946.3	17414.3	17331.18315	13335	-3531.999989	83.11684652	4079.3
2	Delomena	20474.9	20196.878	20798.05788	13258	-278.0220063	-601.1798818	6938.878
3	Ginir	18984.1	20423.7	22167.24602	16445	1439.600003	-1743.546024	3978.7
4	Kibre mengist	24686.5	18316.4	20371.21301	13307	-6370.099995	-2054.813013	5009.4
5	Moyale	12981.9	11791.1	12601.0484	7589	-1190.799996	-809.9483981	4202.1
6	Bore	25516.1	24676.9	24515.55799	21757	-839.199992	161.3420069	2919.9
7	Negele	5437.4	4571.1885	4655.4	3562	-866.2115012	-84.2115017	1009.188498
8	Finchawa	20114.1	15268.4339	16395.37301	15188	-4845.66612	-1126.939126	80.43388549
9	Filtu	4198.748	4213.9	4536.668993	4174	15.15159158	-322.7689929	39.9

Table A0-4 Inter comparison of mean monthly rainfall from different rainfall product

station		Jan	Feb	Mar	Apr	May	Jun	Jul	Aug	Sep	Oct	Nov	Dec
Robe	CHRIPS	9.909091	9.863636	43.77273	79	58.54545	41.59091	73.68182	108.8182	84.59091	60.31818	25.81818	10.22727
	OBSE	15	17.10909	61.4	99.50909	74.07273	53.68182	90.25	139.0727	106.9136	76.70455	38.34545	15.61364
	TAMSAT	11.78573	17.37795	56.96459	106.3297	81.85777	60.6752	105.1311	143.148	111.497	78.24398	42.35145	14.71658
Delomena	CHRIPS	11.95238	6.285714	54.95238	132.4286	128.9048	19.71429	13.2381	27.04762	53.14286	119.0476	53.14286	11.47619
	OBSE	19.75238	19.39524	73.95238	190.6286	195.1095	27.12381	15.27143	31.35714	77.00952	196.5238	97.20476	19.20476
	TAMSAT	14.59756	18.94943	68.08843	199.1954	209.224	31.92195	17.1699	38.14629	68.72352	190.4496	110.1006	23.81695
Ginir	CHRIPS	19.31818	24.18182	56.18182	150.8182	119.9545	26.95455	17.40909	29.77273	71.09091	134.5455	59.5	26.31818
	OBSE	22.10909	29.94545	64.35	190.55	151.0455	38.04091	18.66818	40.69091	93.94545	176.2591	92.55455	35.2
	TAMSAT	21.95177	10.26791	63.8674	211.9839	179.7073	51.15844	24.91036	49.40536	87.46255	181.8951	93.72664	31.26539
Moyale	CHRIPS	9.818182	5.045455	33.31818	93.22727	51.59091	9.454545	8.227273	8	11.09091	61.40909	43.13636	10.63636
	OBSE	16.86364	11.92727	52.25	130.3727	78.65455	13.20909	9.063636	8.045455	15.45909	102.3864	74.78182	22.98182
	TAMSAT	23.08282	17.02509	55.74755	144.1888	71.7106	14.16941	6.381227	6.314727	12.62582	102.9911	85.48755	33.05018
Kibre mengist	CHRIPSS	11.59091	9.181818	52.18182	127.5	117.4545	28.81818	30.63636	30.18182	45.27273	102.1818	39.04545	10.81818
	OBSE	19.10909	13.87727	74.16818	172.4682	156.9818	43.8	36.41818	37.15455	55.42273	147.8545	61.30909	14.35
	TAMSAT	22.00205	10.41182	73.05055	202.4699	166.9957	50.32227	46.79641	43.957	62.40818	156.9677	72.66691	17.91568
Bore	CHRIPSS	16.44444	20.16667	57.05556	153.5	210.8333	147.8333	103.7778	132.4444	160.6111	140.0556	61.88889	21.44444
	OBSE	20.38333	24.78333	67.54444	168.75	246.9222	180.8222	126.7667	158.7778	196.8611	172.3167	75.62222	25.95
	TAMSAT	17.30811	23.35311	77.05744	199.1327	298.1389	208.6489	153.2213	185.5151	211.3472	198.0072	79.34933	29.99733
Filtu	CHRIPS	5.3	12	55.8	118.9	100.1	7.4	1.6	0	21.6	49.7	29.5	15.5
	OBSE	5.16	7.68	45.5	125.61	98.39	9.13	0.68	0.33	10.49	66.76	35.15	16.5
	TAMSAT	4.4457	7.162	56.0133	163.5336	130.8759	13.7276	4.2401	0	20.2626	71.6929	32.85039	20.8628
Negele	CHRIPS	6.375	1.875	52.375	116.75	86.875	8.125	3.375	4.25	23.75	97.625	24.625	19.25
	OBSE	9.7625	3.5	64.8875	142.5625	103.55	10.2625	4.2125	4.7625	28.875	141.0375	40.45	28.0625
	TAMSAT	8.481	3.615	59.97475	151.2355	101.0669	11.30425	8.395375	5.5505	28.80175	133.4995	34.48175	24.99225
Finchawa	CHRIPS	20.36364	12.72727	52.40909	181.2727	122.6818	24.18182	15.04545	23.04545	40.54545	120.8636	62.45455	14.77273
	OBSE	15.36818	9.627273	49.01364	174.8227	123.7682	33.03636	17.04545	31.63636	45.04091	113.9409	72.46818	15.36818
	TAMSAT	18.82118	11.45205	60.03368	178.4393	128.0009	35.04364	19.73632	36.97445	44.0255	127.5864	68.90082	16.23005

Year	Ann. ROBE St	Cum. Of Robe	Av. Surr sta	cum surr st
1996	895.5	895.5	6117.1	6117.1
1997	896.2	1791.7	6863.3	12980.4
1998	929.6	2721.3	5272.278	18252.678
1999	875.5	3596.8	4568.4	22821.078
2000	773.8	4370.6	5416.4	28237.478
2001	819.1	5189.7	4845	33082.478
2002	648.9	5838.6	5619.2	38701.678
2003	891.4	6730	5505.5	44207.178
2004	884.1	7614.1	5423.4	49630.578
2005	675.8	8289.9	5764.2	55394.778
2006	985.4	9275.3	6992.1	62386.878
2007	916.5	10191.8	4929.2	67316.078
2008	827.7	11019.5	5143.4	72459.478
2009	848.6	11868.1	4525.1	76984.578
2010	1067.1	12935.2	6762.7	83747.278
2011	769.2	13704.4	4796.7	88543.978
2012	855.3	14559.7	5814.933885	94358.912
2013	978.9	15538.6	5847.2	100206.11
2014	532.6	16071.2	4215	104421.11
2015	768.8	16840	4190.4	108611.51
2016	574.3	17414.3	2551.7	111163.21
2017			1211.6	112374.81

Station		Observed	CHRIPS	TAMSAT
Robe	Observed	1.000	0.9262	0.8932
	CHRIPS	0.9262	1.0000	0.7502
	TAMSAT	0.8932	0.7502	1.0000
Delomena	Observed	1.000	0.8016	0.8750
	CHRIPS	0.8016	1.0000	0.6604
	TAMSAT	0.8750	0.6604	1.0000
Ginir	Observed	1.0000	0.8974	0.9274
	CHRIPS	0.8974	1.0000	0.8406
	TAMSAT	0.9274	0.8406	1.0000
Kibremengist	Observed	1.0000	0.8202	0.8429
	CHRIPS	0.8202	1.0000	0.7508
	TAMSAT	0.8429	0.7508	1.0000
Moyale	Observed	1.0000	0.8744	0.9117
	CHRIPS	0.8744	1.0000	0.8006
	TAMSAT	0.9117	0.8006	1.0000
Finchawa	Observed	1.0000	0.7474	0.8884
	CHRIPS	0.7474	1.0000	0.6824
	TAMSAT	0.8884	0.6824	1.0000
Negele	Observed	1.0000	0.9616	0.9510
	CHRIPS	0.9616	1.0000	0.9247
	TAMSAT	0.9510	0.9247	1.0000
Filtu	Observed	1.0000	0.8773	0.8641
	CHRIPS	0.8773	1.0000	0.6832
	TAMSAT	0.8641	0.6832	1.0000
Bore	Observed	1.0000	0.9424	0.8277
	CHRIPS	0.9424	1.0000	0.7772
	TAMSAT	0.8277	0.7772	1.0000

Table A-0-5 Inter-comparison of daily rainfall from satellite rainfall products and rain gauge

						statistical indecs					Catagorical Indecs			
STATION		Mini	Max	Mean	ST.dev	R	ME	BIAS	RSME	NSE	POD	FAR	FB	HSS
ROBE	OBSERVED	0.000	112.300	2.393	5.697									
	TAMSAT raw	0.000	55.6	2.734341	6.141082	0.373712	0.045314	1.018939	6.430582	0.033195	0.550865	0.318538	0.808358	0.447763
	TAMSAT corr	0.0000	109.3000	2.9470	8.0355	0.893193	-0.00043	0.999819	2.594137	0.79263	0.773744	0.175439	0.938371	0.683207
	CHRIPS	0.0000	83.0000	1.8413	4.5603	0.926194	-0.55205	0.76932	2.330566	0.832628	0.833263	0.003534	0.836218	0.769677
DELOMENA	OBSERVED	0.0000	109.3000	2.9470	8.0355									
	TAMSAT raw	0.0000	82.0000	2.801135	7.329934	0.265019	0.040929	1.022132	9.548722	-0.41253	0.530752	0.382372	0.859339	0.437905
	TAMSAT corr	0.0000	108.0000	3.0322	8.1220	0.87502	0.085271	1.052026	4.040226	0.747119	0.672551	0.237573	0.882118	0.62202
	CHRIPS	0.0000	83.0000	1.9332	6.0181	0.768893	-0.44862	1.052026	5.249629	0.573064	0.803531	0.106396	0.899203	0.749717
GINIR	OBSERVED	0.0000	162.0000	2.8379	8.8331									
	TAMSAT raw	0.0000	90.0000	2.338445	6.592414	0.387615	0.078876	1.027798	10.30538	0.265518	0.469245	0.374472	0.750159	0.429591
	TAMSAT corr	0.0000	159.0000	3.0660	9.0298	0.927438	0.228094	1.080386	3.415104	0.85048	0.749524	0.206711	0.944832	0.709155
	CHRIPS	0.0000	133.0000	2.2397	6.8379	0.886561	-0.59811	0.789213	4.247007	0.768763	0.863031	0.06972	0.927711	0.867603
KIBREMENGIST	OBSERVED	0.0000	94.0000	2.7444	7.3775									
	TAMSAT raw	0.0000	85.0000	3.139099	7.671638	0.477391	0.082814	1.03018	7.457154	0.02153	0.551895	0.335757	0.830862	0.472268
	TAMSAT corr	0.0000	90.9500	3.0510	7.7411	0.842937	0.306546	1.111717	4.261564	0.666232	0.641406	0.257942	0.86436	0.582509
	CHRIPS	0.0000	68.0000	1.9930	5.0413	0.820244	-0.75129	0.726202	4.40317	0.643682	0.753432	0.174489	0.912685	0.713187
MOYALE	OBSERVED	0.0000	126.2000	1.5445	6.1903									
	TAMSAT raw	0.0000	100.0000	1.641689	6.108773	0.444698	0.141207	1.092055	6.670313	0.062321	0.394262	0.41198	0.670492	0.394355
	TAMSAT corr	0.0000	124.0000	1.6504	6.4030	0.911657	0.106122	1.068619	2.656653	0.81577	0.589344	0.220174	0.755738	0.618921
	CHRIPS	0.0000	102.0000	0.9940	4.5153	0.87437	-0.55025	0.643577	3.182567	0.735609	0.698361	0.019563	0.712295	0.787448
BORE	OBSERVED	0.0000	96.3000	4.5216	8.8091									
	TAMSAT raw	0.0000	92.0000	4.131688	7.20546	0.533719	0.078944	0.982538	9.083087	0.059702	0.605564	0.258516	0.816692	0.440411
	TAMSAT corr	0.0000	94.0000	5.1507	9.3179	0.82353	-0.66661	1.147453	5.460694	0.615618	0.722942	0.198225	0.901677	0.582113
	CHRIPS	0.0000	85.0000	3.7828	7.7295	0.942359	0.738646	0.836612	3.091595	0.876794	0.926067	0.002872	0.928735	0.929945
FILTU	OBSERVED	0.0000	90.3000	1.2116	5.3058									
	TAMSAT raw	0.0000	70.0000	1.386654	5.064305	0.552734	0.22244	1.183647	5.886496	0.006483	0.382212	0.519637	0.795673	0.357632
	TAMSAT corr	0.0000	89.0000	1.5114	5.6214	0.864094	0.299732	1.247459	5.619803	0.705288	0.733173	0.300459	1.048077	0.676354
	CHRIPS	0.0000	87.0000	1.2011	5.2425	0.8773	-0.64244	0.87232	3.21122	0.732212	0.84323	0.00323	0.87888	0.80545
NEGELE	OBSERVED	0.0000	103.0000	1.5913	5.6485									
	TAMSAT raw	0.0000	50.0000	1.158242	4.007861	0.5787	0.062573	1.039226	5.215568	0.148275	0.506073	0.382716	0.819838	0.47629
	TAMSAT corr	0.0000	102.5500	1.5671	5.6598	0.95105	-0.0242	0.984788	1.768763	0.901881	0.730769	0.154567	0.864372	0.743696
	CHRIPS	0.0000	91.0000	1.2211	4.7713	0.960519	-0.37005	0.767375	1.741461	0.904887	0.817814	0.012225	0.827935	0.875739
FINCHAWA	OBSERVED	0.0000	100.7000	2.2023	7.4748									
	TAMSAT raw	0.0000	96	1.8872	5.7896	0.435043	0.296837	1.134804	7.73823	0.067179	0.424932	0.653304	1.22566	0.252722
	TAMSAT corr	0.0000	99.0000	2.3409	7.5316	0.888362	0.138526	1.062909	3.548081	0.774625	0.832575	0.23495	1.088262	0.757778
	CHRIPS	0.0000	100.0000	2.1685	7.5197	0.8715	-0.77445	0.648298	3.907088	0.726709	0.748863	0.057274	0.794359	0.808018

Table A-0-6 Parameter Sensitivity result

		TAMSAT						CHRIPS							
	Dawa at Melka Guba		Welmel at Melka Amana		Dimtu Nr. Bore		Genale at Halwen		Dawa at Melka Guba		Welmel at Melka Amana		Dimtu Nr. Bore		Genale at Halwen	
Parameter	Rank	P-Value	Rank	P-Value	Rank	P-Value	Rank	P-Value	Rank	P-Value	Rank	P-Value	Rank	P-Value	Rank	P-Value
R__CN2.mgt	2	0.302457722	1	0.122177095	2	0.286817183	3	0.037760345	2	0.277068115	1	0.144812090	2	0.028562523	2	0.028562523
V__ALPHA_BNK.rte	16	0.892553366	13	0.332582267	1	0.269957807	18	0.846371683	1	0.254792937	2	0.194728164	4	0.098133386	4	0.098133386
V__CH_K2.rte	11	0.552340775	10	0.265607843	16	0.864748535	12	0.133171589	3	0.328846616	3	0.286155906	8	0.296854261	8	0.296854261
V__SOL_AWC(..).sol	14	0.855777861	17	0.695548247	9	0.518954011	17	0.387222551	4	0.425851809	4	0.391541471	11	0.400451241	11	0.400451241
V__GWQMN.gw	15	0.862508787	9	0.264046531	15	0.833918316	13	0.147862001	5	0.663917705	5	0.503671803	14	0.609171980	14	0.609171980
V__ALPHA_BF.gw	7	0.372584669	16	0.384807230	12	0.557679337	14	0.158737079	11	0.787503227	6	0.560518060	12	0.406052969	12	0.406052969
V__HRU_SLP.hru	6	0.360818427	4	0.223688577	13	0.610174635	2	0.031962848	14	0.870314852	7	0.566635625	1	0.013184128	1	0.013184128
V__EPCO.hru	17	0.901062031	12	0.280983568	17	0.907242180	15	0.159881574	6	0.681187927	8	0.576285448	16	0.822951008	16	0.822951008
V__REVAPMN.gw	5	0.350006016	3	0.219806295	14	0.649763999	5	0.098558510	9	0.738797139	9	0.741221206	13	0.473387639	13	0.473387639
V__SOL_K(..).sol	3	0.322018285	8	0.247260614	7	0.492986168	8	0.111760874	17	0.949636434	10	0.762863994	5	0.231694926	5	0.231694926
V__SURLAG.hru	12	0.578106934	6	0.228865795	4	0.419491018	6	0.104529355	10	0.777644350	11	0.765994644	9	0.375829171	9	0.375829171
V__SLSUBBSN.hru	13	0.681779666	14	0.348839583	6	0.472076129	11	0.132971848	13	0.866059912	12	0.768464207	17	0.834493699	17	0.834493699
V__CANMX.hru	10	0.454077242	7	0.230816815	5	0.468902692	7	0.107032446	8	0.737134674	13	0.773166064	7	0.288005159	7	0.288005159
V__CH_N2.rte	8	0.400048372	15	0.371138914	10	0.542981067	9	0.123515953	15	0.928919190	14	0.849478419	10	0.388145202	10	0.388145202
V__ESCO.hru	18	0.943276948	18	0.816738762	18	0.966006824	16	0.318948831	7	0.733774711	15	0.868988358	18	0.978776889	18	0.978776889
V__GW_REVAP.gw	9	0.400341007	11	0.266336039	8	0.500824097	10	0.125828582	12	0.801728866	16	0.877488615	15	0.806540934	15	0.806540934
V__RCHRG_DP.gw	4	0.332327013	2	0.202302599	11	0.547235352	1	0.015688527	18	0.978167602	17	0.908654372	3	0.030283124	3	0.030283124
V__GW_DELAY.gw	1	0.263324146	5	0.228295593	3	0.303283390	4	0.063050076	16	0.948003135	18	0.942552363	6	0.251840577	6	0.251840577

Table A-0-7 Symbols and description of weather generator parameters (WGEN) used by the SWAT model

S. No	Symbol	Description
1	TMPMX	Average or mean daily maximum air temperature for month (° C).
2	TMPMN	Average or mean daily minimum air temperature for month (°C).
3	TMPSTDMX	Standard deviation for daily maximum air temperature for month (°C).
4	TMPSTDMN	Standard deviation for daily minimum air temperature for month (°C).
5	PCPMM	Average or mean total monthly precipitation (mm H2O).
6	PCPSTD	Standard deviation for daily precipitation for month (mm H2O/day).
7	PCPSKW	Skew coefficient for daily precipitation in month.
8	PR_W1	Probability of a wet day following a dry day in the month.
9	PR_W2	Probability of a wet day following a wet day in the month.
10	PCPD	Average number of days of precipitation in month.
11	SOLARAV	Average daily solar radiation for month (MJ/m2/day).
12	DEWPT	Average daily dew point temperature in month (°C).
13	WNDAV	Average daily wind speed in month (m/s).

Table A-0-8 pcpSTAT result for WGEN generation

Statistical Analysis of Daily Precipitation Data (2000 - 2003)
Input Filename = PCPBORE.TXT

Number of Years = 4
Number of Leap Years = 1
Number of Records = 1461
Number of NoData values = 0

Month	PCP_MM	PCPSTD	PCPSKW	PR_W1	PR_W2	PCPD
Jan.	23.00	2.3420	4.3468	0.1275	0.3182	5.50
Feb.	10.75	1.9930	8.3345	0.1031	0.3125	4.00
Mar.	68.30	4.2974	2.8432	0.2615	0.6780	14.75
Apr.	150.65	8.6968	3.8001	0.5143	0.7765	21.25
May.	261.37	13.1333	2.2972	0.5185	0.8247	24.25
Jun.	235.47	13.6416	2.8597	0.5758	0.7471	21.75
Jul.	139.80	7.4013	2.6691	0.5000	0.8750	26.00
Aug.	167.75	8.2238	2.4191	0.8261	0.7822	25.25
Sep.	150.05	7.3447	2.8177	0.5152	0.7816	21.75
Oct.	226.95	12.6837	4.0568	0.6111	0.8679	26.50
Nov.	65.60	4.9959	3.6780	0.3333	0.6667	15.75
Dec.	47.68	4.1871	3.9332	0.1807	0.5854	10.25

Statistical Analysis of Daily Precipitation Data (2000 - 2003)
Input Filename = PCPDELO.TXT

Number of Years = 4
Number of Leap Years = 1
Number of Records = 1461
Number of NoData values = 0

Month	PCP_MM	PCPSTD	PCPSKW	PR_W1	PR_W2	PCPD
Jan.	23.17	3.0072	5.1942	0.0841	0.4706	4.25
Feb.	6.47	1.8912	9.8718	0.0275	0.2500	1.00
Mar.	58.53	5.9125	5.7507	0.1613	0.5161	7.75
Apr.	222.75	10.5409	1.8739	0.5227	0.6842	19.00
May.	163.90	9.5739	2.5945	0.4032	0.5323	15.50
Jun.	27.07	2.8921	3.8069	0.0909	0.4762	5.25
Jul.	15.85	2.3422	6.8103	0.1509	0.1111	4.50
Aug.	29.23	3.2318	4.6044	0.1275	0.3636	5.50
Sep.	115.95	6.8105	2.6815	0.4151	0.6567	16.75
Oct.	182.33	8.9518	2.1959	0.3429	0.8202	22.25
Nov.	108.45	10.1625	3.8161	0.1605	0.6154	9.75
Dec.	46.65	4.5050	4.4622	0.1327	0.4615	6.50

Statistical Analysis of Daily Precipitation Data (1996 - 1999)
Input Filename = PCPGINIR.TXT

Number of Years = 4
Number of Leap Years = 1
Number of Records = 1461
Number of NoData values = 0

Month	PCP_MM	PCPSTD	PCPSKW	PR_W1	PR_W2	PCPD
Jan.	57.43	7.3121	4.7858	0.0360	0.6154	3.25
Feb.	24.13	5.6543	8.6775	0.0190	0.7500	2.00
Mar.	40.35	3.5731	3.8119	0.1327	0.5000	6.50
Apr.	198.32	12.0924	3.0486	0.3846	0.6765	17.00
May.	119.15	8.9448	3.5033	0.2405	0.5333	11.25
Jun.	64.75	6.6465	4.1237	0.1648	0.4483	7.25
Jul.	21.75	2.4335	4.4228	0.1308	0.1765	4.25
Aug.	25.33	2.9609	5.0779	0.1215	0.2353	4.25
Sep.	80.30	6.4806	3.2287	0.2346	0.5128	9.75
Oct.	208.45	9.2384	2.2010	0.3333	0.8182	22.00
Nov.	132.80	10.9104	3.7795	0.2143	0.7000	12.50
Dec.	37.15	5.2458	6.9712	0.0808	0.6800	6.25

Statistical Analysis of Daily Precipitation Data (1998 - 2002)
Input Filename = PCPKIBRE.TXT

Number of Years = 5
Number of Leap Years = 1
Number of Records = 2188
Number of NoData values = 0

Month	PCP_MM	PCPSTD	PCPSKW	PR_W1	PR_W2	PCPD
Jan.	20.90	3.2578	6.6996	0.0357	0.6000	3.00
Feb.	20.42	2.8360	5.0125	0.0397	0.6000	3.00
Mar.	76.18	6.1942	3.4947	0.1441	0.6136	8.80
Apr.	196.62	10.5181	2.0368	0.4394	0.6548	16.80
May.	158.68	13.6294	4.1379	0.1856	0.6379	11.60
Jun.	22.96	2.9127	5.8283	0.1145	0.1579	3.80
Jul.	24.40	2.3674	5.0352	0.1230	0.4848	6.60
Aug.	32.32	4.4515	7.6619	0.1721	0.3333	6.60
Sep.	76.98	5.0473	3.1499	0.3133	0.6119	13.40
Oct.	196.54	7.8338	1.8243	0.4762	0.7788	22.60
Nov.	41.54	4.6442	4.2852	0.1024	0.3913	4.60
Dec.	28.70	4.4146	7.5268	0.0821	0.4762	4.20

Statistical Analysis of Daily Precipitation Data (2005 - 2007)
Input Filename = PCPMOYALE.TXT

Number of Years = 3
Number of Leap Years = 0
Number of Records = 1096
Number of NoData values = 0

Month	PCP_MM	PCPSTD	PCPSKW	PR_W1	PR_W2	PCPD
Jan.	15.80	2.1222	4.9716	0.0732	0.4545	3.67
Feb.	8.00	1.8547	8.1121	0.0641	0.1667	2.00
Mar.	17.60	2.2421	4.9716	0.0833	0.2222	3.00
Apr.	229.47	15.9675	3.5006	0.3784	0.7170	17.67
May.	85.27	9.6683	5.3953	0.2364	0.6053	12.67
Jun.	12.93	1.4713	6.2713	0.0986	0.5263	6.33
Jul.	4.87	0.7127	6.0170	0.1111	0.2500	4.00
Aug.	4.00	0.4221	3.9528	0.1111	0.1667	4.00
Sep.	17.73	2.2270	5.3222	0.1268	0.4737	6.33
Oct.	157.87	14.7577	5.8048	0.2222	0.6667	13.00
Nov.	107.00	7.6058	2.6685	0.2600	0.6500	13.33
Dec.	17.93	2.3542	4.9450	0.0741	0.4167	4.00

Statistical Analysis of Daily Precipitation Data (1999 - 2001)
Input Filename = PCPROBE.TXT

Number of Years = 3
Number of Leap Years = 1
Number of Records = 1095
Number of NoData values = 0

Month	PCP_MM	PCPSTD	PCPSKW	PR_W1	PR_W2	PCPD
Jan.	19.83	2.9589	5.8570	0.0588	0.2500	2.67
Feb.	4.40	0.7796	7.1856	0.0385	0.5714	2.33
Mar.	87.83	5.8989	2.6492	0.2679	0.5676	12.33
Apr.	91.00	6.3305	3.9608	0.3500	0.7000	16.67
May.	66.53	4.8538	4.5101	0.4894	0.4783	15.33
Jun.	70.67	4.7875	3.4838	0.2857	0.6098	13.67
Jul.	96.80	6.9568	3.6324	0.4091	0.6122	16.33
Aug.	110.27	5.6720	2.6580	0.4857	0.6552	19.33
Sep.	113.17	6.5516	4.0060	0.4375	0.7241	19.33
Oct.	52.63	3.0136	2.2171	0.2979	0.6739	15.33
Nov.	24.17	2.3930	3.1295	0.1096	0.4706	5.67
Dec.	49.17	4.9711	4.0142	0.1127	0.5909	7.33

PCP_MM = average monthly precipitation [mm]
PCPSTD = standard deviation
PCPSKW = skew coefficient
PR_W1 = probability of a wet day following a dry day
PR_W2 = probability of a wet day following a wet day
PCPD = average number of days of precipitation in month

(written by Stefan Liersch, Berlin, August 2003)

Table A-0-9 **dew02 Result For WGEN generation**

```
This file has been generated by the program 'dew02.exe'
Input Filename    = bore.txt
Number of Years   =            1
Number of Records =          365

Number of NoData Values
tmp_max  =          0
tmp_min  =          0
hmd      =          0

Average Daily Dew Point Temperature for Period (2014 - 2014)
```

Month	tmp_max	tmp_min	hmd	dewpt
Jan	20.23	6.99	65.71	8.41
Feb	21.79	8.57	64.15	9.18
Mar	20.19	9.41	71.48	10.37
Apr	18.95	10.12	71.15	9.79
May	18.27	10.42	82.25	11.73
Jun	17.76	9.74	87.69	12.14
Jul	16.25	9.48	90.65	11.65
Aug	16.53	9.18	87.10	11.09
Sep	16.84	9.16	88.30	11.48
Oct	17.09	9.89	83.12	11.00
Nov	17.71	9.09	78.95	10.26
Dec	18.47	7.33	89.53	12.07

```
This file has been generated by the program 'dew02.exe'
Input Filename    = delo.txt
Number of Years   =            1
Number of Records =          365

Number of NoData Values
tmp_max  =          0
tmp_min  =          0
hmd      =          0

Average Daily Dew Point Temperature for Period (2005 - 2005)
```

Month	tmp_max	tmp_min	hmd	dewpt
Jan	31.05	13.76	52.65	13.78
Feb	31.80	15.70	43.52	11.93
Mar	31.38	16.25	57.44	16.01
Apr	28.49	16.69	65.97	16.19
May	27.58	16.97	80.81	19.46
Jun	27.19	17.02	75.29	18.14
Jul	25.64	16.87	72.56	16.55
Aug	27.41	16.90	66.67	16.25
Sep	28.37	17.00	65.79	16.63
Oct	26.64	17.09	74.94	17.70
Nov	27.58	15.68	64.71	15.37
Dec	28.45	15.00	47.54	11.09

```
This file has been generated by the program 'dew02.exe'
Input Filename     = kibre.txt
Number of Years    =                    1
Number of Records  =                  365

Number of NoData Values
tmp_max  =          0
tmp_min  =          0
hmd      =          0

Average Daily Dew Point Temperature for Period (2006 - 2006)
```

Month	tmp_max	tmp_min	hmd	dewpt
Jan	28.68	9.47	59.29	13.16
Feb	29.67	11.42	60.71	14.59
Mar	29.13	12.59	66.94	16.04
Apr	26.52	14.27	76.77	17.06
May	26.08	14.59	78.48	17.26
Jun	24.31	13.86	77.93	15.81
Jul	22.44	13.78	79.13	14.89
Aug	23.75	13.51	78.61	15.44
Sep	25.01	13.47	74.03	15.27
Oct	24.93	14.47	82.16	17.23
Nov	26.32	12.80	74.63	16.07
Dec	26.73	12.25	71.71	15.50

```
This file has been generated by the program 'dew02.exe'
Input Filename     = ginir.txt
Number of Years    =                    1
Number of Records  =                  365

Number of NoData Values
tmp_max  =          0
tmp_min  =          0
hmd      =          0

Average Daily Dew Point Temperature for Period (1991 - 1991)
```

Month	tmp_max	tmp_min	hmd	dewpt
Jan	25.47	13.56	56.79	11.45
Feb	26.14	13.88	63.55	13.52
Mar	25.06	14.56	77.71	16.43
Apr	23.42	14.22	79.77	15.75
May	23.45	14.34	73.01	14.40
Jun	23.17	13.95	79.19	15.38
Jul	21.63	12.61	81.73	14.44
Aug	23.11	12.90	74.74	14.08
Sep	24.77	13.05	67.99	13.68
Oct	24.19	14.24	62.91	12.45
Nov	23.52	12.63	62.55	11.38
Dec	23.99	12.05	52.12	8.40

```
This file has been generated by the program 'dew02.exe'
Input Filename      = moyale.txt
Number of Years     =                    1
Number of Records   =                  365

Number of NoData Values
tmp_max  =                   0
tmp_min  =                   0
hmd      =                   0

Average Daily Dew Point Temperature for Period (2014 - 2014)
```

Month	tmp_max	tmp_min	hmd	dewpt
Jan	31.89	19.14	50.35	15.22
Feb	32.33	19.63	64.75	19.66
Mar	31.92	20.45	75.32	22.12
Apr	30.11	18.99	85.50	22.67
May	27.24	17.63	84.65	20.25
Jun	25.94	17.83	80.60	18.77
Jul	25.19	15.24	71.10	15.33
Aug	26.07	16.88	69.77	16.11
Sep	27.55	16.87	85.60	20.34
Oct	26.03	15.86	89.97	19.85
Nov	26.30	16.19	50.13	10.92
Dec	28.77	15.56	75.32	18.54

```
This file has been generated by the program 'dew02.exe'
Input Filename      = robe.txt
Number of Years     =                    1
Number of Records   =                  365

Number of NoData Values
tmp_max  =                   0
tmp_min  =                   0
hmd      =                   0

Average Daily Dew Point Temperature for Period (2011 - 2011)
```

Month	tmp_max	tmp_min	hmd	dewpt
Jan	23.33	5.69	52.54	6.73
Feb	24.39	6.68	48.69	6.52
Mar	24.34	8.10	50.86	7.43
Apr	24.45	9.03	59.37	10.12
May	22.27	10.34	74.07	12.55
Jun	23.14	10.06	67.81	11.68
Jul	22.51	9.92	71.83	12.09
Aug	21.14	9.64	78.52	12.51
Sep	20.59	9.62	79.55	12.35
Oct	19.88	7.83	71.71	9.09
Nov	20.52	8.37	74.60	10.85
Dec	21.68	5.19	54.80	6.04

```
tmp_max  = average daily maximum temperature in month [°C]
tmp_min  = average daily minimum temperature in month [°C]
hmd      = average daily humidity in month [%]
dewpt    = average daily dew point temperature in month [°C]

(written by Stefan Liersch, August, 2003)
```